2012-08-20

Mechanical Activation Of Valvular Interstitial Cell Phenotype

Angela Quinlan
Worcester Polytechnic Institute

MECHANICAL ACTIVATION OF VALVULAR INTERSTITIAL CELL PHENOTYPE

A Dissertation Presented

By

Angela Marie Throm Quinlan

Submitted to the Faculty of Worcester Polytechnic Institute, Department of Biomedical Engineering and University of Massachusetts Graduate School of Biomedical Sciences, Worcester in partial fulfillment of the requirements for the degree of

Doctor of Philosophy

August 10, 2012

Biomedical Engineering and Medical Physics

Mechanical Activation of Valvular Interstitial Cell Phenotype

A Dissertation Presented

By

Angela Marie Throm Quinlan

The signatures of the Dissertation Defense Committee signify completion and approval as to style and content of the Dissertation

Kristen L. Billiar, PhD, *Thesis Advisor*

Tanja Dominko, DVM, PhD, *Member of Committee*

Jie Song, PhD, *Member of Committee*

Frederick J. Schoen, MD, PhD, *Member of Committee*

Gang Han, PhD, *Member of Committee*

The signature of the Chair of the Committee signifies that the written dissertation meets the requirements of the Dissertation Committee

George D. Pins, PhD, *Chair of Committee*

The signature of the Dean of the Graduate School of Biomedical Sciences signifies that the student has met all graduation requirements of the school.

Anthony Carruthers, PhD.,
Dean of the Graduate School of Biomedical Sciences

Biomedical Engineering and Medical Physics
Worcester Polytechnic Institue and UMass Medical School, Graduate School of Biomedical Science
August 10, 2012

Dedication

I dedicate this work to my family and friends.

To my husband, Ed, thank you for getting me through this. Your personal understanding of the "thesis process" was invaluable. You truly understood the joy of statistical differences, the frustrations of failed experiments, and the occasional necessity of working nights and weekends to take a time point or run an assay "just one more time." This knowledge gave you the unique ability to understand what I was going through and to offer what I needed, be it advice, support, a sounding-board, or ice cream, often, before I knew I needed it. You are my motivator, my cheerleader, and my voice of reason. I could not have asked for a better partner on this journey and look forward to starting the next chapter as Drs. Quinlan.

To my parents, Phil and Kathie Throm, you always told me "You can do anything you put your mind to." I have held this advice close to my heart and draw from these words during difficult times as well as reflect back on them after accomplishments. Not only have you given sage advice, but you self-sacrificed so that I could be afforded opportunities and an education that made "anything" possible. Even at a distance your support an encouragement kept me going. To my brother, Jason, thank you for the comic relief and welcomed distractions. Your pursuit of learning, despite unconventional methods is inspiring (most of the time). To Grandma Norma Bouse, you were one of my first teachers; you taught me so many things from crocheting to canning. As you continue

to embark on new adventures and learn new things, I am reminded where my desire for education came from and hope that I can follow your example of life-long learning and passing along family traditions and recipes. To my grandparents, that took pride in my education and accomplishments. Thank you for all of the love and support, I wish you could all be here to see me complete my degree. Thank you to my numerous aunts, uncles, cousins, and family friends that always asked how things were going and gave words of encouragement.

To my Collinsville and SLU friends, despite long distances and different life paths, we have maintained our friendships and supported each other through school, marriages, jobs, and family. I truly cherish our friendships. To my WPI and Umass friends, we started on this journey together and saw each other at our best (and at our worst). Together we made it through courses, qualifiers, research, and graduation. I am so grateful to have had a group of friends in which to share these accomplishments. Thank you for the fond memories and for making grad school (even the late nights and weekends in the lab) enjoyable.

Acknowledgements

Thank you to my advisor, Kristen Billiar, for all of the education, opportunities, guidance.

I would like to thank the following WPI graduate students for scientific advising and assistance with experiments: Katie Bush, PhD, Kevin Cornwell, PhD, Brett Downing, Jenna Balestrini, PhD, Jeff Johns, Jeremy Skorinko, Jacques Guyette, PhD, Tracy Gwyther, PhD, Jen Makadradis, Pete Driscoll, PhD, Eftim Milkani, PhD, Heather Hinds, Heather Circa, Mehmet Kural, and Christine Lima. Thank you to the The Angles (in the Outfield) for a championship title.

The WPI faculty that guided me through numerous projects: Jill Rulfs, PhD, Nancy Burnham, PhD, John McDonald, PhD, Sakthikumar Ambady, PhD, Venkat Thaladi, PhD, Ray Page, PhD, Marsha Rolle, PhD, and Glenn Gaudette, PhD.

Thank you to my committee members, past and present: Kristen Billiar, PhD, George Pins, PhD, Jie Song, PhD, Tanja Dominko, DVM, PhD, Frederick Schoen, MD, PhD, and Gang Han, PhD.

Dan Tchumperlain, PhD, Fei Liu, PhD, and Justin Mih, PhD of the Harvard School of Public Health for instruction on preparing gels.

I would like to thank Yu Li Wang, PhD and Margo Frey, PhD from UMass for assistance with gels. Thank you to Sue Wheeler for providing tissue for cell isolation. Kendall Knight, PhD, Tony Caurthers, PhD, Mary Ellen Lane, PhD, and Gaile Arcouette-Curtis for helping me navigate the UMass graduate program.

Thank you to the following undergraduate students for assistance with lab work and projects: Danielle Defour, Jaime Day, Lee Sierad, Andy Capulli, Laura Firstenberg, Bhavika Shah, Tim Ebner, Alex Christakis, Joey Lock, Cris Liu, PhD, Molly Conforte, and Jackie Youssef, PhD.

WPI Staff for assistance with administrative items, experimental, and lab support: Pam O'Brien, Debbie Bordage, Jean Siequist, Sharon Shaw, Vicki Huntress, Wayne Atchu, Neil Whitehouse, Adriana Hera, PhD, Sia Najafi, and Lisa Wall.

Abstract

During heart valve remodeling, and in many disease states, valvular interstitial cells (VICs) shift to an activated myofibroblast phenotype which is characterized by enhanced synthetic and contractile activity. Pronounced alpha smooth muscle actin (αSMA)-containing stress fibers, the hallmark of activated myofibroblasts, are also observed when VICs are placed under tension due to altered mechanical loading *in vivo* or during *in vitro* culture on stiff substrates or under high mechanical loads and in the presence of transforming growth factor-beta1 (TGF-β1). The work presented herein describes three distinct model systems for application of controlled mechanical environment to VICs cultured *in vitro*. The first system uses polyacrylamide (PA) gels of defined stiffness to evaluate the response of VICs over a large range of stiffness levels and TGF-β1 concentration. The second system controls the boundary stiffness of cell-populated gels using springs of defined stiffness. The third system cyclically stretches soft or stiff two-dimensional (2D) gels while cells are cultured on the gel surface as it is deformed. Through the use of these model systems, we have found that the level of 2D stiffness required to maintain the quiescent VIC phenotype is potentially too low for a material to both act as matrix to support cell growth in the non-activated state and also to withstand the mechanical loading that occurs during the cardiac cycle. Further, we found that increasing the boundary stiffness on a three-dimensional (3D) cell populated collagen gel resulted in increased cellular contractile forces, αSMA expression, and collagen gel (material) stiffness. Finally, VIC morphology is significantly altered in response to

stiffness and stretch. On soft 2D substrates, VICs cultured statically exhibit a small rounded morphology, significantly smaller than on stiff substrates. Following equibiaxial cyclic stretch, VICs spread to the extent of cells cultured on stiff substrates, but did not reorient in response to uniaxial stretch to the extent of cells stretched on stiff substrates. These studies provide critical information for characterizing how VICs respond to mechanical stimuli. Characterization of these responses is important for the development of tissue engineered heart valves and contributes to the understanding of the role of mechanical cues on valve pathology and disease onset and progression. While this work is focused on valvular interstitial cells, the culture conditions and methods for applying mechanical stimulation could be applied to numerous other adherent cell types providing information on the response to mechanical stimuli relevant for optimizing cell culture, engineered tissues or fundamental research of disease states.

Table of Contents

List of Figures

List of Tables

List of Copyrighted Material

Figure 2.1 was created by Eric Pierce and is licensed under the Creative Commons Attribution-Share Alike 3.0 Unported license granting permission to copy, distribute and/or modify the document.

Figure 2.2 was previously published in an open access journal and no permission is required from the authors or the publishers so long as the original authors and source are cited.

> Hemodynamics and mechanobiology of aortic valve inflammation and calcification.
> International Journal of Inflammation

Figure 2.3 was previously published and copyright permissions were obtained from the publisher.

> The effects of cellular contraction on aortic valve leaflet flexural stiffness
> Journal of Biomechanics
> License Number: 2956730182255

Figure 2.4 was previously published and copyright permissions were obtained from the publisher.

> Dynamic and Reversible Changes of Interstitial Cell Phenotype During Remodeling of Cardiac Valves
> Journal of Heart Valve Disease

Figure 2.5 was previously published and copyright permissions were obtained from the publisher.

> Myofibroblasts and mechano-regulation of connective tissue remodeling
> Nature Reviews Molecular Cell Biology
> License Number: 2956731108757

Portions of **Chapter 3** including figures, tables, and text were previously published and copyright permissions were obtained from the publisher.

> Investigating the role of substrate stiffness in the persistence of valvular interstitial cell activation
> Journal of Biomedical Materials Research

License Number: 2956581237667

Portions of **Chapter 4** including figures, tables, and text were previously published and copyright permissions were obtained from the publisher.

Boundary Stiffness Regulates Fibroblast Behavior in Collagen Gels
Annals of Biomedical Engineering
License Number: 2956590670019

Portions of Chapter 5 including figures, tables, and text were previously published in an open access journal and no permission is required from the authors or the publishers so long as the original authors and source are cited.

Combining Dynamic Stretch and Tunable Stiffness to Probe Cell Mechanobiology *In Vitro*
PLOS One

List of Abbreviations

µm	Micrometer
µN	MicroNewton
2D	Two-dimensional
3D	Three-dimensional
AFM	Atomic force microscopy
ANOVA	Analysis of variance
BSA	Bovine serum albumin
CAD	Computer-aided design
CCD	Charged coupled device
CMR	Cell Mapping Rheometry
DMEM	Dulbecco's modified eagle's medium
E	Young's Modulus
ECM	Extra cellular matrix
Eq	Equation
FBS	Fetal bovine serum
FFT	Fast Fourier transform
FIB	Dermal fibroblasts
FOV	Field of view
G'	Storage modulus
G''	Loss modulus
GAGs	Glycosaminoglycans
HDM	High Density Mapping
HDPE	High density polyethylene
hMSC	Human mesenchymal stem cells
IACUC	Institutional animal care and use committee
KCl	Potassium chloride

kPa	KiloPascal
LDS	Laser displacement system
M	Meter
M	Molar
mL	Milliliter
Mm	Millimeter
mM	Millimolar
mN	MilliNewton
N	Newton
Ng	Nanogram
NIH	National Institutes of Health
Pa	Pascal
PA	Polyacrylamide
PDMS	polydimethyl siloxane
PEG	Polyethylene glycol
PMSF	Phenylmethanesulfonylfluoride
PVA	Polyvinyl alcohol
ROI	Region of interest
SD	Standard Deviation
TCPS	Tissue culture polystyrene
TE	Tissue engineering
TGF-β1	Transforming growth factor beta-1
VICs	Valvular interstitial cells
αSMA	Alpha smooth muscle actin

Chapter 1 - Introduction

Heart valve disease results in nearly 300,000 annual valve replacements worldwide.[1] The aortic valve is the most susceptible to disease and the most frequently replaced with an artificial valve. Valve replacement is considered the standard-of-care; however, both mechanical and bioprosthetic implants are acellular and unable to promote self-repair. Tissue engineered valves offer a promising approach for extending the life of implants and for adaptation to changes in patient size, attributes particularly important for the pediatric patient population. In addition, controlled *in vitro* studies of valvular cells and their role in valve disease add to the fundamental knowledge of valve pathogenesis. The majority of *in vitro* studies on VIC biology have been studied in standard tissue culture environments with stiff, static substrates which do not emulate the soft, dynamic environment of the valves, yet altered mechanical loading, resulting from congenital and/or acquired conditions, is now thought to play a role in aortic valve disease progression. Regions of the valve bearing the highest strains, such as where the leaflet attaches near aortic wall, correlate with regions where calcification is initiated.[2-4] Further, cells isolated from the aortic and mitral valves both on the left side of the heart which experience high pressures, were stiffer and expressed more collagen than cells isolated from the tricuspid and pulmonary valves located on the right side of the heart which experience relatively lower pressures.[5] Taken together these data suggest a strong regulatory role of mechanics in valvular cell function and progression of valvular disease.

Valvular interstitial cells (VICs) are the most abundant cell type found in heart valves and are responsible for the maintenance and repair of the valve leaflet.[2,6,7] The majority of VICs express characteristics of normal fibroblasts in healthy valves,[8] however, activated VICs in diseased valves predominantly express myofibroblastic markers. The defining cytological marker for these highly synthetic and contractile cells is the contractile protein alpha smooth muscle actin (αSMA).[9] Although a small number of activated VICs are required to repair and maintain the valve tissue; in heart valves and in other tissues, the presence of myofibroblasts is associated with fibrosis and disease.

In vitro studies have also demonstrated that VICs are sensitive to the mechanical environment in which they are cultured. Freshly isolated VICs are activated by culturing on tissue culture treated polystyrene.[10,11] Another study demonstrates that VICs cultured on stressed (stiff) collagen matrices express increased levels of αSMA as compared to unstressed (compliant) culture conditions.[10] The addition of the profibrotic cytokine transforming growth factor beta-1 (TGF-β1) further enhances the response in only the "stiff" gels suggesting that a minimum stiffness level is required for activation by TGF-β1.[10] While these studies demonstrated the importance of TGF-β1 and mechanical tension (stiffness) on VIC phenotype, the tension "perceived" by the cells was not quantified. More recently, Kloxin and colleagues, using dynamically modulated hydrogel system, demonstrate that the activation of VICs to myofibroblasts is reversible when the stiffness of the culture environment is decreased.[12] Mechanical loading (stretch) has also been demonstrated to regulate VIC activation. The magnitude and duration of cyclic

loading affects αSMA expression,[13] collagen production,[14,15] and expression of markers that are implicated in the initiation of valve calcification.[16]

Despite the recent increase in studies evaluating the response of VICs to mechanical stimuli, generally only one or two stiffness levels or one or two stretch levels are being evaluated.[12] Thus, there is a need for a more systematic study with combined stimuli of cytokines and mechanical loading. Here we focus on the effects of mechanical manipulations of heart valve cells in an effort to understand valve pathologies and to aid in the rational design of treatments including the development of tissue engineered heart valves. The goal of these studies is to investigate the role of stiffness and stretch in the regulation of VIC response to external stimuli such as TGF-β1. Chapter 2 presents relevant background on heart valve structure and pathology as well as the roles of mechanical and cytokine stimulation in the activation of VICs. Additionally, methods for applying mechanical stimulation to cells in two- and three-dimensional culture systems are also discussed. In Chapter 3 we describe studies where we utilized a well-established, controlled culture system to investigate the effects of the stiffness on VIC activation in the presence and absence of TGF-β1 in the context of a two-dimensional (2D) cell culture environment. Cells were cultured on polyacrylamide (PA) gels with tunable stiffness and the presence of myofibroblast markers was evaluated. This 2D system allowed us to screen many different levels of stiffness in order to establish the range of stiffness levels required for VIC activation. Next, we used a more *in vivo*-like three-dimensional (3D) culture system to determine the response to stiffness. In Chapter 4 we evaluate VIC

phenotype in a novel 3D culture system with mechanically controlled stiffness. The culture model is comprised of cell-populated collagen gels in which the boundary stiffness of the gels is controlled by stainless steel wires of varying diameter. While this system is more complex, the cells are able to create focal adhesions on all surfaces (unlike a 2D culture) and "sense" the stiffness on all sides. After establishing the importance of stiffness in VIC differentiation to the myofibroblast phenotype, we discuss in Chapter 5, the development of a model system to simultaneously control the stiffness and loading (stretch) of the culture environment. VICs were cultured on soft and stiff substrates and subjected to static and equibiaxial stretch conditions. A method of stretching PA substrates was developed and both the stiffness and stretch of the substrate were varied and cell spreading, which is associated with many cell functions, was measured. Chapter 6 is a reflection on the findings presented in this work. Implications of the findings are discussed as well as suggestions for potential future studies. These studies characterize the effect of mechanical stimuli in a variety of culture environments on the activation of VICs. Knowledge of VIC response to material and mechanical stimuli is essential for creating successful therapies for heart valve disease and for the rational design of tissue engineered valves.

Chapter 2 - Background

2.1. Significance

Approximately 330,000 aortic or mitral valve procedures were performed in the United States between 1998 and 2005; of these, 288,000 were valve replacements and 46,000 were valve reparative surgeries.[1] The aortic valve is most frequently diseased and replaced (compared to the other 3 heart valves). Each procedure requires a 6-10 day hospital stay and costs on average $138,000* and $118,000* for an aortic valve repair and replacement respectively (* figures from 2005).[1]

Aortic valve stenosis is the most common condition necessitating heart valve replacement in developed countries.[17] Calcium deposits on the valve tissue cause the valve opening to narrow and the valve tissue to stiffen. During early stages of calcific valve disease, the valve tissue is thickened and does not yet obstruct the flow of blood, at this stage the valves are described as sclerotic. As the disease progresses, the fibrocalcific masses increase in size and there is disruption of both the basement membrane and collagen fiber alignment. Macrophages and lymphocytes also begin to infiltrate the tissue.[18] As the thickness and stiffness of the valve leaflets increases, the valve opening becomes narrowed causing an increased pressure across the valve which results in altered blood flow. Once flow is obstructed, the valve is described as stenotic. The altered blood flow increases the work done by the heart, which if left untreated, leads to heart muscle injury and eventual cardiac failure. Changes to the valve structure and ECM surrounding the

cells in not only the result of valvular mechanical malfunction but changes in the mechanical environment surrounding the cells could regulate the progression of the disease (Review by Chen and Simmons[19]). The current therapies for valve disease are effective, but not without limitations. Mechanical replacement valves can cause thrombosis, requiring the patient to be on long-term anti-coagulant therapy. Biological valves are not as thrombogenic, however, they are less durable and can degenerate faster in young patients. Although these treatments are the clinical standard, they do not fully mimic the structure and function of the native valves. In addition, both types of replacement valves are acellular, eliminating the ability of self-repair. For these reasons, researchers are investigating methods for developing tissue-engineered valves capable of remodeling and growth with the patient, an attribute which is particularly attractive for valve replacement in the adolescent patient population.

2.2. Physiology of Heart Valves

Four valves regulate the flow of blood in and out of the heart: aortic, pulmonary, bicuspid, and tricuspid (Figure 2.1). Due to the prevalence of replacement stated previously, we focus on the aortic valve in this work. The aortic valve is composed of three semilunar cusps (leaflets) inserted into a fibrous connective tissue sleeve. Each cusp is attached to the tissue sleeve along its curved edge and the cusps meet at three commissures which are equally spaced along the circumference of the sleeve at the supra-

aortic ridge. The sinuses of Valsalva are pouches located between the valve sleeve and cusps. During ventricular outflow, the cusps fold back toward the sinuses (Figure 2.2). When the pressure in the aortic root is greater than the ventricular pressure, the valve closes. The heart valve structure allows for its precise motion during each open/close cycle, for 3×10^9 cycles during an average human life span.

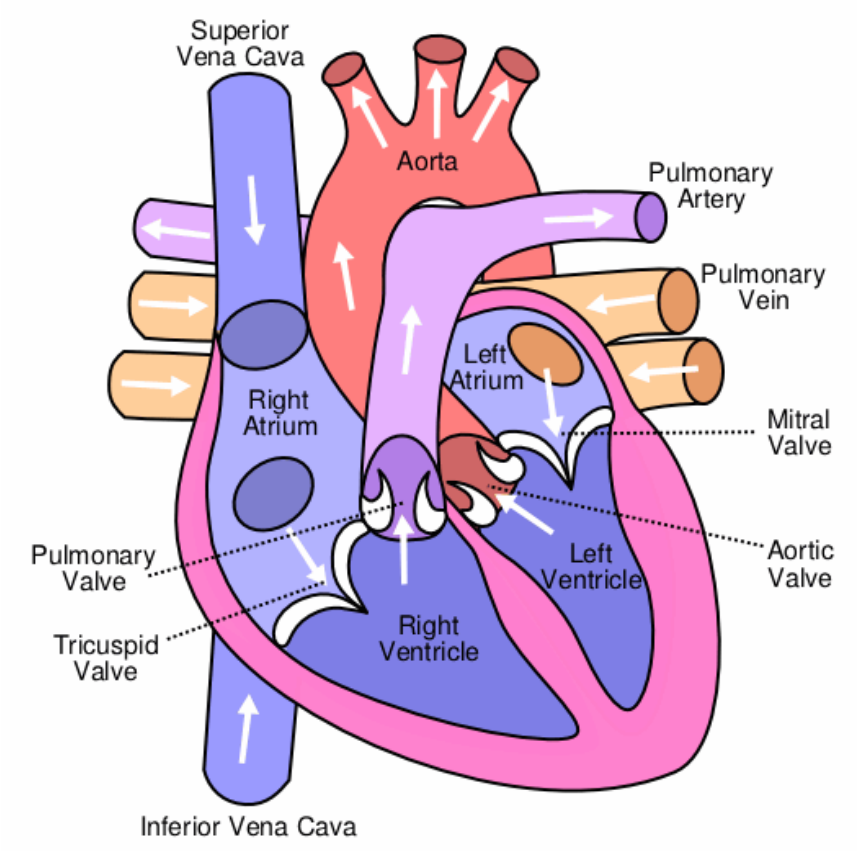

Figure 2.1. The human heart contains four valves: pulmonary, tricuspid, aortic, and mitral (created by Eric Pierce).

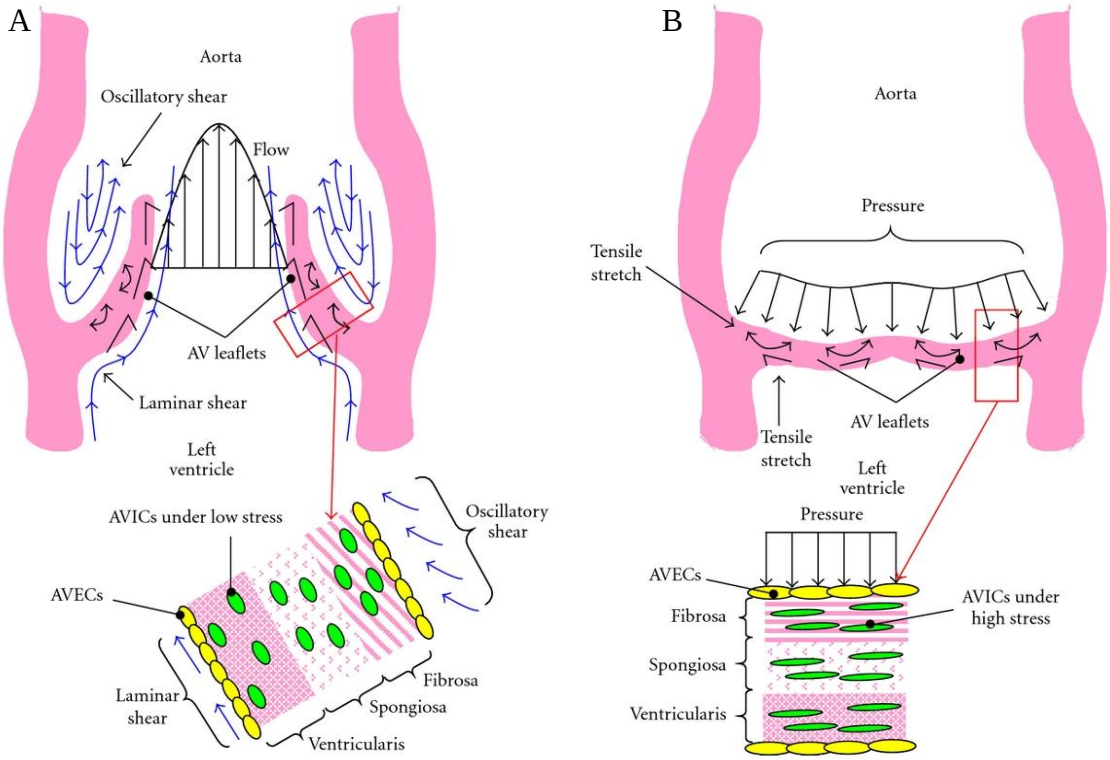

Figure 2.2. Schematic of the aortic valves showing direction of blood flow, the tri-layered structure of the valve cusps, and forces applied to VICs during cusp deformation in systole (A) and diastole (B).[20]

Aortic valves are comprised of cellular and non-cellular components organized into a three-layered architecture: fibrosa, ventricularis, and spongiosa (Figure 2.2 and Figure 2.3). The fibrosa is the innermost layer, composed primarily of collagen with a few fibroblasts and elastic fibers. It spans the full area of the valve and is the major structural support of the valve. The ventricularis is the subendothelial layer on the ventricular surface of the valve. It spans the full area of the valve and is composed of collagen fibers and radially arranged elastin fibers. The spongiosa layer is located between the fibrosa and ventricularis and contains loosely arranged collagen fibers, scattered fibroblasts, less-well differentiated mesenchymal cells, and large amounts of proteoglycans. The spongiosa layer is most prominent in the basal third of the valve. The cellular components of the valve include: cardiac muscle, smooth muscle, VICs and the valve exterior is surrounded by a single layer of endothelial cells.

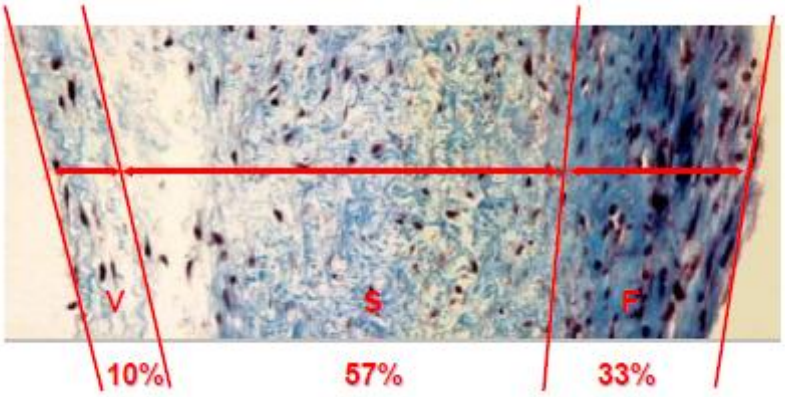

Figure 2.3. Masson's Trichrome stained porcine aortic valve depicting the tri-layered valve structure. Lines show the approximate locations of the three layers and the average thickness of each layer is shown as a fraction of total valve thickness. From the ventral (left) side, ventricularis (V), spongiosa (S), and fibrosa (F).[21]

2.3. Valvular Interstitial Cells

VICs are the most abundant cell type found in heart valves and are responsible for valve structure maintenance and repair of the valve leaflet.[2,6,7] In healthy valves, the majority of VICs are considered quiescent and express characteristics of normal fibroblasts[8] such as ease of *in vitro* culture, slow proliferation, adherence to tissue culture plastic, and elongated morphology with filopodia. VICs are found throughout the valve and make connections to each other and to the extracellular matrix (ECM) creating a network within the valve structure.[22] VICs maintain the valve structure through secretion of ECM components including collagen, fibronectin, chondroitin sulfate and prolyl-4-hydroxlase.[23] Many tissues, including heart valves can respond to alterations in physical signals by reversible phenotypic modulation of cells (Figure 2.4).[8] Unlike healthy valves, with a majority of VICs exhibiting a quiescent fibroblast-like phenotype, VICs in developing, diseased, and adapting valves are predominantly activated myofibroblasts. The defining cytological marker for these highly synthetic, proliferative, and contractile cells is the expression of the contractile protein αSMA.[9] Myofibroblasts are present in fibrotic tissues throughout the body and are often associated with wound healing. While myofibroblasts are the hallmark of diseased valves (and of fibrotic tissue in general), a small percentage of myofibroblasts is required for maintenance of the structure of the valve leaflet.[6,24] In healthy valve tissue, myofibroblasts are found in regions that correlate with high stiffness, loaded regions such as the edge of the leaflets, where the valves meet to form a seal, and where more matrix repair and remodeling are required.[8] Healthy

porcine aortic valves immuno-stained for αSMA were found to have less than 1% αSMA expressing cells while in sclerotic valves (thickened tissue without obstructing blood flow), 31% of cells were immuno-stained for αSMA.[11]

In addition to expressing αSMA, activated VICs also express the intermediate filament protein vimentin, matrix metalloproteinase 13 (collagenase-3), and the motor protein, non-muscle myosin heavy chain (SMemb).[8] However, since some of the proteins are expressed by quiescent fibroblasts and others are expressed by smooth muscle cells, only αSMA is considered the defining marker of myofibroblasts. More recently, cofilin, an actin-binding protein that disassembles actin filaments, has been found to be expressed in both diseased valves and VICs activated *in vitro*.[11] siRNA mediated depletion of cofilin did not affect αSMA expression; however, αSMA incorporation into stress fibers was significantly impaired. Further, depletion of cofilin reduced the contractility of VICs, as evidenced by the inability of VICs to contract collagen gels. This suggests that cofilin may be required for the activation of VICs to the myofibroblast phenotype.[11] Calcific deposits are generally co-localized with the areas of the highest stresses in the valve.[4] Since calcific valves have a high percentage of activated VICs it is hypothesized that VIC activation to the myofibroblast phenotype and VIC expression of calcific markers.[10,25] Since these studies were proposed, other groups have evaluated VICs for the expression of osteogenic markers in addition to that of αSMA. Yip et al. evaluated the expression of osteonectin, osteocalcin, bone transcription factor core binding factor α1, and alkaline phosphatase activity of VICs cultured on substrates of varying stiffness in standard and

calcifying media (standard media supplemented with β-glycerophosphate, ascorbic acid and dexamathesone).[26] Interestingly, Monzack and Masters found that culturing VICs in mineralization medium caused an increase in calcific markers and decreased expression of myofibroblastic markers indicating that differentiation to the myofibroblast phenotype may not be required to reach a calcific cellular profile.[27]

Researchers postulate that VICs are activated from the relatively quiescent fibroblast phenotype to the activated myofibroblast phenotype by elevated matrix stiffness,[10] dynamic loading of the valve,[2,8,28,29] and elevated TGF-β1 levels[10] (Figure 2.4). However, how the factors integrate to regulate VIC activation in healthy and diseased valves remains controversial[28] and VIC responses to each of these stimuli are examined in this study.

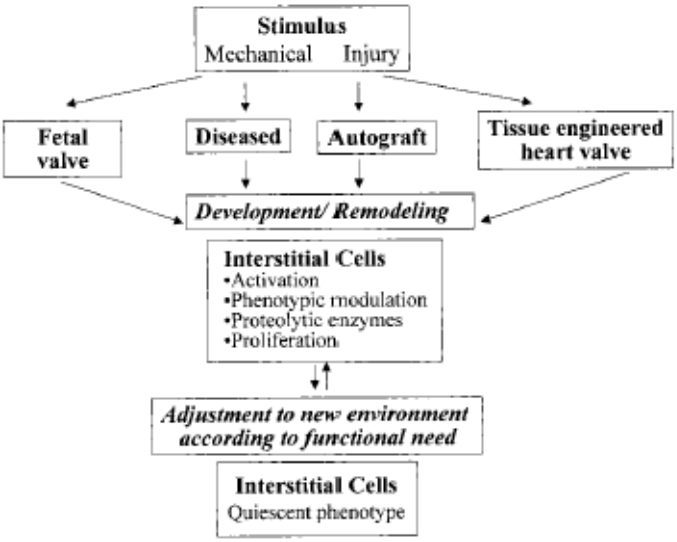

Figure 2.4. Valve interstitial cells respond to mechanical stimuli by making adjustments to the valve structure in order to return to a quiescent state.[8]

2.4. VICs are Sensitive to the Stiffness of Their Surrounding Environment

The phenotypic transition from fibroblast to myofibroblast is known to require mechanical tension, cellular fibronectin, and TGF-β1 (Figure 2.5).[30] Tension can be generated by the cell itself against a relatively stiff matrix or substrate (inside-out signaling) or by external loads and deformations that apply forces to the cell (outside-in signaling).[31] As the fibroblast transitions to the myofibroblast phenotype, stress fibers composed of cytoplasmic actin develop.[30] The myofibroblasts generate tension which results in contraction of the surrounding matrix.[30] Myofibroblast activation has primarily been studied by altering the stiffness of the environment as discussed below; studies of outside-in signaling will be described in the section 2.5.

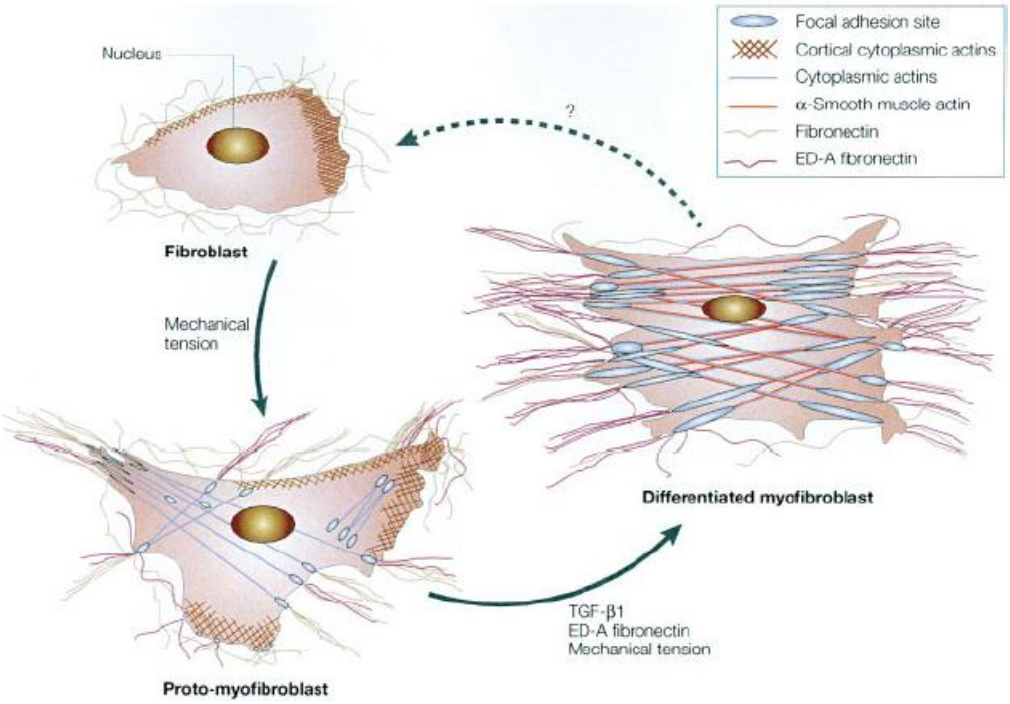

Figure 2.5. Proposed cycle of differentiation from fibroblast to myofibroblast.[32]

Fibroblast response to stiffness (tension) has been extensively studied *in vivo* in granulation and fibrotic tissues. Methods for altering stiffness *in vivo*, including wound splinting and release of pressure from a dermal wound bed by removal of fluid, have demonstrated that the myofibroblast phenotype is linked to mechanical tension.[33] The fibroblast-to-myofibroblast transition has been described *in vitro* on soft 2D gels (method described in detail in section 2.7.1) as well as within 3D gel matrices (biopolymer[34-36] and synthetic (reviewed by Tibbitt and Anseth[37])). Both 2D and 3D culture systems can be modified using chemical or mechanical methods to change the relative stiffness that the cells experience. Regardless of the culture system used, fibroblasts have been demonstrated to be sensitive to the stiffness of the culture environment as well as to biochemical stimulation. Biochemical stimulation can be mediated by ECM proteins attached to the surface of the gel to facilitate cell attachment, the protein composition of 3D biopolymer gels, or through the addition of exogenous cytokines to the culture system. Numerous other cell types have shown sensitivity to the stiffness of the culture environment including mesenchymal stem cells, which can be differentiated down specific lineages (neural, muscular, osteogenic) with defined stiffness levels.[38] A theoretical model that predicts stem cell stress fiber alignment and contractility in response to matrix rigidity has been developed demonstrating the importance of substrate mechanics in stem cell differentiation.[39]

VICs are fibroblast-like cells that demonstrate sensitivity to environmental stiffness cues. This phenomenon is observed when VICs are isolated from valve tissue and cultured *in*

vitro using standard cell culture techniques. Healthy valves are known to have few activated (αSMA expressing) cells (<1%, as reported by Pho et al.).[11] VICs isolated from freshly harvested heart valves are also minimally activated; however, culturing these cells on plastic significantly increases αSMA expression. Levels of VIC activation range from 20-65% when cultured on tissue culture-treated polystyrene (TCPS).[10,11] Substrate stiffness has been shown to affect cell proliferation. Yip et al. showed that VICs cultured on soft substrates in standard media proliferated more rapidly than those cultured on stiff substrates.[26] Tchumperlin et al. demonstrated an increase in cell proliferation with stiffness for primary and immortalized cell lines; however, two of the cell types appeared insensitive to stiffness with regard to proliferation.[40] Cells showed increased tractional forces with the addition of TGF-β1 but only at stiffness levels above the physiologic range,[41] suggesting a minimal stiffness level for cell responsiveness to TGF-β1. Given the variability in cellular proliferative responses and that TGF-β1 is an inhibitor of proliferation, combinatorial studies of various cell types and TGF-β1 concentration are required to determine the interactions between these two stimuli.

In addition to playing a role in VIC activation and proliferation, ECM stiffness has also been shown to be a co-factor in valve calcification. VICs cultured on unmodified TCPS expressed calcific markers (calcific nodule formation, alkaline phosphatase activity, and calcium accumulation) and the addition of TGF-β1 enhanced the expression of these markers.[42] Modifying TCPS surfaces with fibronectin or fibrin represses calcific marker expression and VICs cultured on soft PEG gels have repressed calcific marker expression

regardless of surface modification.[42] More recently, a dynamically modulated hydrogel system was used to demonstrate that the activation of VICs to the myofibroblast phenotype is reversible.[12,43]

Similar to fibroblast studies, 3D culture systems have also been used to evaluate the response of VICs to the stiffness of the culture environment. VICs cultured within stressed (stiff) attached gels in the presence of TGF-β1 are more contractile with increased αSMA expression compared to cells cultured within unstressed (compliant) free floating gels.[10] While this study demonstrates the importance of mechanical tension on VIC phenotype, the tension (stiffness) "perceived" by the cells was not quantified and the stiffness of the collagen gels was not measured or modulated.

Stiffness is a primary stimulus for activation of fibroblasts to the myofibroblast phenotype. Effects of stiffness on cell response have been studied for many cell types over a wide range of stiffness levels. Recently, several groups have described the response of VICs to several levels of substrate stiffness; further studies are required to fully characterize the response. Modification and control of stiffness in 2D culture systems is of relatively low complexity and numerous studies have documented cellular responses under these conditions. However, applying a defined tension level (stiffness) to cells cultured in a 3D culture system remains challenging.

2.5. VICs are Responsive to Dynamic Loading

The sensitivity of cells to dynamic stretch *in vitro* was first described by Leung et al.[44] who demonstrated altered protein production by smooth muscle cells that underwent equibiaxial cyclic stretch. Subsequent studies describe a wide range of cellular responses that are induced by stretch including cytoskeletal remodeling, ECM protein synthesis, and altered expression of many of genes.[45,46] The most visible effect of stretch is observed when cells reorient "away" from the direction of maximal cyclic stretch which is accompanied by pronounced remodeling of the actin cytoskeleton.[47,48] In a recent study, application of cyclic compressive stretch was shown to direct stem cell fate.[49] The magnitude and direction of the strain are also important in directing stem cell differentiation. Mesenchymal stem cells subjected to equibiaxial strain had decreased αSMA expression while stem cells subjected to uniaxial strain had increased αSMA expression.[50] A recent translational study that mechanical preconditioning of stem cells prior to implantation to cardiac infarcts had improved function within the heart.[51]

Heart valves undergo complex mechanical loading withstanding circumferential strains of 9-11% and radial strains of 13-25%. In diseased tissue, these values increase to >15% and 15-31% for circumferential and radial strains respectively.[52] The deformation (stretch) of the valve leaflets is related to the pressure the heart valve cusps experience.[53] The valves on the left side of the heart (aortic and mitral) experience higher transvalvular pressures and subsequently display increased expression of αSMA and heat shock protein 47 (surrogate for collagen) compared to cells isolated from the right side valves

(pulmonary, tricuspid)[5] indicating a role for valve leaflet deformation in VIC activation and collagen synthesis. αSMA expression in native (quiescent) VICs in intact valves is relatively low, suggesting that the surrounding ECM stress shields resident cells from cyclic mechanical loading during the cardiac cycle.[32]

Several *in vitro* and *ex vivo* studies have evaluated the effects of cyclic loading on isolated VICs using various stretching devices. Cyclic stretch is shown to induce dose dependent collagen expression in isolated VICs[14] and explanted valve tissue.[13] Using a Flexcell® system to apply stretch VICs stretched to 10-20% had increased collagen synthesis and interestingly mesenchymal stem cells stretched to 14% had similar collagen synthesis as VICs stretched to the same magnitude.[14] Further, compared to VICs cultured under 'normal' strains (10%), VICs cultured under 'pathological' strains (15%) exhibit stronger calcification response.[16] Interestingly, GAG content was decreased for stretched and statically incubated valves compared to freshly isolated valves.[13] αSMA expression increases in stretched leaflets and decreases in statically incubated leaflets compared to fresh leaflets.[13] Tissue-engineered (TE) heart valves are also sensitive to stretch, TE valves that undergo cyclic flexure have increased stiffness and collagen production; further, there is a positive linear relationship between the stiffness of the TE valves and the mean collagen concentration.[15]

Like many adherent cells, VICs are sensitive to the magnitude and duration of stretch. Understanding the role of stretch in VIC activation is especially important due to the complex mechanical environment of the heart. Further studies are required to characterize

the response to stretch in the presence of other stimuli.

2.6. VICs are Responsive to Stimulation by TGF-β1

TGF-β1 is a 25 kDa protein that has been studied extensively with regard to its role in wound repair. Many cells secrete and/or are responsive to exogenous TGF-β1. TGF-β1 in combination with intercellular tension is a known stimulus for the activation of VICs and other fibroblasts to the myofibroblast phenotype.[25,30,54] Plasma levels of healthy individuals and patients with aortic stenosis were 9.8 and 24.2 ng/mL respectively.[55] Another study found that plasma levels of TGF-β1 in control group were approximately 6 ng/mL while patients with liver or lung fibrosis were 20 and 25 ng/mL respectively.[56] Walker et al. found maximum response in VICs treated with 5 ng/mL TGF-β1.[10] Levels used for these studies were based on values found in literature however the local concentration of TGF-β1 exposed to the cell remains unclear.

Increased levels of TGF-β1 have been associated with aortic valve calcification and the promotion of VIC calcification via apoptosis.[57] *In vitro*, treatment of VIC culture with exogenous TGF-β1 initiates a cascade of events including cellular migration and aggregation, formation of apoptotic akaline phosphatase enriched nodules, and calcification of the apoptotic nodules.[57] Injuring a confluent monolayer of VICs by scratching the culture plate results in increased TGF-β1 and αSMA protein expression in cells at the wound edge.[54] Treatment of VICs with TGF-β1 increases stress fiber

formation and alignment. In addition, TGF-β1 enhances contractility and inhibits myofibroblast proliferation without increasing apoptosis.[10]

TGF-β1 is a potent regulator of VIC activation; however, the relationship between TGF-β1 and mechanical tension is still unclear and requires further investigation. Specifically to determine a threshold cellular tension that is required for VICs to be sensitive to TGF-β1. Numerous model systems have been developed to study the effects of mechanical stimulation on adherent cell culture, some of which will be discussed in the next section.

2.7. Model Systems for Controlling the Mechanical Environment of Cultured Cells

In vitro studies of cells, and VICs in particular, have resulted in many important findings regarding the significance of disease and the importance of the mechanical environment on cell function and signaling. Devices used to modulate the mechanics of the culture environment must be non-toxic and non-leaching if in contact with the cells. Materials must be able to withstand elevated temperatures and high levels of humidity which limits the use of powered devices within an incubator and a closed culture system is required to prevent bacterial contamination. Despite these constraints and limitations, many devices have been successfully developed for mechanical stimulation of isolated cells or explanted tissues during *in vitro* culture.

2.7.1. Methods for Changing Stiffness in 2D

Numerous systems have been developed to isolate and evaluate the effects of mechanical stimulation on cells and tissues and even control cell differentiation in a controlled environment (Review by DeForest and Anseth[58]). In early studies, cells were cultured on a thin film of polymerized silicone which was layered on an unpolymerized silicone substrate to evaluate the effects of tissue stiffness on cellular responses. The forces cells exert on the silicone were evaluated by observing the wrinkling of the thin polymerized silicone layer.[59] More recently, researchers have used polydimethyl siloxane (PDMS) to evaluate the effects of substrate stiffness on cells. The stiffness of the substrate can be modified by changing the ratio of polymer base to curing agent over a range of 48 to 1800 kPa.[60] The surface of the PDMS can be modified with proteins (covalently attached or passively absorbed to the surface) and the concentration of attached proteins is independent of stiffness.[60] A method has been developed for utilization of PA gels coupled with matrix proteins to evaluate the effects of a range of substrate stiffness levels on adherent cells (fibroblasts and endothelial cells)[61] which is now a widely accepted model system for mechanobiology studies.[62,63] When polymerized, PA is a clear, elastic gel and the stiffness of the gel is easily modified by changing the ratio of acrylamide to bis-acrylamide. PA gels are primarily used for protein separation, therefore they are inert and cells do not interact with the gel structure. PA gels require the conjugation of ECM proteins to the surface of the gels to facilitate cell adhesion. One method of covalently binding ECM proteins to the surface is with the UV activated heterobifunctional cross-

linker sulpho-SANPAH. Sulpho-SANPAH has been used to attach collagen,[64] fibrinogen, fibronectin, and polylysine to PA gel surfaces.[65] In our experience, monomeric collagen exhibits the best attachment. While cells are sensitive to both chemical and mechanical cues, a study that evaluated the effects of substrate stiffness and type and concentration of surface protein found that the cells were more sensitive to stiffness than protein type or concentration.[62] PA gel systems have been utilitized to measure focal adhesions (identified by immunostaining)[66] and traction forces exerted by the cell onto the PA gel surface by tracking the movements of fluorescent beads embedded in the gel.[66] These studies revealed that as the substrate stiffness increases, fibroblasts become more spread, have increased contractile forces, and have less motility.[61] Fluorescent labeling of focal adhesions revealed that cells cultured on stiff substrates had stable focal adhesions with normal morphology while cells cultured on soft substrates had highly dynamic focal adhesions with irregular morphology.[61]

Given the importance of cues from ECM proteins, researchers have developed gel systems made entirely of ECM proteins and other natural hydrogels to support cell culture in 2D or 3D culture systems. Proteins such as collagen, fibrin, laminin have been used for these studies (reviewed by Tibbitt and Anseth[37]). The stiffness of the matrices is controlled by altering the concentration of the protein. Since the entire gel is prepared from ECM proteins, the cells can interact with and migrate through the matrix. This makes these substrates less than ideal for cellular traction force measurements or cell morphology studies given the difficulties of imaging cells moving in 3D. In addition,

changing the concentration of ECM protein in the gel alters the biochemical profile presented to the cell. Polysacchrides such as alginate and agarose have also been used but require the addition of a cross-linker such as glutaraldehyde to maintain the gel structure.

Microfabrication techniques offer an alternative method for dictating the stiffness of a cell culture substrate such as modifying the stiffness cells "sense" by creating a surface with 3-10 μm diameter posts and by adjust the height of the posts, the perceived stiffness can be changed.[67]

2.7.2. Methods for Changing the Stiffness of the Culture Environment in 3D

Cell signaling and function in 2D matrices differ than those observed in 3D matrices (reviewed by Cukierman et al.[68]). Not only does cell morphology differ between 2D and 3D culture systems, but there are also differences in cells' biological responses to mechanical stimuli.[69] Forces applied to the cells differ greatly in 2D and 3D systems.[69] In 2D culture systems we can easily control cell density and have few "edge" or "interface" effects in the culture sytem. Conversely, in a 3D system, we can control cells/volume but it is difficult to control the distance between cells in a 3D culture system, particularly as the cells migrate through and remodel the 3D matrix. Elsdale and Bard first described the utilization of a 3D collagen matrix to support cell growth and noted that morphologies of cells encapsulated in the gels are similar to morphologies found *in vivo* during wound healing.[70] The gels are prepared as floating (free, zero tension) or anchored matrices

(fixed, infinite tension) to represent early and late stage wound healing respectively.[71] An alternative method of culture utilizes a culture force monitor (CFM) to apply tension to a cell-populated gel and measure the resulting contractile force as the cells generate tension across the gel during matrix remodeling.[34] In order to shield themselves from the strain applied by the CFM, fibroblasts residing in the collagen gels aligned to the direction of strain.[34] A similar method utilizes polyethylene bars attached to the cell populated gels and the gels are loaded by attaching free hanging weights onto the polyethylene bars.[72]

Controlling the tension across a cell-populated gel can have a large effect on the cellular responses. However, understanding the specific contributions of the material stiffness of the matrix and the cell generated tension within the matrix remains challenging. Additional studies are also required to discern the differences in cell-perceived tension applied through inside-out (stiffness) versus outside-in (stretching) methods. In the next section we review methods for applying stretch to cells.

2.7.3. Methods for Stretching Cells

Many custom devices, with a variety of different loading mechanisms, including uniaxial and biaxial stretch, bending, distention, compression, and shear stress have been described for the mechanical stimulation of cells (reviewed by Brown et al.[73]) Commercial devices are available such as Flexcell®, which uses vacuum pressure to stretch a circular silicone membrane over a fixed loading post (up to 20%), and STREX

which utilizes dual motors to stretch square or rectangular wells biaxially. Protein-coated silicone membranes are commonly used as dynamic (stretched) culture substrates due to their low cost, chemical inertness, and elastic properties. Silicone dynamic culture substrates have been used to study cellular mechanisms of stretch sensing as well as to model specific disease states such as ventilator injury.[74]

Another approach applies mechanical force to cells by binding magnetic beads to the actin cytoskeleton.[75] A magnetic field is applied causing oscillating torque to twist the beads and subsequently transfer the twisting motion to the actin cytoskeleton.[75]

Each method for stretching cells has strengths and limitations. Often precision is sacrificed in more high-throughput methods where populations rather than individual cells are studied. The devices described in this section have varying potential to be combined with other stimuli such as exogenous growth factors or culture substrate stiffness.

2.7.4. Methods for Combining Stiffness and Stretch

There are few studies that evaluate the combination of mechanical stimuli. Cells cultured on soft PA gels would move in response to the soft substrate being pulled or pushed with a pipette near front or rear edge of a cell[63] suggesting that cells can respond to tensile and compressive forces (strains) applied to relatively soft gels, however multiple combination of these stimuli were not evaluated. More recently, two approaches have been developed

for measuring the traction forces resulting from deformative forces applied to cells cultured on compliant substrates. Fredberg and colleagues stretched single cells on PA gels locally by pressing indentors around/next to the cells while simultaneously imaging (and subsequently measuring) the displacement of beads within the gels to quantify stretch and traction forces.[76] Other groups developed methods for stretching beds of compliant PDMS posts on which cells are cultured.[77,78] These short-term experiments, focus on changes in subcellular traction forces with time and further studies are required to understand the interactions between and cell sensing mechanisms for stretch and stiffness.

2.8. Rationale for Metrics Used in these Studies

For these studies αSMA expression was evaluated as it is the hallmark of the myofibroblast phenotype Methods for detection included immunofluorescent staining of individual cells to determine the organization of αSMA into stress fibers, Western Blotting for αSMA to semi-quantitatively determine expression levels, and immunohistochemistry to assess αSMA expression by cells within a 3D matrix. Cell area, perimeter and shape factor are used to describe cell morphology and relative amount of spreading. Cell morphology can be an indicator of cell fate; rounded cells are likely approaching apoptosis while flat, spread cells are in growth phase (Review by Ingber[79]). Traction force measurements and 3D gel contraction offer a functional snap-shot of cell

activation by measuring the force the cells exert onto the surrounding matrix. Mechanical testing of remodeled tissue is another functional measure of VIC remodeling.

2.9. Summary

In summary, it is clear that the behaviors of VICs, like other fibroblastic cells, are highly dependent upon biochemical cues and the mechanical environment in which they are cultured. Recent studies have demonstrated the importance of the mechanics of the culture environment on VICs. Specifically, the sensitivity to changes in this environment and reversal of the myofibroblast phenotype in response to stiffness,[12,43] which illuminated the pathobiology of heart valve disease. Ultimately, the rational design of TE heart valves and the development of effective treatments for heart valve disease will require more detailed mechanobiological studies to determine functional dependencies between combined levels of stiffness, stretch, and cytokines. In Chapter 3 we evaluate the effects of substrate stiffness and cytokine stimulation, specifically TGF-β1 on VIC activation to the myofibroblast phenotype.

Chapter 3 - Investigating the Role of Substrate Stiffness in the Persistence of Valvular Interstitial Cell Activation

Angela M. Throm Quinlan,[1,2] and Kristen L. Billiar[1,3]

[1]Department of Biomedical Engineering, Worcester Polytechnic Institute, Worcester, MA

[2]Graduate School of Biomedical Sciences, University of Massachusetts Medical School, Worcester, MA

[3]Department of Surgery, University of Massachusetts Medical School, Worcester, MA

The following chapter was accepted for publication in the Journal of Biomedical Materials Research, Part A on February 28, 2012. Additional sections have been added to the original publication as supplementary data.

3.1. Abstract

During heart valve remodeling, and in many disease states, VICs shift to an activated myofibroblast phenotype which is characterized by enhanced synthetic and contractile activity. Pronounced αSMA-containing stress fibers, the hallmark of activated myofibroblasts, are also observed in VICs cultured on stiff substrates especially in the presence of TGF-β1; however, the detailed relationship between stiffness and VIC phenotype has not been explored. The goal of this study was to characterize VIC activation as a function of substrate stiffness over a wide range of stiffness levels including that of diseased valves (stiff), normal valves (compliant), and hydrogels for heart valve tissue engineering (very soft). VICs obtained from porcine aortic valves were cultured on stiff tissue culture plastic to activate them, then cultured on collagen-coated PA substrates of predefined stiffness in a high-throughput culture system to examine the persistence of activation. Metrics extracted from regression analysis demonstrate that relative to a compliant substrate, stiff substrates result in higher cell numbers, more pronounced expression of αSMA-positive stress fibers, and a larger spread area which is in qualitative agreement with previous studies. Our data also indicate that VICs require a much lower substrate stiffness level to "deactivate" them than previously thought. The high sensitivity of VICs to substrate stiffness demonstrates the importance of the mechanical properties of materials used for valve repair or for engineering valve tissue.

3.2. Introduction

VICs are the primary cell type found in heart valves and are responsible for the maintenance and repair of valve structure. In healthy valves, a majority of VICs exhibit characteristics of normal fibroblasts.[8] However, in remodeling and disease states, when rapid matrix repair and remodeling are required, VICs express αSMA,[8,80] the defining immunological marker for the myofibroblast phenotype. Fibroblasts expressing αSMA-positive stress fibers have increased contractility,[81] and myofibroblasts exhibit increased matrix production and remodeling capabilities relative to quiescent fibroblasts.[8] These activities are necessary for successful restoration of tissue following injury, and a small percentage of myofibroblasts is necessary for maintenance of the structure of the leaflet.[24] However, excessive numbers of myofibroblasts are observed in pathological heart valve matrix remodeling,[80] occurring with stenosis,[7] myxomatous degeneration,[80] and fibrocontractive diseases. Understanding how to modulate VIC phenotype offers the potential for more effective treatment strategies for heart valve pathologies.

VIC activation (towards the myofibroblast phenotype) has been shown, directly or indirectly, to be regulated by environmental stimuli such as dynamic loading of the valve,[8,28] elevated levels of profibrotic cytokines (most notably TGF- β1;[10] and elevated matrix stiffness.[10-12] Even in healthy valves, VICs expressing αSMA are generally found near the outer edges of the fibrosa[82] and ventricularis.[28] These areas are relatively stiff, experience large stresses,[5,28,83] and are adjacent to the endothelium and blood stream which could contribute to cytokine stimulation; thus, it is difficult to parse out the

primary source(s) of VIC activation. The specific levels of the factors that regulate VIC activity and how they may interact in healthy and diseased valves remains poorly understood.[28]

In 2D *in vitro* studies, where fibroblasts (from various sources) are cultured on substrates of tunable stiffness (e.g. PA gels), the mechanical environment has clearly been shown to modulate a broad range of cell functions,[62,84] and sufficient substrate stiffness is necessary for fibroblast force generation and myofibroblast differentiation.[71] In light of the large body of literature demonstrating the importance of stiffness on fibroblasts-to-myofibroblast differentiation, it is surprising that the effects of stiffness on VIC phenotype have been largely overlooked until recently. Several *in vitro* studies clearly show that the percentage of VICs expressing myofibroblast characteristics is elevated on stiff 2D substrates relative to soft substrates.[10,11,85,86] However, only a few levels of stiffness over a limited range are utilized in these studies, thus critical levels of stiffness (thresholds for activation, saturation levels, etc.) and how different stimuli interact have not been elucidated. A notable exception is a recent study by Anseth and colleagues (2010) who cultured VICs on hydrogels with tunable stiffness gradients (7-32 kPa).[12] The authors found that VIC activation occurs on substrates with Young's modulus greater than or equal to about 15 kPa and also that, by reducing the gel stiffness from ~30 kPa to ~7 kPa, the cells could be deactivated as demonstrated by reduction in αSMA-positive stress fibers. These data represent an important step in identifying critical parameters for VIC sensitivity to stiffness; however, the range of stiffness is limited in this study, and

the cells were cultured at very high density. In high density monolayers, cells sense traction from neighboring cells which confounds the interpretation of stiffness-dependent results.[87,88] Further characterization of VIC responses to mechanical stimuli is needed for both understanding of disease progression and for proper selection and culture of replacement cells for disease therapeutics or tissue engineered valves.

To systematically evaluate the effects of stiffness on the persistence of the activated VIC phenotype, we utilized a novel high-throughput system allowing parallel culture of cells over a broad range of stiffness levels *in vitro*. There is no one single characteristic stiffness level of the native aortic valve due to the non-linear strain-, direction-, and location-dependent properties of the tissue.[89] Further, the valve has a tri-layered structure with relatively stiff fibrous outer layers surrounding a soft core. Therefore, the stiffness levels chosen for this study span a large range. Following pre-activation on stiff tissue culture plastic, VICs were cultured on eleven levels of PA gel stiffness over four orders of magnitude with and without exogenous TGF-β1. The isolated cells were cultured at low density to minimize physical and chemical interactions between adjacent cells. Collagen coated surfaces, high serum (15%), and exogenous TGF-β1 were utilized to push the VICs toward a fibrotic state. Cells were evaluated for spreading area, morphology, and the presence of αSMA-positive stress fibers. By studying the cellular response over a large range of stiffness levels and utilizing regression models, we are able to identify specific thresholds for the transition to the activated phenotype.

3.3. Methods

3.3.1. Substrate Preparation

Collagen-coated PA substrates were prepared based on standard protocols[65] adapted to a 96-well format as previously described[90] and generously donated by the Tschumperlin laboratory at the Harvard School for Public Health. Briefly, the wells of glass bottom 96-well plates were activated using 0.4% aqueous solution of *g*-methacryloxypropyltrimethoxysilane (Acros Organics) and PA gel solution consisting of 0.15% tetramethylethylenediamine (Biorad), 0.075% ammonium persulfate (Biorad), and acrylamide:bisacrylamide (Biorad) of varied ratio to control stiffness was applied to the center of each well. Coverslips (5 mm diameter) were made hydrophobic to prevent adhesion to the gels by treating with Surfacil (Pierce) and then rinsing with methanol. The coverslips were placed in each well until gel polymerization after which they were removed. Sulfosuccinimidyl 6 (4-azido-2-nitrophenyl-amino)hexanoate (Sulfo-SANPAH, Thermo Scientific) was applied to the surface of each gel and activated with UV light as previously described[61] and 100 μg/mL type I collagen (Purecol, Advanced Biomatrix) was applied to the surface of each gel and incubated for four hours at room temperature. Gels were rinsed with PBS and UV sterilized prior to cell seeding. Eleven substrate stiffness levels were prepared (n=8 per stiffness) ranging from 3%/0.04% (acrylamide/bis-acrylamide) to 12%/0.585% (for specific formulations and corresponding stiffness see Table 3.1). Glass substrates were used as positive (rigid) control.

Table 3.1. Polyacrylamide formulations and corresponding modulus values from AFM.

% Acrylamide	3.0	3.0	3.0	3.0	7.5	7.5	7.5	7.5	12	12	12
% Bisacrylamide	0.04	0.05	0.06	0.11	0.03	0.05	0.12	0.24	0.12	0.24	0.58
E (Hertzian, AFM, Pa)	150	300	600	1200	2400	4800	9600	19200	38400	76800	153600
Measured G' (Rheometer, Pa)	35	128	236	188*	909	2506	4670	9856	11130	20075	38985

*dataset contained significant outliers

3.3.2. Substrate Characterization

Stiffness of the substrates was determined using an atomic force microscope (AFM) and verified using macroscopic rheometric measurements. For AFM measurements, force-displacement curves were acquired (Asylum MFP 3D) with silicon nitride tips with 5 µm diameter borosilicate spheres and a nominal spring constant of 0.06 N/m. Prior to testing, the spring constant of the tip was measured using thermal calibration. The Young's Modulus (E) was calculated using Hertzian mechanics and a Poisson's ratio of ν=0.2 and is provided in Table 3.1.[61,91] The low Poisson's ratio is appropriate for the surface analysis (not bulk) as previously demonstrated.[92,93]

The bulk stiffness of the gels was confirmed by oscillatory shear rheometry using an AR-G2 rheometer (TA Instruments). The normal force was held at 1 N and the storage modulus (G') and loss modulus (G") were measured at a frequency of 1 Hz. One

measurement was made on each gel (n = 2) and values were averaged. As G" was over an order of magnitude lower than G', the gels were considered elastic.

3.3.3. Cell Culture

VICs were isolated from porcine hearts obtained from a local abattoir by standard methods.[94] The isolated VICs were cultured in standard medium (Dulbecco's Modified Eagle's Medium (DMEM), 100 U/mL penicillin G sodium, 100 μg/mL streptomycin sulfate, and 250 ng/mL amphotericin B supplemented with 15% fetal bovine serum (FBS, Hyclone)) at 37°C with 10% CO_2. VICs at passage 2-5 were used for all experiments (mixed cultures). High serum (15%) and stiff substrates (plastic) during passaging resulted in a high level of VIC activation. Activated VICs were seeded onto the PA substrates at a density of 2000 cells/cm^2 and cultured in standard media; in the TGF-β1+ group the media was supplemented with 5 ng/mL TGF-β1 (EMD).

3.3.4. Immunofluorescent Staining, Microscopy, and Image Analysis

After two days of culture, VICs were fixed and permeabilized on the PA substrates with a 5.3% formaldehyde (Ted Pella) and 4 μM Triton X-100 (Calbiochem) solution. The cells were blocked with a 1% bovine serum albumin (BSA, Sigma) solution in PBS, probed for αSMA with the clone 1A4 antibody (Sigma), and visualized with Alexa 546-conjugated

goat anti-mouse IgG (Invitrogen). Nuclei were visualized with Hoechst 33342 stain (Invitrogen). Cells were imaged with an epifluorescent microscope (Zeiss) with a charge-coupled device camera. Five images were acquired from each substrate (n = 3 per stiffness done in duplicate). The resulting images were analyzed using Image J for the area of αSMA expression per image. The number of cells per image, the percent of cells expressing αSMA in stress fibers, and the cell morphology were manually verified for each image. Cell morphology was visually assessed and each cell was identified as having a cubodial (round or square) or elongated (spindle-like with multiple extensions or fillipodia) morphology. Many cells stained positive for αSMA in their cytosol without αSMA organized into stress fibers, and stress fiber size and density varied between cells, thus a semi-quantitative scale was developed to characterize the extent of expression of αSMA in stress fibers; specifically, the number of αSMA-positive cells was manually counted and each cell was identified as having weak or pronounced expression of αSMA in stress fibers. “Weak expression” cells exhibited mostly cytosolic αSMA with some expression in stress fibers, and “pronounced expression” cells had highly pronounced expression and stress fibers were well defined. Examples of cells with “weak” and “pronounded” αSMA expression are shown in Figure 3.1.

In order to quantify αSMA protein expression in response to substrate stiffness via Western Blot, three formulations of larger format (22 mm diameter) PA gels (acrylamide/bis-acrylamide 8/0.02, 5/0.01, 8/0.08) were prepared as described above. VICs were seeded onto the gels as described above, cultured for seven days, and lysed

with a solution containing NP40 Lysis Buffer (Biosource), PMSF (Pierce), and Halt Protease Inhibitor (Pierce). The protein quantified using the BCA Protein Assay (Pierce). 10 µg of protein was added to each well of a 12% bis-acrylamide SDS page gel and protein was separated by electrophoresis. The protein was transferred to PVDF membrane via semi-dry transfer. The membrane was placed in a 5% milk in PBST block for 2 hours and probed with the αSMA (clone 1A4) antibody overnight at 4˚C. The antibody was removed and the membrane was washed with PBST buffer for 4-10 minutes washes. Anti IgG-alkaline phosphatase conjugated antibody (Sigma) was used for secondary detection and was incubated for 1 hour at room temperature. The membrane was washed 6 times for 10 minutes per wash and the signal was detected by chemiluminescence (Lumi-Phos WB chemiluminescent substrate for AP, Pierce), on the Geldoc (Biorad).

3.3.5. Traction Force Microscopy

Traction force microscopy was performed as described by Munevar.[95] Briefly, the deformation of the PA caused by cellular traction forces relative to the relaxed substrate was determined by the use of a pattern recognition algorithm. Large format (22 mm diameter) PA substrates were prepared as described above with the addition of 0.2 µm diameter Fluoresbrite® Yellow Green Microspheres (Polysciences) and were equilibrated in standard culture medium for ~30 min at 37° C. VICs were seeded onto the substrates

and cultured for 48 hours. Images of cells and substrate-embedded fluorescent beads were acquired with a Zeiss Axiovert fluorescent microscope equipped with a charge-coupled device camera. First, a phase contrast image of a single cell on the substrate was acquired, next the focal plane was lowered 5 μm and fluorescent images of the fluorescent microspheres suspended within the gels were imaged. A total of 10 cells were imaged per substrate. 10X trypsin was applied to the gels for 10 minutes in order to remove the cells from the substrate, the trypsin was removed leaving the original volume of fluid on the gels and the same location and focal plane of beads was imaged in the "relaxed" state (without the cell attached to the surface). All images were collected and processed for background subtraction by custom programs which measures the displacement of the beads within the gel and combined with the stiffness of the PA gel, the subcellular forces are calculated.[66,96,97] (Custom traction force computation software generously donated by Dr. Dembo of Boston University). Traction forces in the x- and y-direction were averaged over the area of the cell for n=3 cells per stiffess gel. Representative plots were output from the custom software.

3.3.6. Statistical Modeling and Analysis

For each metric (cell density, spread area, and αSMA expression), two-way analysis of variance (ANOVA) and non-linear regression analysis were performed using commercial statistical software (Sigmaplot 11.0, Systat Software Inc.). The two-way ANOVA

allowed for the determination of overall effects of stiffness and TGF-β1, and if significant differences were found, post-hoc analysis identified differences between individual groups via the Holm-Sidak method for pair-wise multiple comparison procedures with $p<0.05$ considered significant.

Regression analysis provides metrics for trends in the response of the cells as a function of stiffness including levels of stiffness where transitions occur between types of behavior (e.g., rounded vs. spread) and where saturation levels of each metric occur (e.g., maximum spreading area) allowing for comparison to other published studies as well as selecting stiffness levels for tissue engineering applications. Data from cells plated on the glass controls were excluded from models due to difference in surface chemistry from the PA gels.

All metrics (i.e., density (cells/mm^2), projected cell area (μm^2), percentage of αSMA-positive cells (%), and percentage of cells that have pronounced expression of αSMA organized in stress fibers (%)) increased monotonically from a baseline through a transition to a saturation level, thus a four-parameter sigmoid distribution was used to model each data set:

$$y = y_0 + \frac{a}{1 + e^{-\left(\frac{E-E_t}{b}\right)}}, \qquad \textit{Equation 3.1}$$

where y is the metric being analyzed, y_0 is the baseline level, a is the saturation level, b

indicates the steepness of the transition region, and E_t is the stiffness where transition occurs between the baseline and saturation levels. The units of y_0 and a match the metric being analyzed, and b and E_t have units of stiffness (Pa). In cases where the baseline parameter, y_0, resulted in over-parameterization, a three-parameter sigmoid distribution was utilized (i.e., y_0 set to zero). To investigate the dependence of αSMA expression on cell area, the values for area/cell and the fraction of pronounced αSMA-positive cells from both experiment runs were fit to a linear regression model and the correlation determined.

3.4. Results

3.4.1. Gel Stiffness

The Young's modulus of the gels ranged from 150 Pa to 154 kPa (Table 3.1); the values from AFM and rheological measurements were highly correlated (r^2=0.98). Stiffness values from AFM measurements were used in the tables and graphs below. VICs attached and spread on the PA gels in a stiffness-dependent manner, the spread-area and cell morphology over the range of 11 stiffness levels is shown in Figure 3.2. Diffuse staining for αSMA was ubiquitous and the extent of expression of αSMA was an important quantification metric in this study (Figure 3.1).

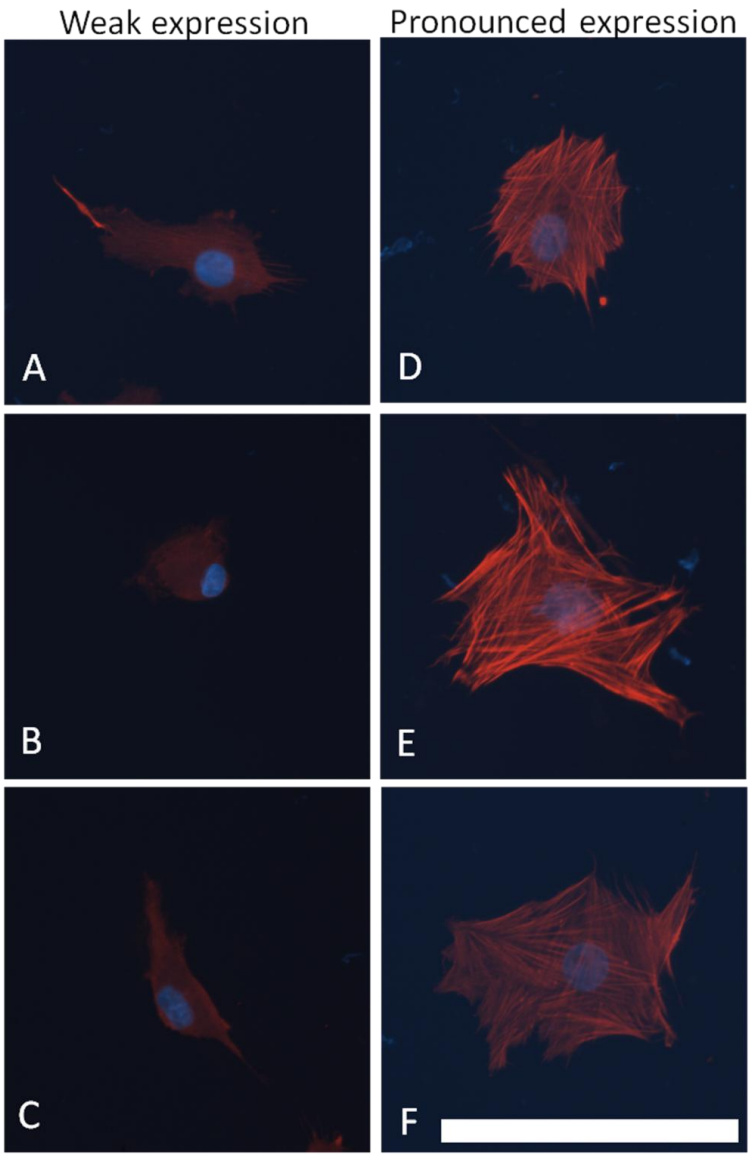

Figure 3.1. Cells with "weak" or "pronounced" expression of αSMA. "Weak expression" cells (A-C) exhibited mostly cytosolic αSMA with some expression in stress fibers, and "pronounced expression" cells (D-F) had highly pronounced expression and stress fibers were well defined. Scale bar is 100 µm.[98]

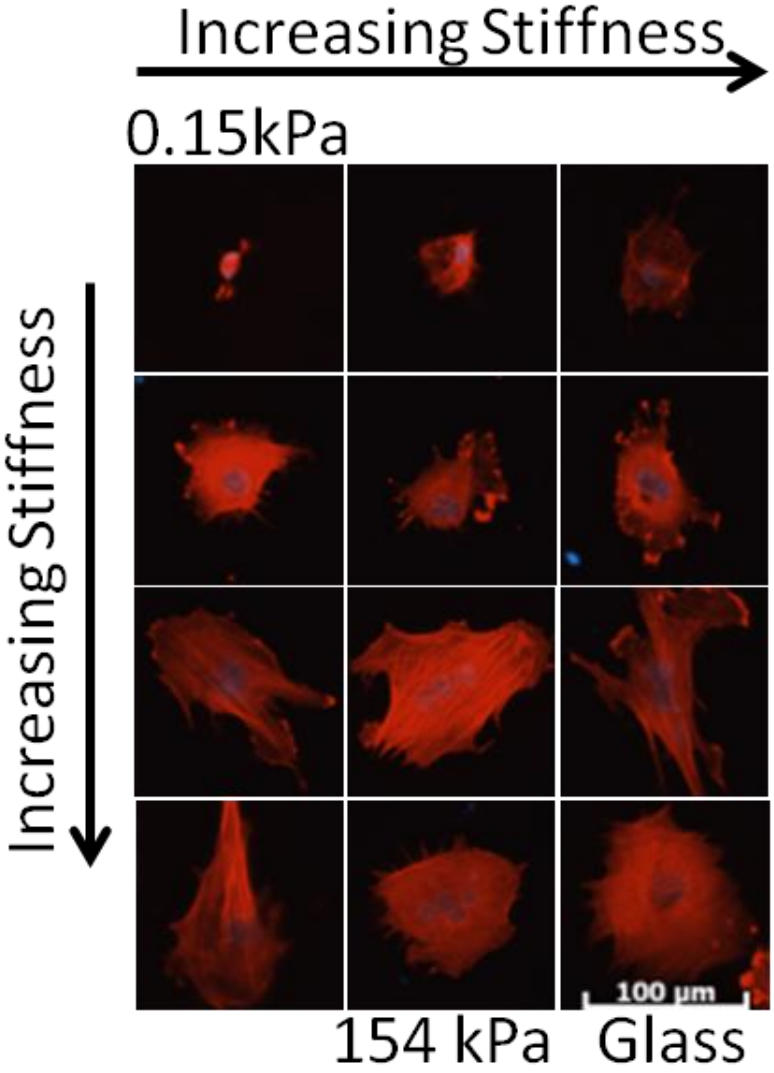

Figure 3.2. Substrate stiffness has a pronounced effect on VICs cultured on PA gels of increasing stiffness. VICs cultured on PA gels ranging 4 orders of magnitude in stiffness (0.15-150 kPa) plus glass with DMEM+15% FBS without TGF-β1 for two days. Cells were probed for αSMA (red) and nuclei (blue). Scale bar is 100 µm.[98]

3.4.2. Cell Culture

VICs were plated at a relatively low density to minimize cell-cell interactions and analysis focused on single cells. Figure 3.3 shows that adjacent cells (cells that are nearly touching each other) are more spread, have longer projections, and migrate towards each other demonstrating the importance of analyzing only individual cells in isolation, especially on soft substrates.

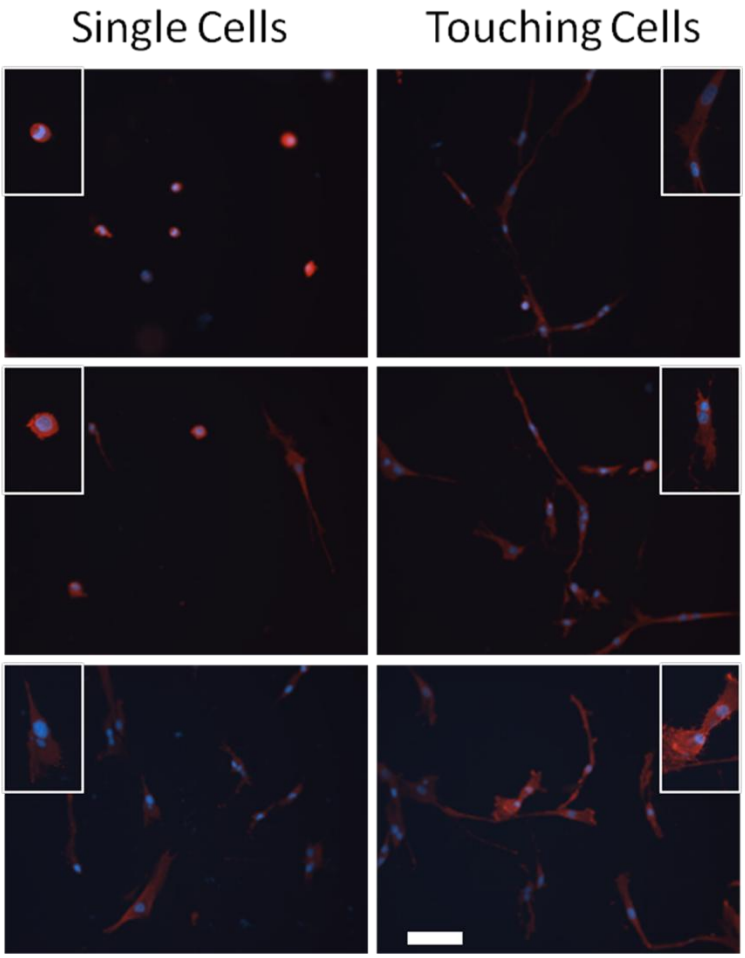

Figure 3.3. Cell-cell contact increases cell size and enhances cell projections. Three representative images of touching and non-touching cells are shown in this figure. Insets show detail of individual cells. Scale bar is 100 μm.[98]

3.4.3. Data Models

Data from both experimental runs are provided in Table 3.2 with statistically significant differences listed in Table 3.3. Statistical differences between stiffness levels (column headings) are indicated by the letters (corresponding metrics are listed below the table). For example, for area/cell, 150 Pa is only significantly different from 76.8 kPa and 154 kPa groups (designated by letters j and k). Data from the first experimental run are shown in the graphs; the trends in the second run were consistent with the first. The only substantial difference between runs was that the cell density of the second experimental run was roughly twice that of the first run. The variability between runs could be attributed to non-uniform cell adhesion across the substrate. The gel was homogenous across the center region but the ridge at the edge of the gel provided a topographical cue and in some samples this region had a higher cell density (only the homogenous center of the gel was included in the analysis). Differences between groups determined by the two-way ANOVA are provided in Table 3.3; however, in this study we focus on the trends more than statistical differences between specific groups since our goal is to describe the relationships between substrate stiffness and cell behaviors. All fits had an r^2 greater than 0.5 with an average r^2 for all fits of 0.8.

Table 3.2. Parameters from regression analysis: y0 is the baseline level, a is the saturation level, b indicates the steepness of the transition region, and Et is the stiffness where transition occurs between the baseline and saturation levels. The units of 'y0' and 'a' match the metric being analyzed, and b and Et have units of stiffness (Pa). In cases where the baseline parameter resulted in over-parameterization, a three-parameter sigmoid distribution was utilized (i.e., y0 set to zero).

Metric	TGF-β1	Run	a (units of metric)	b (Pa)	y_0 (units of metric)	E_t (Pa)	r^2
Cell Density (cells/mm^2)	-	1	41.8	99.2	N/A	181.1	0.72
		2	19.2	222.5		*	0.18
	+	1	39.8	441.0		191.6	0.76
		2	17.6	100.4		*	0.42
Cell Area (μm^2)	-	1	409	172	56645	1770	0.59
		2	2621	6305	*	1269	0.74
	+	1	966	176	917	1034	0.81
		2	3476	2489	*	350	0.83
Fraction αSMA+ stress fibers (%)	-	1	0.98	49.1	N/A	148.1	0.98
		2	0.81	114.1		3.70	0.75
	+	1	0.85	280.4		85.8	0.95
		2	0.76	370.0		80.8	0.89
Fraction pronounced αSMA+ stress fibers (%)	-	1	0.15	1215	N/A	2449	0.892
		2	0.33	2399		3416	0.88
	+	1	0.11	1307		2843	0.845
		2	0.36	603		1871	0.92

*value below lowest stiffness level

Table 3.3. Significance between groups from the two-way ANOVA; ($p<0.05$) by post hoc analysis.

Stiffness (Pa)	150	300	600	1200	2400	4800	9600	19.2k	38.4k	76.8k	154k
Area/cell	j,k	n.s.	n.s.	n.s.	n.s.	n.s.	n.s.	n.s.	n.s.	n.s.	n.s.
Pronounced αSMA	f,g,h,i,j,k	f,g,h,i,j,k	f,g,h,i,k	i,k	i,k	n.s.	n.s.	n.s.	n.s.	n.s.	n.s.
Cubodial	c,d,e,f,g,h,i,j,k	n.s.	n.s.	n.s.	n.s.	n.s.	n.s.	n.s.	n.s.	n.s.	n.s.
Density	d,e,f,g,h,i,j,k,	n.s.	n.s.	n.s.	n.s.	n.s.	n.s.	n.s.	n.s.	n.s.	n.s.
Fraction αSMA	c,d,e,f,g,h,i,j,k	n.s.	n.s.	n.s.	n.s.	n.s.	n.s.	n.s.	n.s.	n.s.	n.s.

TGF-β1 did not have a significant effect and values are not shown. No groups were significant in the percent elongated cells and are therefore not shown in the table.

Letters indicate stiffness levels where the response is statistically different than a given group;
c = 600, d = 1200, e = 2400, f = 4800, g = 9600, h = 19.2k, i = 38.4k, j = 76.8k, and k = 154k, n.s. = no significant differences

3.4.4. Cell Density

Cell density (number of cells per area) increased with substrate stiffness ($p<0.01$); the presence of 5 ng/mL exogenous TGF-β1 did not have a significant impact ($p>0.05$). The

softest gel (150 Pa) has significantly fewer cells than all levels greater than 600 Pa. The 300 Pa gel also has significantly fewer cells than the 4.8 kPa gel; however, even at the highest cell density, the cells were generally still sparse enough for single cell analysis. The three-parameter sigmoidal distribution fit the cell density data well (Figure 3.4) and identified a transition modulus of approximately 180 Pa and a saturation density of approximately 40 cells/mm^2 irrespective of the addition of 5 ng/mL TGF-β1. The cytokine decreased the slope of the curve in the low stiffness range (the *b* parameter was approximately four times greater in TGF-β1 group).

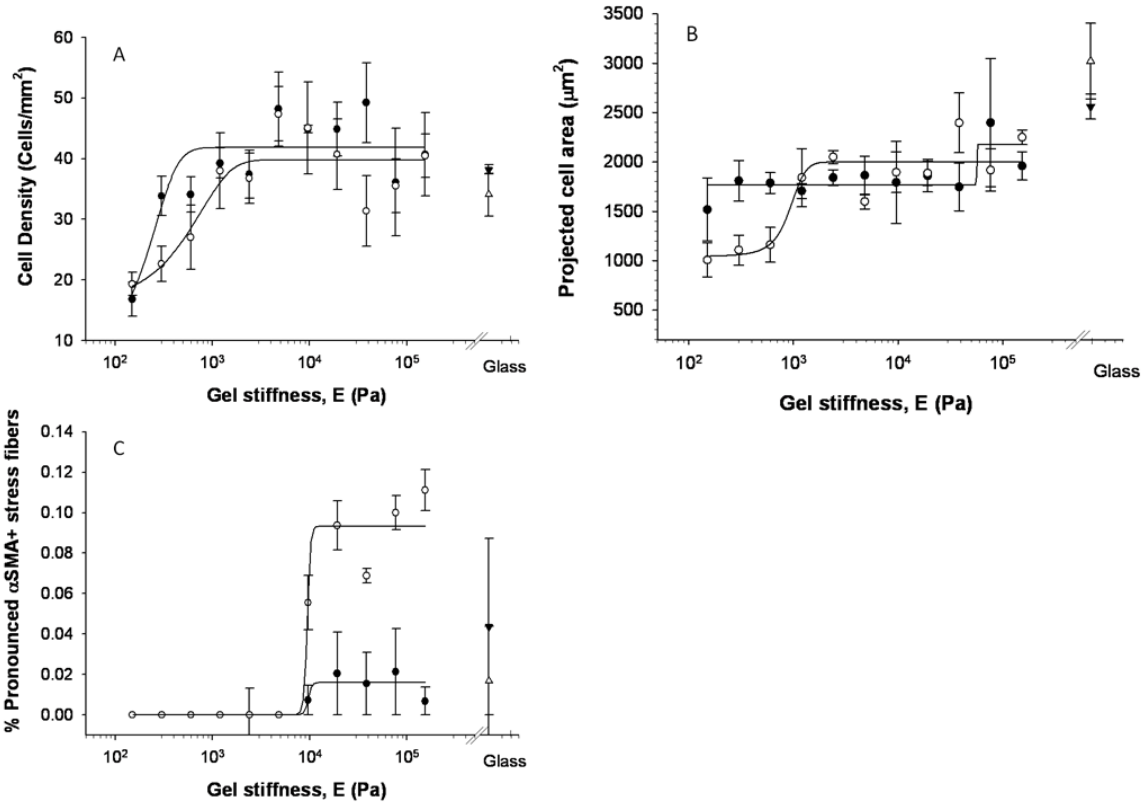

Figure 3.4. Regression analysis of VIC responses to substrate stiffness. Each point represents the average of 3 wells with SEM of cells cultured in standard (closed symbols) or TGF-β1 supplemented (open symbols) media.[98]

Increased cell spreading correlated with increased stiffness as shown in Figure 3.2 and Figure 3.4. The cell area was significantly different ($p<0.01$) for cells between stiffness levels; specifically, cells on the softest gel (150 Pa) had significantly smaller spread area than those on the two stiffest gels (76.8 and 154 kPa), but there was not a strong trend in cell area with stiffness. The addition of TGF-β1 produced a more pronounced trend with stiffness, although it did not have an overall statistically significant effect compared to the control group. As the trend without TGF-β1 was not strong ($r^2=0.56$ for the first run), the parameter values cannot be viewed as accurate and are thus not provided in Table 3.2. The data from TGF-β1 treated group were fit well by the model and provided a transition modulus of just under 1 kPa and a saturation level of approximately 1000 μm^2 for the first run.

3.4.5. Cell Morphology

The cell morphology was also significantly impacted by the stiffness of the substrate ($p<0.01$); the addition of TGF-β1 did not have a significant impact on the cell shape. Specifically, the fraction of cubodial cells on the softest (150 Pa) gels was significantly greater than all stiffness levels greater than 600 kPa (data not shown). The fraction of cuboidal cells decreases from 60% to 30% as stiffness increases with the form of an inverted sigmodial curve. There were few elongated cells on the low stiffness gels, a peak of elongated cells at an intermediate stiffness, and then slow decrease in numbers on the

high stiffness gels, but the differences were not statistically significant.

3.4.6. αSMA Expression

A portion of the VICs cultured on each stiffness level expressed at least a low level of αSMA (with the exception of the lowest stiffness, 150 Pa) (Figure 3.4). The fraction of cells positive for αSMA was significantly altered ($p<0.01$) with both stiffness and additional TGF-β1. Specifically, the softest gels had significantly lower fractions of αSMA-positive cells than gels with stiffness levels greater than 600 Pa. This trend was verified by immunoblot detection of αSMA (Figure 3.5), although additional studies are required to determine statistical significance. VICs cultured on 30 kPa gels express more αSMA (relative to tubulin) than those cultured on 10 kPa gels. VICs cultured on 75 kPa gels express roughly equivalent levels of αSMA as those cultured on 30 kPa gels. Dermal fibroblasts expressed slightly lower levels of αSMA compared to VICs cultured on 10 kPa substrates. Surprisingly, the presence of exogenous TGF-β1 significantly decreased the expression of αSMA overall ($p<0.01$) possibly due to high serum levels (see Discussion). The three-parameter sigmoid model fit the total fraction of cells positive for αSMA very well (r^2 values of 0.98 and 0.95 for standard media and TGF-β1+ groups, respectively). The transition modulus was somewhat smaller for the TGF-β1 treated group (86 Pa vs. 148 Pa) but the transition region for the TGF-β1 groups was more spread out with a lower saturation level (85% vs. 98%) occurring at a higher stiffness

level (~1.2 kPa vs. 300 Pa). On the stiffer gels, VICs exhibited pronounced staining for αSMA with highly aligned stress fibers. The fraction of cells with pronounced αSMA-positive stress fibers, a more appropriate metric for activation to the myofibroblast phenotype than diffuse αSMA staining, was significantly increased ($p<0.01$) with both stiffness and addition of TGF-β1 (Figure 3.4). Despite the statistical differences between control and TGF-β1+ groups, the fit parameters were similar for standard media and TGF-β1+ groups in both experimental runs with transition modulus ~2.4-2.8 kPa and a saturation level of 11 to 15% of the exhibiting pronounced αSMA expression. The percentage of cells with pronounced αSMA expression on glass was somewhat higher at 20 to 25%.

The cell size and amount of αSMA stress fibers were highly positively correlated; large cells had a high number of bright, highly aligned stress fibers (see Figure 3.1). Specifically, the area/cell and fraction of pronounced αSMA-positive cells were fit to a linear regression ($y=mx+b$) with similar slopes ($m=0.0001$ fraction with pronounced αSMA staining/μm^2 for both groups) and y-offsets (-0.1445 and -0.1891 for standard and TGF-β1 groups respectively). Good correlations were found for both standard media ($r^2= 0.74$) and TGF-β1 ($r^2= 0.82$) groups.

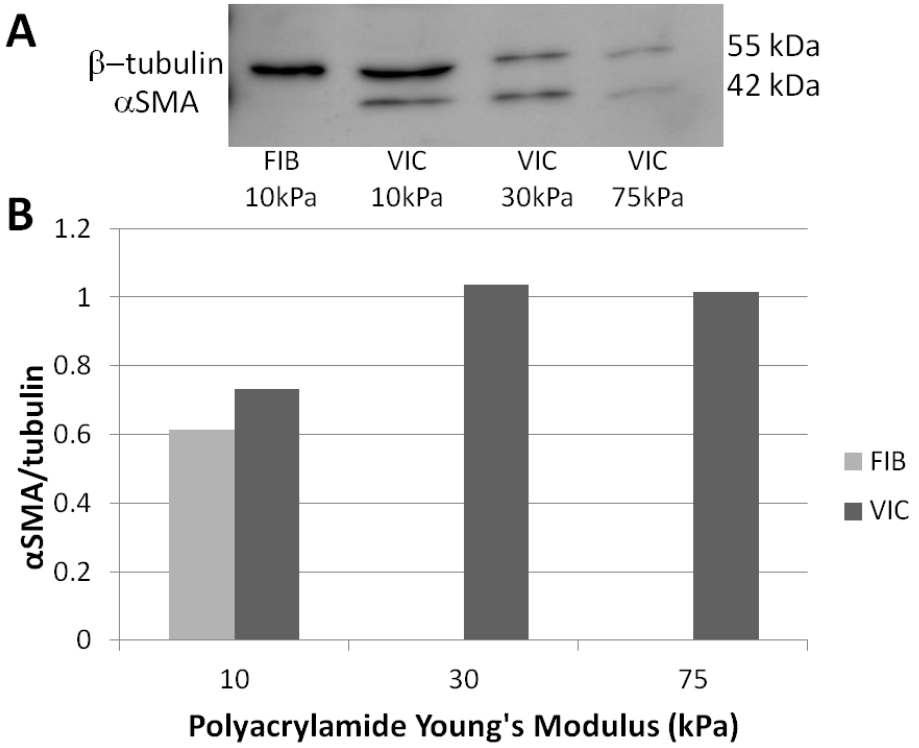

Figure 3.5. αSMA expression in response to substrate stiffness (A). Plots (B) represent cellular levels of αSMA normalized to tubulin (n=1). VICs and dermal fibroblasts (FIB) were cultured on 22 mm diameter PA gels for seven days.

3.4.7. VIC Traction Force

Larger traction forces were observed in cells plated on stiff 70 kPa gels than on soft 30 kPa gels ($p<0.05$) (Figure 3.6). Compared to dermal fibroblasts VICs tended to have smaller traction forces although the differences were not statistically significant. Similar to other published reports, standard deviations are very large.[63] Traction force microscopy was also attempted on softer (10 kPa) gels; however, reliable traction force maps were not achievable.

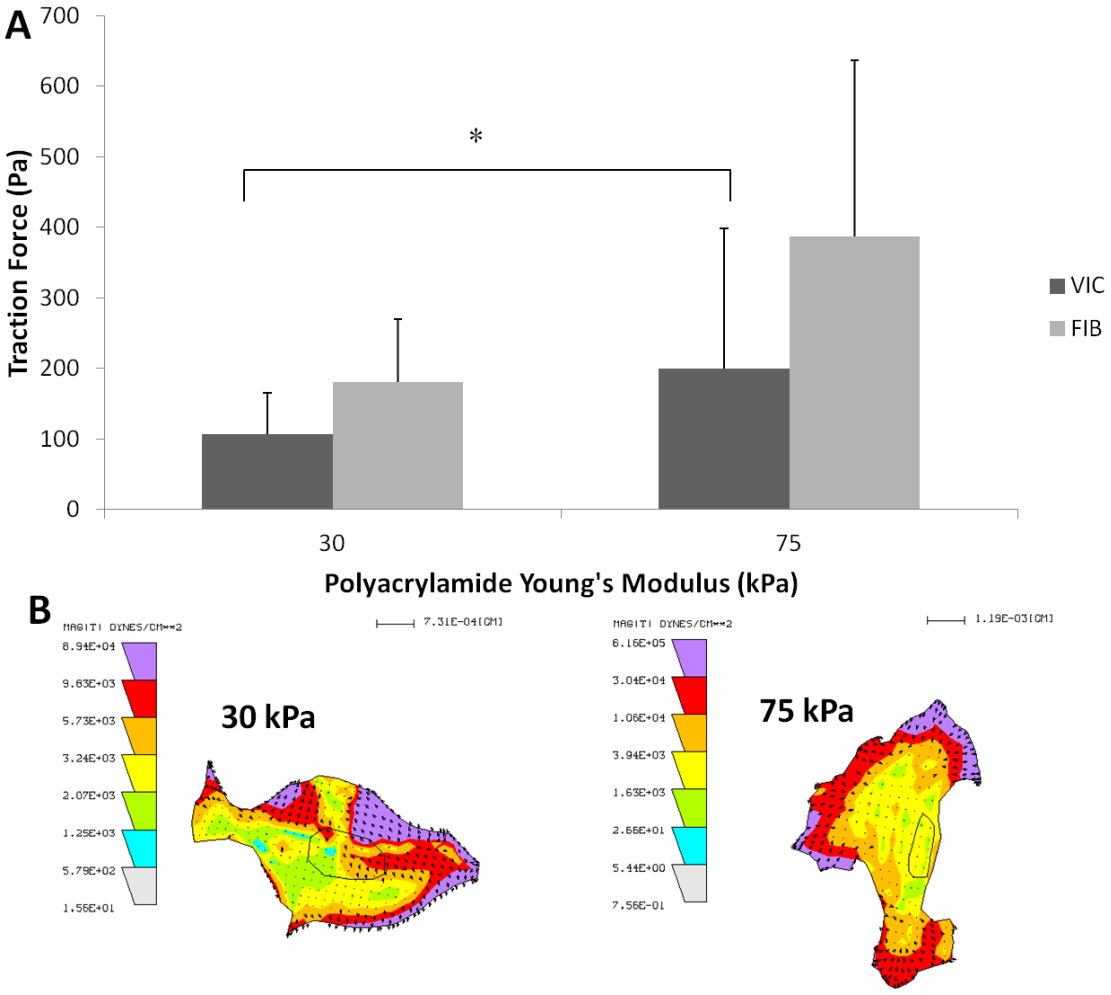

Figure 3.6. The traction forces exerted by individual cells on substrates were measured using an image correlation method. Images of fluorescent beads embedded within the substrate in the stressed and unstressed positions were used to obtain the bead displacement which, with the substrate stiffness was used to calculate the average traction in areas of significant traction forces. (n=10; * denotes p-value < 0.05).

3.5. Discussion

In this study, we analyzed the response of porcine aortic VICs to substrate stiffness over a wide range of levels using a high-throughput method. We found pronounced expression of αSMA (defined as organization of αSMA into stress fibers) above a threshold of approximately 2.5 kPa with and without 5 ng/mL TGF-β1 supplementation. Our data demonstrate that VIC activation (in the presence of 15% serum) is sensitive to a lower range of substrate stiffness levels than previous studies have demonstrated for both VICs[12] and other fibroblastic cells[81,99] in terms of αSMA expression and organization, cell density, size, and morphology. The high sensitivity of VICs to substrate stiffness demonstrates the importance of mechanical properties of materials used for valve repair or for engineering valve tissue. The data presented herein can be used as a reference for culturing VICs *in vitro* and for the design of tissue engineered valves.

3.5.1. High-Throughput, Low Density, Interaction Study

A high-throughput approach was utilized to facilitate assessment of the effects of a large range of stiffness levels encompassing soft glycosaminoglycans characteristic of spongiosa, fibrotic (myofibroblast-populated) tissue,[99] and osteogenic substrates which potentiate calcific deposits[26] characteristic of heart valve disease.[99,100] Gel stiffness levels chosen for this study range from those similar to hydrogels used for tissue engineered valves (E ~ 100 Pa, estimated from rheometric measurements of shear modulus)[101] to

values well above those calculated immediately prior to valve damage and/or failure of native and tissue engineered valves.[102] Biaxial mechanical characterization of porcine heart valve leaflets found the modulus to range from 30-150 kPa depending on the direction of extension(radial or circumferential) and the strain level.[89] The stiffness of (thawed) cryopreserved human valve leaflets (E ~ 1.7 kPa)[103] is in the mid-range of stiffness values tested in this study.

The large number of stiffness levels allows thresholds to be determined quantitatively with and without the soluble factor TGF-β1, an important regulator of the myofibroblast phenotype. In order to minimize the effects of cell-cell signaling and elucidate the cellular responses to substrate rigidity, we cultured the VICs at a low density, allowing for analysis of single cell behavior. Cellular interaction causes cells to modify their shape and αSMA expression as shown in the images of "touching" and "non-touching" cells in Figure 3.3.

Matrix stiffness may also affect cell proliferation resulting in changes in cell density. The effect of matrix molecules bound to the substrates on VIC attachment has been studied extensively,[25,104,105] yet the effects of matrix stiffness on VIC proliferation have largely been ignored. Proliferation may be beneficial in certain applications (e.g., populating an acellular scaffold), yet excessive proliferation can be detrimental to tissue development (i.e., production of ECM to replace a degrading scaffold). We found that cell density increased with stiffness until it saturated between 10 kPa and 20 kPa. Interestingly, cell density observed on the glass control is lower than that observed for cells on the stiff PA

gels, whereas, the majority of other metrics evaluated in this study (cell spread area and percentage of cells with pronounced αSMA expression) saturate towards the level observed on the glass control. Similar findings were reported by Chen et al.[106] where MSCs cultured on fibronectin-coated PA gels exhibited maximum proliferation when cultured on gels with stiffness of 10 kPa when compared to higher or lower stiffness ranges.

3.5.2. Cell Area, Morphology, and Forces

Changes in cell area and morphology are readily visible indicators of changes in cytoskeletal organization and focal adhesions,[61] and control of cell shape can itself modulate cell function.[107] In a recent study by Liu et al.,[108] six distinct VIC morphologies were identified. The different morphologies have different cell motility and cell matrix interactions, and all morphologies showed variable amount of αSMA. We chose to categorize the phenotypes into two categories based on cell morphology: cubodial cells were more round or square in appearance with few, if any extensions; elongated cells were bipolar or had many extensions.

In our study, VICs on the lower stiffness gels remained small and rounded, and as the stiffness level increases VICs exhibit not only greater area but also more extensions and fillapodia. In a study by Engler et al.[62] a similar increase in projected cell area with stiffness was found, albeit over a smaller range of stiffness (1-40 kPa with 3 or 4 levels of

stiffness). The authors fit the response to a hyperbolic function and a power law; we utilized a sigmoidal model to recapitulate the baseline response transitioning through an intermediate region, and saturating at higher stiffness levels observed for TGF-β1-treated VICs over broad stiffness range studied herein (Figure 3.4b). We do not attempt to assign any physiologic significance to the parameters, although the E_t parameter is especially useful for quantifying the transition between what the cell type "feels" as "soft" ($E<E_t$) or "stiff" ($E>E_t$). Figure 3.6 shows representative plots of the average traction forces across the cell. These forces are a functional measure of VIC activation to the myofibroblast phenotype. Cellular traction forces are increased during migration and the highest forces are co-localized with the leading- and tail-end of the cell.[109] Generally, rounded cells have lower tractional forces as they have fewer focal adhesions to the culture substrate.

3.5.3. αSMA Expression and Localization

Expression of the contractile protein αSMA is the primary indicator of the myofibroblast phenotype[8,80] and the organization of αSMA into stress fibers has been correlated with increased myofibroblast contractility.[81] The threshold stiffness level for the appearance of αSMA-positive stress fibers in this study is lower than previously reported for both VIC (~15 kPa)[12] and fibroblast activation (16-20 kPa).[81,99] The *in vivo* the ECM threshold stiffness required for the presence of αSMA in stress fibers appears to be ~20 kPa for rat wound granulation tissue.[99] However, in previous studies, limited ranges and numbers of

levels of stiffness have been utilized and relatively simplistic measures of stiffness employed, thus precise thresholds are difficult to determine from previous data. Compared to a recent study with a transition stiffness of roughly above 7 kPa,[12] we found the transition stiffness is somewhat lower (4.80 kPa to 9.60 kPa) for all groups and stress fibers were seen on relatively soft substrates. Further, our preliminary data with fibroblasts indicate that VICs may have a lower set-point for activation with regard to stiffness; VICs expressed more αSMA when cultured on soft PA gels when compared to dermal fibroblasts (Figure 3.5). Additional studies are required to determine statistical significance of αSMA expression between stiffness levels and cell types. In these studies we normalized αSMA expression to β-tubulin, a microtubule protein. However, since β-tubulin is a structural protein which are often affected by changes in the mechanical environment we recommend the use of other reference proteins not directly involved in the transfer of forces across the cell for future studies such as GAPDH or anti-histone H1.[110]

Interestingly, despite having greater expression of αSMA, VICs had lower traction forces compared to dermal fibroblasts. Since traction force measurements produce relatively high standard deviations,[63,97] further experiments are required to compare the traction forces of VICs and fibroblasts. We are the first to report the traction forces of VICs on a 2D gel surface; however, utilizing a culture force monitor, Smith and colleagues observed 34% variability of contraction forces produced by VICs in 3D culture.[111]

3.5.4. TGF-β1 and Serum Levels

It is widely accepted that myofibroblasts are regulated by profibrotic cytokines, most notably TGF-β1, which can be secreted by endothelial cells or the VICs themselves during repair of damaged valves or diseases affecting the valve tissue.[112] Previous studies have shown that VICs cultured in the presence of exogenous TGF-β1 concentrations ranging from 0 to 5 ng/mL had increased αSMA expression with increased TGF-β1 concentration.[10,25] Further, TGF-β1 has been shown to interact with mechanical stimuli in the stimulation of myofibroblast activation.[71] It is hypothesized that a minimal stiffness (tension) is required for the activation of latent TGF-β1.[81] A single level (5 ng/mL) was chosen for this study to maximize VIC activation based on previous work by Walker et al.[10] In general, we observe few differences with the addition of exogenous TGF-β1, indicating that under these specific culture conditions, VIC phenotype is more sensitive to environmental stiffness than exogenous TGF-β1. This finding adds to the controversy of the role of TGF-β1 in VIC activation.

The relatively low stiffness threshold for VIC activation may also be due, in part, to the high level of serum (15%) chosen to stimulate the cells; at this level, TGF-β1 actually inhibited some metrics of the myofibroblast phenotype. In a previous study, VICs were cultured in 15% serum allowing for cells to attach and undergo the cell cycle and then cultured in low serum (1%) during experimentation to minimize cell proliferation.[12] Another study showed that serum concentrations from 1 to 15% had no effect on αSMA

expression.[25] The VICs used in this study were not serum starved, prior to addition of TGF-β1. The lack of additional response to 5 ng/mL supplemental TGF-β1 could also be explained by the TGF-β1 in the serum or autocrine production of TGF-β1 by the VICs.

3.5.5. Matrix Molecules

In addition, the choice of matrix proteins bound to the surface also has an effect on VIC phenotype; VICs cultured on collagen-coated surfaces have been shown to express decreased levels of αSMA (compared to fibronectin and heparin).[25] Other matrix proteins such as fibronectin and heparin have TGF-β1 binding interactions, which were found to increase VIC αSMA expression.[25] Cell phenotype is clearly regulated by both matrix composition and mechanical properties (and combinations of these).[62,113] As our main focus was to assess effects of graded stiffness levels and interaction with a soluble factor (TGF-β1), we chose to use a single concentration of a single ubiquitous ECM protein (collagen) to reduce the number of variables. Type I collagen was chosen as the attachment protein as it is the most prominent matrix component of the native valve and has been used extensively in PA gel studies.[61] Previous studies have shown that collagen density does not vary with PA gel concentration and thus stiffness.[61]

3.5.6. Limitations

Evaluating other markers in combination with αSMA expression could perhaps reduce the variability attributed to VIC phenotype as well as provide additional insight on the role of matrix stiffness in the progression of valve disease. Other cellular markers correlating with VIC activation are vimentin, matrix-metalloproteinase-13/collagenase-3 and sMemb (combined with expression of αSMA).[8] Recent studies of VICs have also investigated pathological markers associated with valve disease such as cofilin expression[11] or calcification markers.[26] In the study by Yip et al., calcific markers were observed in VICs cultured on all stiffness levels tested in the presence of osteogenic media (standard media supplemented with β-glycerophosphate, ascorbic acid and dexamathesone).[26] VICs cultured on substrates of varying stiffness in standard media did not express calcific markers[26] thus we did not expect to observe calcific markers. We recommend that in future studies, evaluation of calcific markers should be included in the experimental design.

The sensitivity of VICs to passaging could also be a possible explanation for lower activation stiffness levels than previously found and for differences between runs. To obtain the large number of cells analyzed in this study, passage 2-5 (mixed populations) VICs were used. The trends for the two experimental runs were similar, yet there was notable variation within and between groups for most metrics. As with most published studies, the VICs were passaged on tissue culture plastic prior to seeding on PA. Previous studies showed that αSMA decreases with passage number (on tissue culture plastic)[25].

While freshly isolated VICs more closely replicate *in vivo* behavior, ultimately, VICs will require passaging to obtain enough cells for large-scale studies and tissue engineering applications.

Finally, this study focuses on cellular responses to substrate rigidity in a 2D system, allowing for isolation of two specific stimuli (TGF-β1 supplementation and substrate stiffness), providing the foundational information necessary for more complex studies, such as evaluating dynamic changes in stiffness and more *in vivo*-like 3D environments. Recently, researchers have developed methods to reduce the stiffness of 2D gel culture systems using photodegradable hydrogels[12,114] allowing for real-time observations of changes in cellular response to its surrounding mechanical environment. Data from the latter study indicate that activated VICs can be deactivated to quiescent cells by decreasing the stiffness of the culture substrate below ~7 kPa;[12] this value is somewhat higher but within the range of the 2.5 kPa transition modulus we observe for VIC activation. However, the stiffness required for reversal (as observed in the 2D experiments) may differ in a 3D model system, further necessitating studies in 3D systems that build off the results observed here and in the stiffness reversal studies. Further, the absolute stiffness magnitude that produces specific cell behaviors (e.g., spreading) may be orders of magnitude different in 3D tissues compared to 2D culture,[69] thus it is imperative to move to 3D models for future studies. We have recently published on the effects of stiffness in a novel 3D system.[115] The data presented herein can be used in the design of future, 3D studies with regards to transition or saturation stiffness levels

for VIC activation.

3.5.7. Summary

This study builds on previous research on the modulation of VIC phenotype by the mechanical and chemical properties of the culture environment. We examine the phenotypic response of VICs to substrate stiffness ranging over four orders of magnitude encompassing immature to fibrotic tissue with and without exogenous TGF-β1. The 96-well, high-throughput approach facilitated the evaluation of VIC responses to gel stiffness in a highly parallel manner over a wide range of levels and allowed the identification of trends in the data such as threshold stiffness levels and saturation points - analysis not previously possible with a small number of stiffness levels. The high-throughput method should be extended to study interactions with soluble factors (cytokines, serum) and bound matrix molecules, which likely alter important stiffness threshold levels.

Although myofibroblasts have desirable ECM synthesis characteristics for injury repair and initial generation of matrix for tissue engineering applications, excessive numbers of highly activated VICs are implicated in fibrocontractive disease states[80] and should likely be avoided for heart valve engineering. However, utilizing materials with lower than 2.5 kPa stiffness may be problematic as fibroblastic cells form cell aggregates on materials of this low stiffness,[87] and scaffolds below this threshold stiffness would deform excessively

under the physiological loading, characteristics that are non-desirable for a biomaterial scaffold. These factors indicate that cultured VICs may not be an appropriate cell type for tissue engineering of valves if quiescent (non-myofibroblast) cells are desired to minimize neofibrotic behavior.

3.6. Acknowledgements

The authors would like to thank Justin Mih and Dan Tschumperlin, PhD of Harvard School of Public Health for preparing the PA gels. We thank Bhavika Shah and Stephan Koehler, PhD for performing rheological measurements and Laura Firstenberg for assisting with validation of the gels. The authors would also like to thank Dr. Dembo of Boston University for the generous donation of the LIBTRC traction force software. This project was supported in part by American Heart Association grant SDG 0535265N (KLB) and National Institutes of Health grant 1R15HL087257 (KLB).

Chapter 4 - Boundary stiffness regulates fibroblast behavior in collagen gels.

Jeffrey John[1], Angela Throm Quinlan[1,2], Chiara Silvestri[3], and Kristen Billiar[1,4]

[1]Department of Biomedical Engineering, Worcester Polytechnic Institute, 100 Institute Road, Worcester, MA 01609, USA

[2]Graduate School of Biomedical Sciences, University of Massachusetts Medical School, Worcester, MA 01655, USA

[3]Department of Civil Engineering, Worcester Polytechnic Institute, Worcester, MA 01609, USA

[4]Department of Surgery, University of Massachusetts Medical School, Worcester, MA 01655, USA

The following chapter was accepted for publication in the Annals of Biomedical Engineering on November 20, 2009. Only portions of the full publication are included in this chapter and additional sections have been added as supplementary data.

4.1. Abstract

Numerous studies have examined cellular migration, interactions, and behaviors within a 3D matrix. Fibroblasts cultured in 3D collagen gels exhibit morphologies similar to those observed *in vivo*. In addition, the methods for culturing the cell-populated gels can induce cellular behaviors similar to those observed in wound healing. Restrained gels, left attached to the culture dish mimic granulation tissue and free gels, released from culture dishes shortly after preparation, mimic normal dermis. This chapter describes a novel device for applying controlled, intermediate levels of boundary stiffness to cell-populated collagen gels and provides preliminary data demonstrating the devices' use and efficacy. Results demonstrate that increasing boundary stiffness resulted in increased cellular contractile forces, αSMA expression, and gel (material) stiffness. We present this novel device and methods for applying predefined boundary stiffness to cell-populated gels; a useful tool for studying cellular response to environmental stiffness important in studying wound healing, tissue mechanics and tissue engineering.

4.2. Introduction

Traditional 2D culture systems have been instrumental in studies of cellular mechanobiology. Natural and synthetic culture substrates have been used to examine the role of substrate stiffness in cell motility, differentiation, and numerous other cell functions.(review by Disher, Jamney, and Wang, 2005)[31] 2D substrates provide a simplistic means of evaluating cellular contraction and migration by limiting cellular movements to the surface of the gels. The fibroblasts cultured on 2D substrates, however, exhibit a flattened morphology, unlike spindle or stellate morphologies observed *in vivo*. 3D culture matrices were developed to overcome limitations of 2D culture systems and to provide cells with a more *in vivo*-like environment.

Numerous 3D culture systems have been used to study cellular migration and interactions with a 3D matrix. Synthetic materials used for 3D gel systems include polyethylene glycol (PEG), polyvinyl alcohol (PVA), and acrylates along with many other polymers. These synthetic gels can be engineered to have specific stiffness, porosities, and water content but cannot mimic the biochemical environment of natural tissues. Other groups have utilized natural polymers such as collagen, fibrin, gelatin, alginate, chitosan or combinations of natural and/or synthetic polymers. For this study we focus on collagen gels as collagen is the main structural protein in many fibrous tissues. We also focus on fibroblast and fibroblast-like cells because, as discussed in Chapter 2, they are especially sensitive to changes in environmental stiffness and are integral to fibrosis and wound healing. Further, fibroblasts differentiated into αSMA expressing myofibroblasts are

present in granulation tissue during wound contraction and *de novo* collagen synthesis.

Fibroblasts cultured in a 3D cell-populated collagen gel had morphologies similar to connective tissue fibroblasts observed *in vivo*.[70] Additionally, differences were noted in cell behavior when the gels were restrained (attached to culture dishes) or free (released from culture dishes).[70] This study and others have shown that without attachment to a culture dish, the collagen matrix compacts inward with a significant reduction in diameter (review by Grinnell and Petroll).[116]

The compaction of the matrix is a result of fibroblast remodeling; if the boundary is fixed, cells orient the collagen fibers parallel to the direction of the restraint causing tension to develop in the matrix.[36] In contrast, if the collagen matrix is released from the culture dish (free floating) the cells do not orient the collagen fibrils in a specific direction and no tension develops in the matrix.[36] These two distinct culture systems have been used to study wound healing; tension-free (free floating) gels mimics normal dermal tissue and restrained (fixed boundary) gels mimic granulation tissue.[117]

Here we present a mechanical method for controlling the boundary stiffness of fibroblast and VIC-populated collagen matrices and subsequently the effective stiffness local to the cells. These methods allow for the study of cellular behavior at intermediate level boundary stiffness levels when previous studies have only compared free or fixed boundaries.

4.3. Methods

4.3.1. Device Principle

The device used to culture cell-populated collagen gels under controlled boundary tension is originally described by John et al.[115] The cell-populated collagen gel is cast into four porous anchors and the boundary stiffness is controlled by thin vertical cantilever beams (attached to the porous anchors) acting as springs of various tension levels (Figure 4.1).

The culture devices are easily constructed from low cost materials and can withstand multiple autoclave cycles. The inertness of the materials allows for extended culture duration. The frame of the device is constructed from high density polyethylene (HDPE) (McMaster Carr Inc.). The diameter of the stainless steel cantilever beams (Small Parts, Inc.) dictates the boundary stiffness (spring stiffness) applied to the gel and is calculated from the equation for bending of a cantilever beam:

$$K = 3 \cdot \frac{EI}{L^3} \qquad \textit{Equation 4.1}$$

where K is the spring constant (N/m), E is the Young's modulus of the beam (Pa), L is the length of the beam (m), and I is the moment of inertia (m^4) given by $\pi r^4/4$ for a beam of circular cross section, where r is the radius of the beam (m).

The stiffness of the beam is a fourth-order function of its radius and spring stiffness and is related to the beam diameter. The stainless steel beams were calibrated by fixing one

end of the beam and placing the free end on a digital electronic balance.[115] The fixed end was displaced downward with a screw gauge micrometer and the resulting force was measured with the electronic balance. The K values were calculated from the force-displacement curve by linear regression.

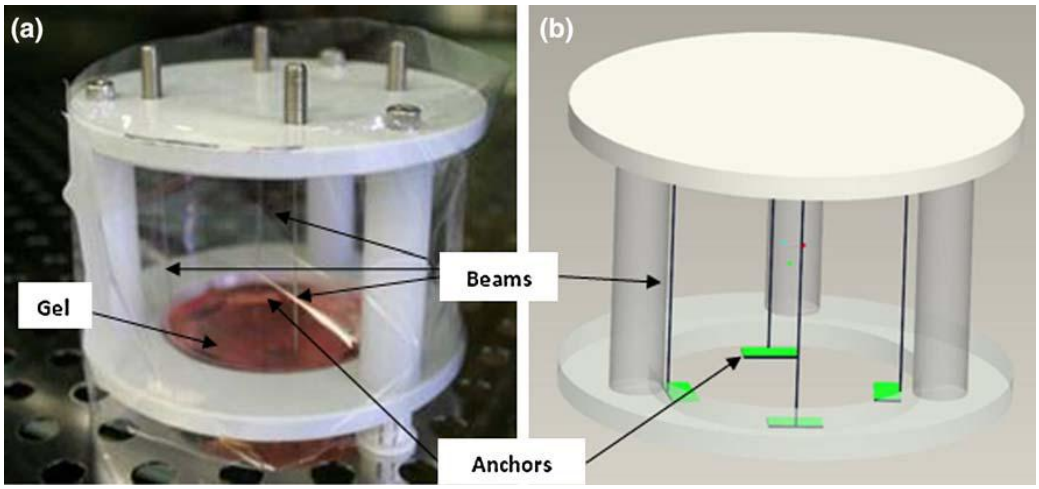

Figure 4.1. Controlled boundary stiffness device showing the four stainless steel beams that act as compliant springs and the porous anchors that attach to the gel (a) photograph and (b) computer aided drawing.[115]

4.3.2. Device Operation

Four porous anchors (Vyon, Porvair Co.) are attached to the ends of the four stainless steel beams and a 60 mm untreated tissue culture dish lid is placed in the bottom of the device.[115] The cell-populated collagen gels are prepared and poured into the tissue culture dish lid prior to gelation. Once solid, the gels are submerged in standard culture media and the device is wrapped in a thin polypropylene sheet providing cover for the device for the duration of the culture.

As the gel compacts and contracts, the pads and beams are displaced and the magnitude of displacement in the x and y direction is measured through analysis of images acquired with a Cannon Rebel XT 6.5 megapixel digital camera and a macro lens (fixed 60 mm focal length) mounted at a fixed length from the base of the device. Images acquired over the duration of the culture are analyzed using Image J (NIH). From the images, the cell–generated forces are calculated along the x and y axis:

$$F = K\frac{\Delta x}{2} \qquad \textit{Equation 4 2}$$

K is the spring stiffness from Eq. (1) and Δx is the change in distance between the two beams along one axis, with each beam contributing half of the change in distance between the pads (Figure 4.2). The theoretical resolutions for the stiffest and the most compliant boundaries are 7.2 μN and 0.48 μN respectively (based on optical resolution) and the repeatability for all beams is approximately 25 μN.[115]

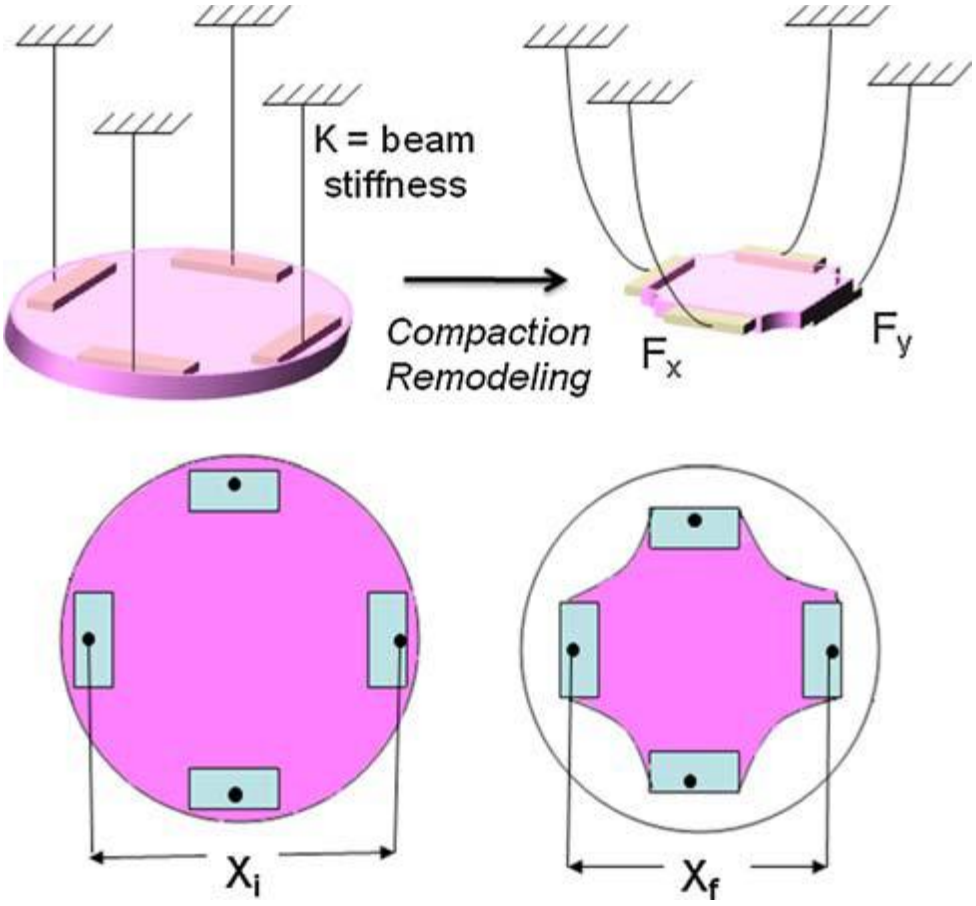

Figure 4.2. Schematic of method to measure cell force by measuring the displacement of the pads; $F_x = 1/2K(X_i - X_f)$where F_x is the force in the 'x' direction and K is the stiffness of the beams.[115]

4.3.3. Cell Culture

Human dermal fibroblasts from neonatal foreskin (ATCC) were expanded to obtain adequate cell numbers in T-150 flasks (BD Biosciences) at 37˚C in humidified 10% CO_2 conditions with DMEM, Mediatech Inc.) supplemented with 10% bovine calf serum (Hyclone) and 1% penicillin/streptomycin/ampothericin B (Invitrogen). Fibroblasts used for the experiments were either passage 8 or 9. VICs, used for a subset of experiments, were isolated from adult porcine aortic valves[94] and expanded as described above with 15% fetal calf serum (Hyclone). VICs used for the experiments were passage 3–5. In a subset of samples, 5 ng/mL TGF-β1 was added to the culture media.

4.3.4. Collagen Gel Fabrication

Fibroblast and VIC-populated collagen gels were prepared by the methods outlined by Bell et al.[118] Type 1 collagen was acid extracted from rat tail tendon, dehydrated and dissolved in 5.0 mM HCl.[70] To prepare each 6 mL gel, the following were combined: 2.64 mL of 5 mg/mL collagen; 1.32 mL 5x DMEM; 0.26 mL of NaOH and 1.91 mL of concentrated cell solution (1x DMEM, 10% or 15% fetal bovine serum for fibroblast and VIC gels respectively, and 1% penicillin and streptomycin). The initial collagen concentration of each gel was 2 mg/mL and the cell concentration was 0.5×10^6 cells/mL. The cell-seeded gels were incubated at 37˚C in humidified 10% CO_2 conditions.

4.3.5. Measurement of Cell-Generated Forces

A culture period of 72 hours allows for the compaction of the gel and cellular response to the altered boundary stiffness.[71,119] The cell generated forces during compaction were monitored over the culture period by measuring the displacement of the pads at 12 hour intervals. A subset of gels were treated with 90 mM potassium chloride (KCl) and the resulting active cellular contraction was measured. KCl depolarizes the cell membrane of muscle and muscle-like cells such as myofibroblasts, allowing for the quantitative evaluation of myofibroblast differentiation.[120] As the cells migrate through and remodel the gels, the matrix itself is brought under tension, to measure this passive tension, resultant from cellular remodeling, gels were treated with cytochalasin D (6 µM, Sigma) for 4 h to disrupt the actin cytoskeleton, controlling for active forces present.[121,122]

4.3.6. Mechanical Testing

Uniaxial mechanical tests were performed on a subset of the VIC-seeded collagen gels to quantify the effect of boundary conditions on the intrinsic stiffness of the gels.[115] After the culture period, the gels were removed from the device and the thickness of each gel was measured using a laser displacement system (LDS, LK-081, Keyence Corporation, Woodcliff Lake, NJ) as previously described by Billiar et al.[123] A 12.5 mm wide strip was excised from the center portion of the gel, placed in an isotonic saline bath, and using custom grips, mounted on a magnetic drive uniaxial testing machine (ElectroPuls 1000,

Instron Corp.) with custom low force transducer (±0.001 N, Interface, Inc.) and optical marker tracking (SVE, Instron). Two barbed markers were placed in the center of the sample to facilitate optical measurement of sample deformation. The sample was tared to a load of 1 mN, the gauge length was measured, and the sample was cyclically stretched for eight cycles between stretch ratios of 1.0 to 1.1. The Lagrangian stress–stretch ratio (σ–λ) data were fit to an exponential model:

$$\sigma = A\left(e^{B(\lambda-1)} - 1\right) + \sigma_0 \qquad \textit{Equation 4.3}$$

where A and B are material parameters and σ_0 is the initial (tare) stress. The maximum tangent modulus, MTM, was calculated (MATLAB, Mathworks) as a metric of the maximum intrinsic stiffness of the gel. The structural stiffness, K, at 0.1 mN was calculated as a functional measure of the matrix stiffness at a level corresponding to the force generated by a population of cells:

$$K = \frac{AE}{L} \qquad \textit{Equation 4.4}$$

Where A is the cross-sectional area of the sample, E is the Young's modulus, and L is the gauge length of the sample.

4.3.7. Immunohistochemistry

Sections of the gel were excised, prepared for immunohistochemistry, and probed for cells positive for αSMA. After mechanical evaluations, the strips of gel were affixed to a

PDMS substrate, fixed for 7 hours with 10% neutral buffered formalin, and then transferred to 70% ethanol. The gel sections were dehydrated in a graded ethanol series, embedded in paraffin, and cut into 5 µm sections on a microtome. Sections were probed with the αSMA antibody (Clone 1A4, Dakocytomation) followed by biotinylated goat anti-mouse IgG2A (Vector Laboratories). Samples were then counterstained with Harris hematoxylin (Richard-Allan Scientific). Slides were viewed with an upright epifluorescent microscope (Eclipse E600, Nikon) and images acquired with a RT Color Spot camera (Diagnostic Instruments, Inc.).

4.3.8. Western Blot

In order to quantify αSMA protein expression in response to substrate stiffness via Western Blot, VIC-populated gels were prepared and cultured as described above. At the end of the culture period, the cell-populated gels were manually homogenized by crushing a conical tipped probe in a microcentrifuge tube, and the cells were lysed with a solution containing NP40 Lysis Buffer (Biosource), PMSF (Pierce), and Halt Protease Inhibitor (Pierce). Total protein was quantified using the BCA Protein Assay (Pierce) according to the manufacturer's specifications. 10 µg of protein was added to each well of a 12% bis-acrylamide gel and protein was separated by electrophoresis. Protein was then transferred to Polyvinylidene fluoride (PVDF) membrane, which was then was blocked in 5% milk in PBST for 2 hours at room temperature and probed with the αSMA

(clone 1A4, Sigma) antibody overnight at 4˚C. The antibody was removed and the membrane was washed thoroughly with PBST prior to incubation with anti IgG-alkaline phosphatase conjugated antibody (Sigma) for 1 hour at room temperature. Following thorough washing with PBST, signal was detected by chemiluimence (Lumi-Phos WB chemiluminescent substrate for AP, Pierce), on the Geldoc (Biorad).

4.4. Results

4.4.1. Increased Cell-Generated Forces with Boundary Stiffness

VIC-populated gels (n=1) were cultured as described above with either compliant (diameter = 0.127 mm, K=0.048 ± 0.007 N/m) or stiff boundaries (diameter = 0.241 mm, K=0.409 ± 0.012 N/m). After 48 hours of culture, increased cell-generated forces were measured on gels cultured with stiff boundaries compared to gels cultured with compliant boundaries. These forces were increased further through the addition of 5 ng/mL TGF-β1 (Figure 4.3). Addition of TGF-β1 to gels cultured with compliant boundaries did not have an effect compared to gels cultured in standard media.

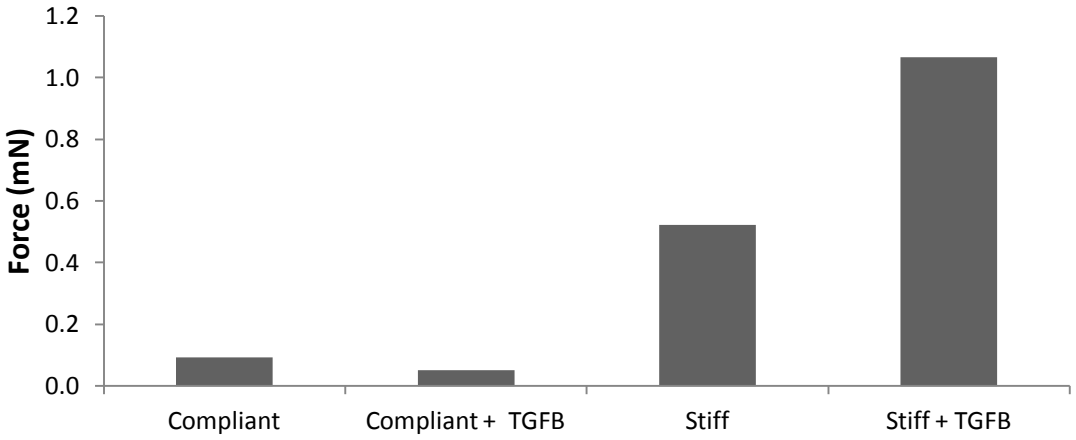

Figure 4.3. Preliminary data (n=1) showing the average contractile force (in x and y plane) exerted by VIC-populated collagen gels. VICs were seeded in collagen gels with stiff, compliant, or free boundary and were cultured for 2 days. Forces were measured by porous anchor displacement from position at t_o.

4.4.2. Material Stiffness is Correlated with Boundary Stiffness

Uniaxial mechanical testing showed that the stiffness of the gel increased with boundary stiffness (Table 4.1). The maximum tangent modulus (stiffness) of the gels cultured in standard media was 43.5, 86.9, and 149.1 kPa for the free, compliant, and stiff boundary groups respectively. The compliant and stiff boundary gels supplemented with 5 ng/mL TGF-β1 during culture had increased stiffness compared to the same groups cultured in standard media; the maximum tangent modulus was 96.0 and 530.8 kPa for the compliant and stiff boundaries, respectively. Notably, the gel stiffness of the stiff boundary group increased 3.5 fold to 530 kPa following the addition of TGF-β1. As expected, the thickness of the free gels was greater than the gels with compliant and stiff boundaries; however, there was no difference in thickness with the addition of TGF-β1. The stress-strain data from all samples fit the expediential model well (Equation 4.3). The compliant and stiff boundary groups had an r^2 value above 0.95 and the free boundary samples had an r^2 values above 0.81.

Table 4.1. Pilot results from uniaxial tensile testing on strips of VIC-populated collagen gels after 72 h cultured free floating (‘‘Free’’) or anchored to compliant (0.048 N/m) or stiff (0.41 N/m) springs in the absence or presence of 5 ng/mL TGF-β1. From John et al.[115]

Boundary condition	TGF-β1 (+/−)	Width (mm)	Thickness (mm)	L_0 (mm)	σ_0 (kPa)	A (kPa)	B (−)	K (N m^{-1})	MTM (kPa)	RMS (kPa)	r^2 (−)
Free	–	6.86	0.30	16.92	0.156	0.115	26.5	0.52	43.5	0.12	0.93
Free	+	5.67	0.31	21.14	0.000	0.286	15.5	0.44	20.9	0.15	0.81
Compliant	–	12.19	0.11	22.49	0.160	0.248	26.2	0.51	86.9	0.20	0.95
Compliant	+	11.73	0.13	24.5	0.220	0.306	25.2	0.57	96.0	0.13	0.98
Stiff	–	10.08	0.17	18.74	0.084	0.280	29.1	0.90	149.1	0.15	0.99
Stiff	+	10.82	0.14	21.5	0.068	0.029	57.4	0.39	530.8	0.20	0.99

The low root mean square error (RMS) and the high coefficient of determination (r^2) indicate that the exponential model fit the data well. One sample from each group was tested.

4.4.3. Differrences in Tissue Morphology with Boundary Stiffness

After 72 hours of culture the displacement of the beam resulting from gel compaction was observed. Notably, the gel cultured with the compliant boundary has displaced beams (Figure 4.4a & b) more than the gel cultured with the stiff boundary (Figure 4.4c). Representative histological images are shown for compliant boundary without (Figure 4.4d) and with (Figure 4.4e) 10 ng/mL TGF-β1 supplementation. Gels cultured with stiff boundary (Figure 4.4f) were thinner and qualitatively had less αSMA expression (brown staining) compared to gels with compliant boundary.

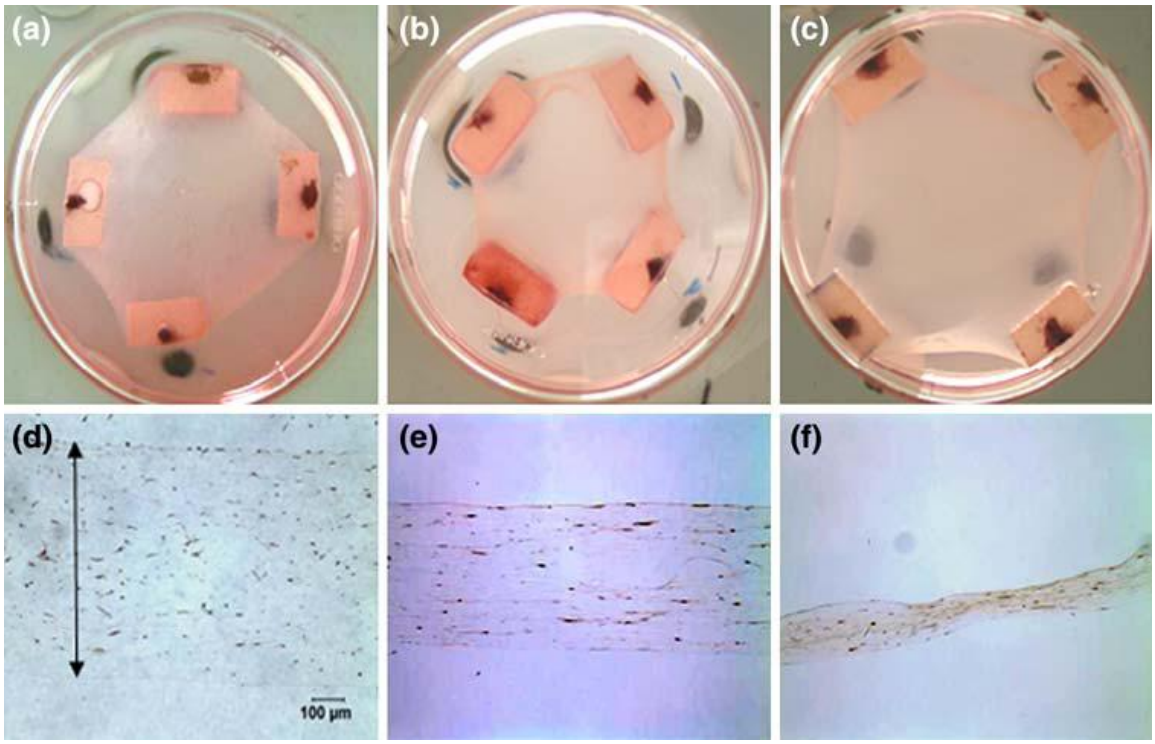

Figure 4.4. Compaction of the gels after culturing for 3 days with (a, d) compliant boundary (beams with K = 0.048 N/m) cultured in standard media (b, e) compliant boundary cultured with 10 ng/mL TGF-β1 and (c, f) gels cultured with stiff boundary (beams with K = 0.57 N/m) in the presence of 10 ng/mL TGF-β1. Images a-c show the gels after three days of culture. Images d-f show representative histological sections of each boundary condition listed above. Sections were probed for αSMA (brown) and counterstained with Harris hematoxylin. The diameter of the dish is 60 mm and original magnification is 200X (d, e, and f).[115]

4.4.4. Increased αSMA Protein Expression with Increased Boundary Stiffness

Given that immunohistochemical staining qualitatively suggested that culture with stiff boundaries increased the cellular expression of αSMA, we addressed this directly using western blot analysis. Cells cultured in gels with fixed boundaries (unreleased gel) had significantly higher αSMA expression compared to those cultured in free boundary gels (Figure 4.5).

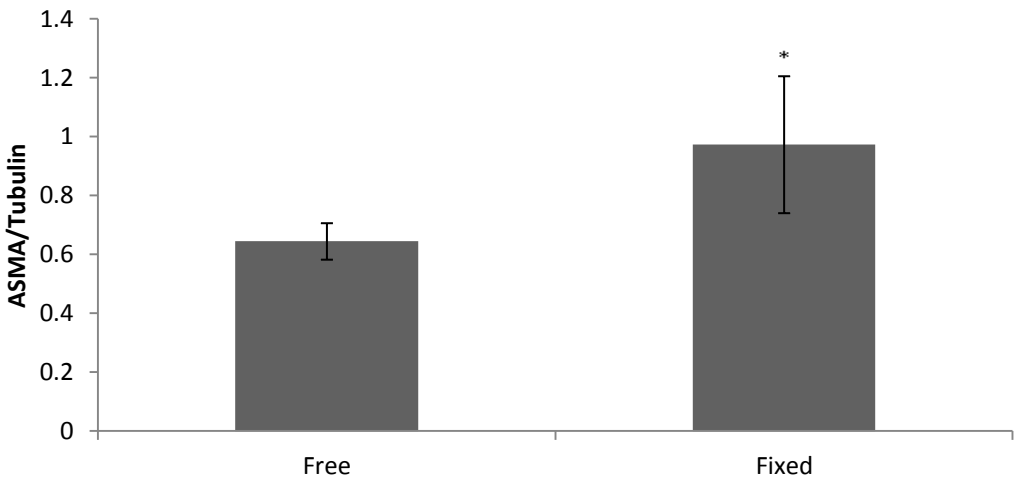

Figure 4.5. Preliminary data showing the relative quantity of αSMA (normalized to tubulin) in free (zero stress boundary) and fixed (infinite stress boundary) gels. VIC-populated gels were cultured for 72 hours. n=5, $p<0.05$, significance determined by Mann-Whitney Rank Sum Test.

4.5. Discussion

Here we describe a culture device for investigating the effects of mechanical properties, specifically the boundary rigidity on cells cultured in a 3D matrix. Previous culture methods allow for only the two extreme conditions to be tested (zero and infinite boundary) which is analogous *in vivo* to splinting wounds.[33] We present a method for applying intermediate levels of boundary stiffness during the culture of cell-populated gels. We include preliminary data from fibroblasts and VICs cultured in collagen gels with and without TGF-β1 supplementation; however, the methodologies presented herein could be applied to numerous other cell types and potentially other biopolymer matrices such as fibrin, chitosan, or alginate. In the two cell types evaluated we found that the cells have increased contractile forces when cultured with stiff boundaries when compared to gels cultured with compliant boundaries; interestingly there was variation in average forces produced by cells from different anatomical locations. Human fetal lung fibroblasts generated higher forces (~1.0 mN, data not shown) than VICs (~0.41 mN) and dermal fibroblasts (~0.35 mN) (beam stiffness of 0.41 N/m and 0.5 million cells per mL in all cases).

The contractile forces of VICs (~0.41 mN per $3x10^6$ cells) were approximately two fold lower than forces reported by Smith et al. (0.31 mN per 10^6 cells).[111] The differing values could be attributed to differences in methodologies for force measurement or the time period over which the measurements were acquired. We saw an increase in force over the first 36 hours after which the force would appear to saturate.[115] Legant et al. developed a

micro-scale system of micropatterned polymer pillars to apply "boundary stiffness" to cells.[124] The beam stiffness was controlled by varying the lengths of the beams and similar to our findings, cellular forces were higher when gels were attached to stiff beams (compared to compliant beams) however αSMA expression and resulting gel stiffness (after culture period) were not evaluated.[124] We found that gels cultured with stiff boundaries and supplemented with TGF-β1 had increased forces compared to non-supplemented gels; however, this trend was not observed for free gels (zero boundary). This response could be related to the need for a basal tension level required by the cells for them to experience an effect of TGF-β1.[98] The average contractile forces (for in the x and y planes) shown in Figure 4.3 represent n=1 and additional samples are required to show statistical significance. In these studies we evaluated one cell density. Interestingly, Smith et al. show, that as VIC density decreases, the contractile force increases[111] suggesting that cell density is yet another important variable in cell contractile force.

Western Blot analysis shows significantly increased αSMA expression in fixed (infinite stiffness boundary) gels compared to free (zero boundary) gels and similar trends with respect to αSMA expression and boundary stiffness were observed in the immunohistochemical results. This trend is consistent with a phenotypic shift towards myofibroblasts and in previous studies was attributed to the intrinsic gel stiffness[33,71] rather than the boundary condition. Additional studies are required to determine the levels of αSMA expression for gels cultured with stiff and compliant boundaries. Since separate gel sections (from each sample) were required for mechanical testing,

immunohistochemistry, and Western Blotting we were often limited by amount of gel available and in several samples, there was not adequate protein to complete the experiment. When sampling the cell-populated collagen gels for testing after the culture period (e.g. mechanical testing) we were careful to avoid the edges of the gel. Gel edges would likely have edge effects such as uniaxial loading patterns which could result in cell alignment. Additionally, edge effects could also occur at the top and bottom surfaces of the gel. Cells at the gel/liquid interface would likely undergo alternative loading than cells in the central region of the gel. While this heterogeneity across of the thickness of the gel could be a concern, it was not controlled for in these experiments. Additional studies are required to determine if there are in fact "interface" effects on cell responses. In addition, the cells on the surface of the gel are in direct contact with the media and thus no diffusion barrier unlike the cells encapsulated within the central region of the gel.

In developing this method, we found the device construction materials to be important. Early prototypes used a two-part epoxy adhesive, which was later found to be mildly cytotoxic. The current device design used Medical Grade Silicone Adhesive, which is non-cytotoxic but requires an extended curing time compared to the epoxy adhesives.

To determine if boundary stiffness had an effect on cell proliferation we evaluated two methods for counting the cells in the gels at the termination of the experiment, CyQUANT® assay from Invitrogen and collagenase digestion of the matrix followed by manual counting with a hemocytometer. Each method had both advantages and limitations. The CyQUANT® assay accurately measures small numbers of cells, however

it requires manual or chemical dissolution of the gel and auto-fluorescence of the collagen could alter results. Collagenase digestion of the collagen matrices requires careful monitoring, prolonged incubation in the collagenase solution caused extensive cell death. While the collagenase digestion is more time consuming, we felt it provided more accurate cell counts than the CyQUANT® assay, as the results were not affected by autofluorescence.

In summary, this chapter expands upon the 2D studies described in Chapter 3 by utilizing a 3D culture system with controlled levels of stiffness. We describe a novel device for applying controlled levels of boundary stiffness to cell-populated collagen gels and provide preliminary data demonstrating the device's use and efficacy. Results demonstrate that increasing boundary stiffness results in increased cellular contractile forces, αSMA expression, and gel (material) stiffness. TGF-β1 supplementation seemed to augment responses in gels with stiffer boundaries suggesting that a minimum boundary stiffness may be required. More studies are required to complete the data set presented here and many more studies are possible, with the addition of more levels of boundary stiffness, changing the boundary stiffness throughout the culture period by using "sleeves" of predefined stiffness on the beams, and evaluating the numerous combinations of cell and gel types. This device and methods described herein provide useful tool for studying cellular response to environmental stiffness which is crucial for the study of wound healing, tissue mechanics and tissue engineering. Chapters 3 and 4 describe the sensitivity of VICs to substrate stiffness in 2D and 3D culture environments.

In Chapter 5 we continue to investigate the role of stiffness in VIC activation by combining multiple levels of substrate stiffness with equibixial stretch.

Chapter 5 - Combining Dynamic Stretch and Tunable Stiffness to Probe Cell Mechanobiology *In Vitro*

Angela M. Throm Quinlan[1,2], Leslie N. Sierad[1], Andrew K. Capulli[1], Laura E. Firstenberg[3], and Kristen L. Billiar[1,4]

[1]Department of Biomedical Engineering, Worcester Polytechnic Institute, Worcester, MA 01609, USA

[2]Graduate School of Biomedical Sciences, UMass Medical School, Worcester, MA 01655, USA

[3]Franklin W. Olin College of Engineering, Needham, MA 02492, USA

[4]Department of Surgery, University of Massachusetts Medical School, Worcester, MA 01655, USA

The following chapter was published in PLoS One on August 15, 2011.

PLoS ONE 6(8): e23272. doi:10.1371/journal.pone.0023272.

5.1. Abstract

Cells have the ability to actively sense their mechanical environment and respond to both substrate stiffness and stretch by altering their adhesion, proliferation, locomotion, morphology, and synthetic profile. In order to elucidate the interrelated effects of different mechanical stimuli on cell phenotype *in vitro*, we have developed a method for culturing mammalian cells in a 2D environment at a wide range of combined levels of substrate stiffness and dynamic stretch. PA gels were covalently bonded to flexible silicone culture plates and coated with monomeric collagen for cell adhesion. Substrate stiffness was adjusted from relatively soft (G' = 0.3 kPa) to stiff (G' = 50 kPa) by altering the ratio of acrylamide to bis-acrylamide, and the silicone membranes were stretched over circular loading posts by applying vacuum pressure to impart near-uniform stretch, as confirmed by strain field analysis. As a demonstration of the system, porcine aortic valve interstitial cells (VIC) and human mesenchymal stem cells (hMSC) were plated on soft and stiff substrates either statically cultured or exposed to 10% equibiaxial or pure uniaxial stretch at 1Hz for 6 hours. In all cases, cell attachment and cell viability were high. On soft substrates, VICs cultured statically exhibit a small rounded morphology, significantly smaller than on stiff substrates ($p<0.05$). Following equibiaxial cyclic stretch, VICs spread to the extent of cells cultured on stiff substrates, but did not reorient in response to uniaxial stretch to the extent of cells stretched on stiff substrates. hMSCs exhibited a less pronounced response than VICs, likely due to a lower stiffness threshold for spreading on static gels. These preliminary data demonstrate that inhibition of

spreading due to a lack of matrix stiffness surrounding a cell may be overcome by externally applied stretch suggesting similar mechanotransduction mechanisms for sensing stiffness and stretch.

5.2. Introduction

Proper spatiotemporal distributions of dynamic physical cues are necessary to guide the development, maintenance, and healing of tissues. Cells such as fibroblasts, endothelial cells, and muscle cells actively sense both the external loading applied to them (outside-in signaling) and the stiffness of their surroundings (inside-out signaling). They respond to these stimuli with changes in adhesion, proliferation, locomotion, morphology, and synthetic profile (reviewed in[31,125]). Although some likely candidates for sensing stiffness and stretch exist, it remains unclear if the same mechanotransduction pathways are responsible for inside-out and outside-in signaling, or if there are mechanosensing and mechanoregulation machinery specific to each stimulus. A better understanding of how complex combinations of mechanical stimuli regulate cell behavior is critical for the rational engineering of tissues *in vitro* and for guiding proper regeneration *in vivo*.

Leung et al.[44] first described the sensitivity of cells to dynamic stretch *in vitro* by demonstrating a change in protein production in equibiaxially cycled smooth muscle cells, and subsequent studies have demonstrated that mechanical stretching induces a wide range of cellular responses including cytoskeletal remodeling, synthesis of numerous ECM proteins, and altered expression of a multitude of genes.[45,46] Cell reorientation "away" from the direction of maximal cyclic stretch is the most visible effect of stretch and is accompanied by pronounced remodeling of the actin cytoskeleton.[47,48] *In vitro* investigations into the role of stretch on cell behavior are most commonly carried out on protein-coated silicone substrates. Countless custom loading

devices have been developed for both uniaxial[126] and biaxial[127] stretch patterns. Commercial devices are also available such as Flexcell®, which uses vacuum pressure to stretch a circular silicone membrane over a fixed loading post, and STREX which utilizes dual motors to stretch square or rectangular wells biaxially. As cells are not able to appreciably deform the relatively stiff silicone substrates used in standard cell-stretch systems (Young's modulus ≈ 150 kPa), it is not possible to quantitatively investigate the effects of stretch on the traction forces the cells exert on the substrate or to determine the effect of substrate stiffness (and resulting prestress) on the cellular response to stretch.

Cells are influenced by the stiffness of their surroundings and exert tension on their environment, a phenomena first described by Harris[59] with cells wrinkling the membrane on which they were cultured. Since that time, it has been clearly shown that the stiffness of the culture environment is a potent stimulus for a variety of cell functions. Stiffness induces wide-ranging effects on cell behavior, the most obvious being spread area and level of prestress. For example, fibroblasts cultured on soft substrates (E ≈ 1 kPa) have significantly smaller spread area and shape factor than those cultured on stiff substrates (e.g., glass, E ≈ 1 GPa).[62] Changes in cytoskeletal organization,[128] matrix adhesions,[62] migration, growth,[84] maturation,[129] contractile force generation,[88] and myofibroblast differentiation[71] have also been reported. Recent studies indicate that stem cell differentiation can be guided by stiffness.[38,130] *In vitro* investigations into the role of stiffness on cell behavior are most commonly carried out on 2D PA substrates by changing the polymer chemistry to alter the substrate stiffness as described in the work of

Y-L Wang and colleagues,[61] although other polymer systems have also been utilized both in 2D and 3D configurations, e.g., polyethylene glycol (PEG)[12] and polydimethyl siloxane (PDMS).[59] Cellular deformation of these compliant substrates has also been exploited to quantify the forces that the cell exerts on the substrate utilizing powerful traction force microscopy techniques.[97]

Recently, Fredberg and colleagues[76] developed an indenter-based method (termed "Cell Mapping Rheometry, CMR") to locally deform single cells cultured on soft PA substrates. The authors probed the time-course of changes in cell traction forces following single and multiple cycles of biaxial and uniaxial stretch and demonstrated cytoskeletal fluidization or reinforcement in response to uniform and non-homogeneous strain fields, respectively. In its current configuration, CMR is ideal for the study of single cells in short duration studies of the dynamics of traction forces and cytoskeletal stiffness. However, a larger format system for combining levels of stretch and stiffness would be of benefit for elucidating mechanotransduction pathways requiring large numbers of cells for gene and protein regulation analyses, and for cell differentiation studies requiring long culture duration.

The goal of this work is to develop an *in vitro* method to investigate the combined role of substrate stiffness and dynamic stretch on cell behavior. Due to common pathways reported for outside-in (stretch-induced) and inside-out (stiffness-induced) cell signaling, we hypothesize that the application of cyclic stretch to cells cultured on soft hydrogels will induce responses commonly observed in cells cultured on stiff substrates. From the

many possible means of controlling substrate stiffness and membrane stretch, we chose to covalently bind PA, the most common “tunable” stiffness substrate, to a widely used dynamic cell culture substrate available commercially (Bioflex Culture Plates, Flexcell International) to ensure that the method could be implemented widely. Although seemingly a straightforward approach, the tight control of the process variables necessary for robust linkage of the PA to the silicone membrane required for large amplitude dynamic deformation has been a common stumbling block. To verify that the strain field presented to the cells by the silicone membrane is not altered by the thin PA gel, we utilize High Density Mapping (HDM) analysis. As a demonstration of the utility of this method we examine the spreading behavior of adherent valvular and stem cells using these mechanical stimuli in concert; most notably we investigate initially rounded cells on very soft substrates subjected to equibiaxial stretch and report a novel outcome. Implications of our preliminary results are discussed along with potential future investigations made possible with the method described herein.

5.3. Methods

5.3.1. Culture Plate Preparation

PA gels of defined stiffness levels were chemically attached onto standard 6-well flexible silicone membranes. To facilitate attachment, untreated Bioflex Culture Plates (Flexcell International) were functionalized using a protocol modified from that of Silver et al.[131] The plates were oxygen plasma treated for 2 minutes (Plasma Prep II, SPI) and then immediately treated with 4.7 mM 3-(Trichlorosilyl)propyl methacrylate (Sigma) in a 4:1 solution of heptanes and carbon tetrachloride for five minutes, after which the solution was removed and the silicone was rinsed with hexane. The plates were transferred to a vacuum chamber and negative pressure was applied for five minutes to remove volatile solvents from the silicone. The vacuum was released from the vacuum chamber and the chamber was flushed with nitrogen gas. STREX chambers (10 cm^2, B-Bridge International, Inc.) with flexible silicone culture surfaces were also treated with the above protocol for comparison.

Collagen-coated PA substrates were prepared based on standard protocols using a hetero-bifunctional UV activated crosslinker[61] adapted to the silicone-bottomed flexible well format (Figure 5.1). Briefly, 50 µL of a PA gel solution consisting of 0.15% tetramethylethylenediamine, 0.075% ammonium persulfate, and acrylamide:bisacrylamide (all from Biorad) of varied ratio (Table 5.1) to control stiffness was applied to the center of each well. Coverslips (22 mm diameter) were made

hydrophobic to prevent adhesion to the gels by treating with undiluted Surfacil (Pierce) for one minute and then rinsing with methanol. The treated coverslips were placed on top of the unpolymerized gel solution and left undisturbed until gel polymerization (under nitrogen flow) after which they were removed. The photo-activatable, heterobifunctional cross-linker, sulfosuccinimidyl 6 (4-azido-2-nitrophenyl-amino)hexanoate) (Sulfo-SANPAH, Thermo Scientific) was applied to the surface of each gel and activated with UV light as previously described[63] and 100 µg/mL type I collagen (Purecol, Advanced Biomatrix) was applied to the surface of each gel and incubated for four hours at room temperature. Gels were rinsed with PBS and UV sterilized prior to cell seeding.

Table 5.1. Average strain (± SD) within central region of PA gel used for analysis of cell morphology for equibiaxial stretch (round loading post) and uniaxial stretch (Arctangle™ loading post).

Stretch	Gel Stiffness	Average Strain
	0.3 kPa	9.3 ± 0.4%
Equibiaxial	50 kPa	7.9 ± 0.6%
	No gel	11.1 ± 0.6%
	0.3 kPa	10.9 ± 0.6%
Uniaxial	50 kPa	7.83 ± 0.3%
	No gel	9.1 ± 0.9%

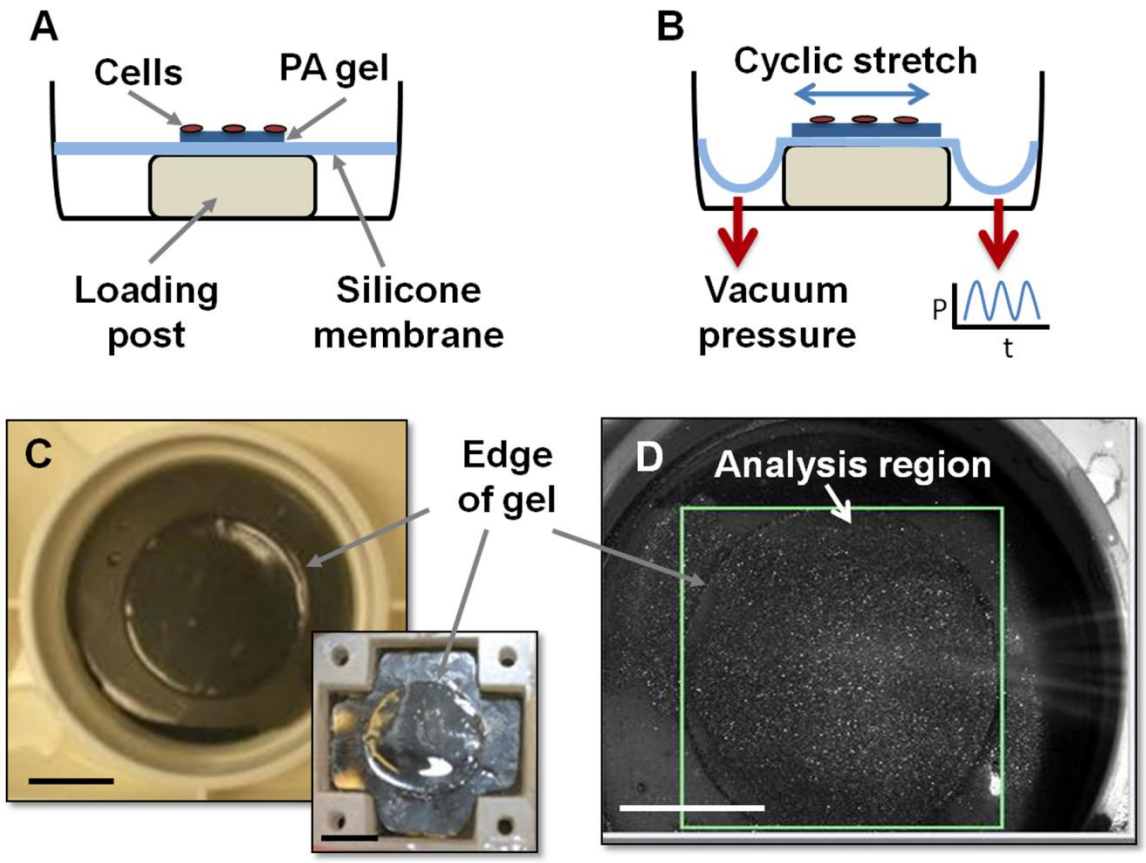

Figure 5.1. Schematic of PA gel on flexible silicone membrane under static (A) and stretched (B) conditions. Top view of a 22 mm diameter collagen-coated gel (~70 µm thickness) is cast into a 35 mm diameter flexible-bottomed Flexcell™ well (C) and STREX well (C, insert). Image of Flexcell™ well (D) stretched above an Arctangle™ loading post and labeled with retroreflective beads for strain field analysis. Rectangle shows region analyzed in HDM software, arrows point to edge of gel. Scale bars = 10 mm in all panels.[132]

5.3.2. Polyacrylamide Gel Stiffness

The bulk stiffness of the gels was measured by oscillatory shear rheometry using an AR-G2 rheometer (TA Instruments). A volume of 155 µl of PA solution was placed on the Peltier plate of the rheometer and a 40 mm diameter parallel plate geometry was lowered to a gap of 100 µm. After polymerizing for 10 minutes, 1X PBS was added around the circumference of the testing geometry to minimize drying, and the temperature was brought to 37°C. Following a 1 Hz 0.1% strain-controlled time sweep to monitor PA polymerization, a 1 Hz stress sweep between 10 and 1000 Pa was performed with the normal force held at 1 N, and the storage modulus (G') and loss modulus (G") were measured. Three measurements were made on each gel, gels were measured in duplicate, and values were averaged. As G" was over an order of magnitude lower than G', the gels were considered elastic. A wide range of acrylamide:bisacrylamide combinations were tested and two formulations were utilized for subsequent cell culture experiments: one low stiffness (3% acrylamide, 0.058% bisacrylamide, G' = 0.3 kPa) and one high stiffness (7.5% acrylamide, 0.117% bisacrylamide, G' = 50 kPa).

5.3.3. Polyacrylamide Gel Stretch Validation

Samples were marked with silicon carbide particles (40 µm diameter) and retro-reflective beads (60 µm diameter) to create a random light intensity distribution in the region of interest (ROI) and stretched to 10% using the Flexcell FX-4000T system (Flexcell

International, Figure 5.1). Digital images were acquired at a rate of 50 frames per second using a 1280 × 1024 pixel resolution CMOS camera (Photron Model # Fastcam-X 1280 PCI) with an 8 bit pixel depth while the Bioflex plates were cycled at 1 Hz from 0 to 10% strain. The strain distributions across the stretched samples were evaluated using digital image analysis. Specifically, the components of the 2D deformation field ($u1$ and $u2$ along the $X1$ and $X2$ camera axes, respectively) were determined from the images by measuring light distribution patterns using High-Density Mapper (HDM) software.[133] In brief, HDM converts the light distribution to the spectral domain using a fast Fourier transform (FFT) and through the use of an interference function, the displacement and rotation are found. The displacements are then converted back from the spectral domain to Cartesian coordinates using an inverse FFT. The chosen field of view (FOV) resulted in a camera resolution of 0.02 mm/pixel. Displacements were measured using a 1.28 mm (64 pixel) sub-image size with a corresponding step size of 0.64 mm (32 pixel shift) yielding a 25 × 20 matrix of $u1$ and $u2$ values for a ~16 × ~13 mm ROI.

5.3.4. Cell Culture

VICs were isolated[94] from porcine tissue samples obtained from a local abattoir (Blood Farm) or from the University of Massachusetts Medical School Department of Animal Medicine, from the carcasses of recently euthanized animals that had been used in other, non-related, animal studies, ***which had appropriate IACUC approval***. Once the

animals are euthanized, use of the carcasses and tissues are no longer covered by the IACUC and, thus, the tissue harvest process has no protocol number associated with it. The aortic valve was excised and rinsed in 1X phosphate buffered saline. The valve leaflets were incubated in a 600 U/mL solution of Type II collagenase (Worthington Biochemical) in DMEM, (Mediatech) with 100 U/mL penicillin G sodium (Sigma), 100 μg/mL streptomycin sulfate, and 250 ng/mL amphotericin B (Invitrogen) for 20 min on a rocking platform in a 37°C incubator. After incubation, the surface of the valves were scraped with a cell scraper to remove endothelial cells, rinsed in sterile 1X PBS (Mediatech), and cut into 1 mm pieces with a scalpel. The valve pieces were incubated in a fresh 600 U/mL collagenase solution as described above for 2 hr on a rocking platform in a 37°C incubator. The resulting cell/tissue solution was filtered through a nylon mesh, pelleted, and resuspended in standard medium (DMEM, 100 U/mL penicillin G sodium, 100 μg/mL streptomycin sulfate, and 250 ng/mL amphotericin B supplemented with 15% FBS (Hyclone)) at 37°C with 10% CO_2. VICs at passage 2-5 were used for all experiments. VICs were seeded onto the PA substrates at a density of 2000 cells/cm^2 and cultured in standard media.

Human mesenchymal stem cells (hMSCs, Lonza) were cultured in mesenchymal stem cell growth medium (Lonza) in a 37°C incubator with 5% CO_2. hMSCs at passage 11 were used for all experiments and were seeded onto the PA substrates at a density of 660 cells/cm^2.

5.3.5. Immunofluorescent Staining, Microscopy, and Cell Metrics

After six hours of static or dynamic culture (cyclic strain ~10% at 1Hz), cells were fixed and permeabilized on the PA substrates with a 5.3% formaldehyde (Ted Pella, prod #18505) and 4 µM Triton X-100 (Calbiochem) solution. The cells were labeled for f-actin (phalloidin, green, Invitrogen) and nuclei were visualized (Hoechst 33342, blue, Invitrogen). Cells were visualized with an epifluorescent microscope (Zeiss) and images acquired with a CCD camera. Images of 20 cells were acquired from each substrate (n=3 per group, experiment run in duplicate). The resulting images were analyzed using Image J (NIH) for the cell spread area and perimeter, and the shape factor (Eq. 1) was computed.

$$ShapeFactor = \frac{4\pi \cdot Area}{Perimeter^2} \qquad \textit{Equation 5 1}$$

5.3.6. Statistics

All values are reported as mean ± standard deviation. Each group consisted of 3 samples. Statistical comparisons were made across all groups (soft, stiff, static, and stretched) using two-way analysis of variance (ANOVA). Differences between groups were determined by post-hoc analysis using the Holm-Sidak method (Sigma Stat). A significance level of 0.05 was used in all the statistical tests performed.

5.4. Results

The protocol for covalently attaching the PA to the silicone membranes is relatively straight-forward in theory, but difficult in practice due to multiple critical processing steps. In order to develop a robust protocol to repeatedly produce gels of defined stiffness capable of dynamic stretch, we had to address both the polymerization and covalent attachment of PA onto silicone. We found that oxygen plasma is necessary for the covalent attachment, and that both vacuum and nitrogen flow were required to dry the silicone to allow for polymerization. Gels of low (0.3 kPa) and high (50 kPa) shear stiffness (G') were able to be polymerized in silicone-bottomed culture wells for two different commercially available stretching systems: Flexcell® and STREX. The gels could also be prepared with unmodified fluorescent polystyrene beads; however, we found that modified beads can inhibit polymerization, possibly due to the surface charges (data not shown). We suspect that this process may not work on all silicone as we experienced difficulty polymerizing the gels on the "uniaxial" STREX wells whereas the gels polymerized on the "biaxial" STREX plates; however, the reason is not clear at this point.

Gels polymerized onto silicone membranes had identical appearance as those polymerized on glass. Cells cultured on the PA gels had similar responses for both glass and (static) silicone supports. The PA gels attached to silicone membranes can be stretched equibiaxally to 15% at 1 Hz triangle waveform for 12 hours and still remain attached under culture conditions. Longer stretch cycles are currently being investigated.

The gels can be fabricated and stored (pre-collagen coating) at 4°C for multiple weeks without any apparent degradation in performance as assessed by visual appearance during manual stretching.

5.4.1. Strain Field Transmission

Strain is transferred through gel and exhibits similar strain patterns compared to unmodified Flexcell® wells although the average value is slightly lower (Figure 5.2). The lower average strain likely reflects imperfect transfer of strain rather than restriction of membrane deformation due to the presence of the very thin and soft gel (Table 5.1); however, it is conceivable that the stiff gel may somewhat restrict the motion of the membrane as it is a similar stiffness (50 kPa shear stiffness = 150 kPa Young's modulus if incompressibility is assumed). Alternatively, the treatment with solvents may stiffen the membrane resulting in lower stretch at a given vacuum pressure. The equibiaxial stretch loading posts provide approximately 3.8 cm^2 homogeneous region in the center (Figure 5.2). The Arctangle™ loading post produces complex strain field, as expected with roughly pure uniaxial strain in discrete areas along the primary stretch axis (Figure 5.3).

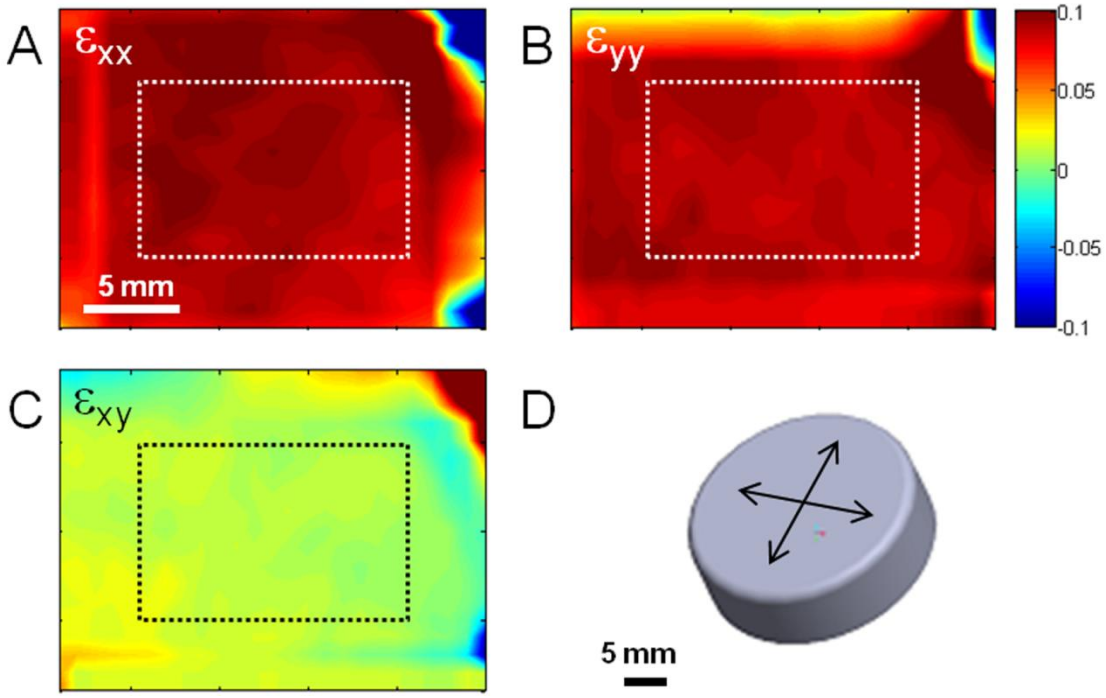

Figure 5.2. Strain field in region of interest is roughly uniform for equibiaxial stretch. Strain maps for a soft gel (0.3 kPa) undergoing equibiaxial strain in the X (A), Y (B), and XY (shear, C) directions demonstrating relatively homogenous strain and minimal shear within the area of analysis of cell morphology (dashed box). (D) CAD representation of the circular loading platen over which the silicone membrane is stretched by vacuum pressure. Scale bars = 5 mm.[132]

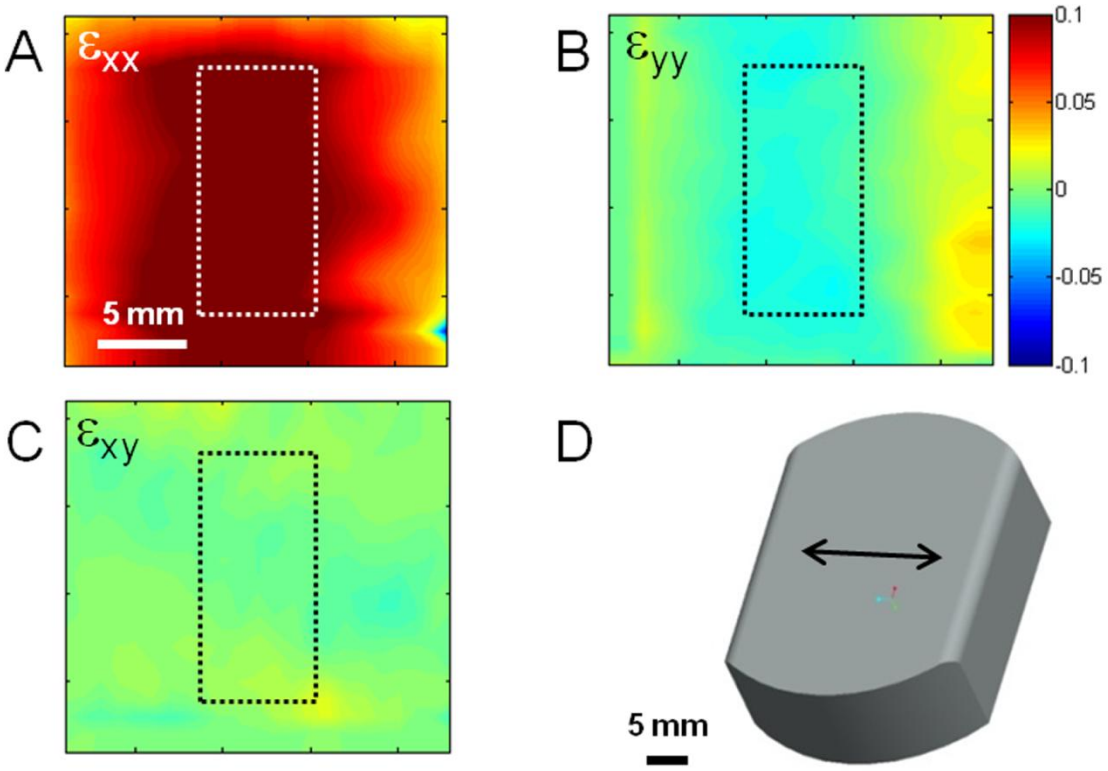

Figure 5.3. Strain field in region of interest is roughly uniform for pure uniaxial stretch. Strain maps for a soft gel (0.3 kPa) undergoing pure uniaxial strain in the X (A), Y (B), and XY (shear, C) directions demonstrating relatively homogenous strain and minimal shear within the area of analysis of cell morphology (dashed box). (D) CAD representation of the Arctangle™ loading platen over which the silicone membrane is stretched by vacuum pressure. Scale bars = 5 mm.[132]

5.4.2. Cell Culture Results

VICs cultured on static soft gels were small and round and developed pronounced stress fibers with stretch (Figure 5.4). The spread area of the VICs increased ~3-fold with stretch of cells on soft gels, but decreased ~25% for cells on stiff gels with 10% equibiaxial stretch (Figure 5.5). The spread area of VICs on soft-stretched gels was not significantly different than on stiff-stretched gels ($p<0.05$), although the perimeter was smaller ($p < 0.05$). The shape factor (function of area and perimeter, indicating relative amount of cellular extension) decreased approximately two-fold with stretch of cells on soft gels and did not change significantly for cells on stiff gels (Figure 5.5). Stretching hMSCs cultured on soft gels affected cell spread area to a lesser extent (compared to VICs) which was likely due to the ability of hMSCs to spread on lower stiffness substrates (thus little additional spreading occurred with stretch, Figure 5.6). VICs cultured on soft substrates (0.3 kPa) and subjected to uniaxial stretch showed minimal alignment perpendicular to the direction of stretch, whereas VICs on stiff substrates under the same stretch conditions had pronounced alignment perpendicular to the stretch direction (Figure 5.7).

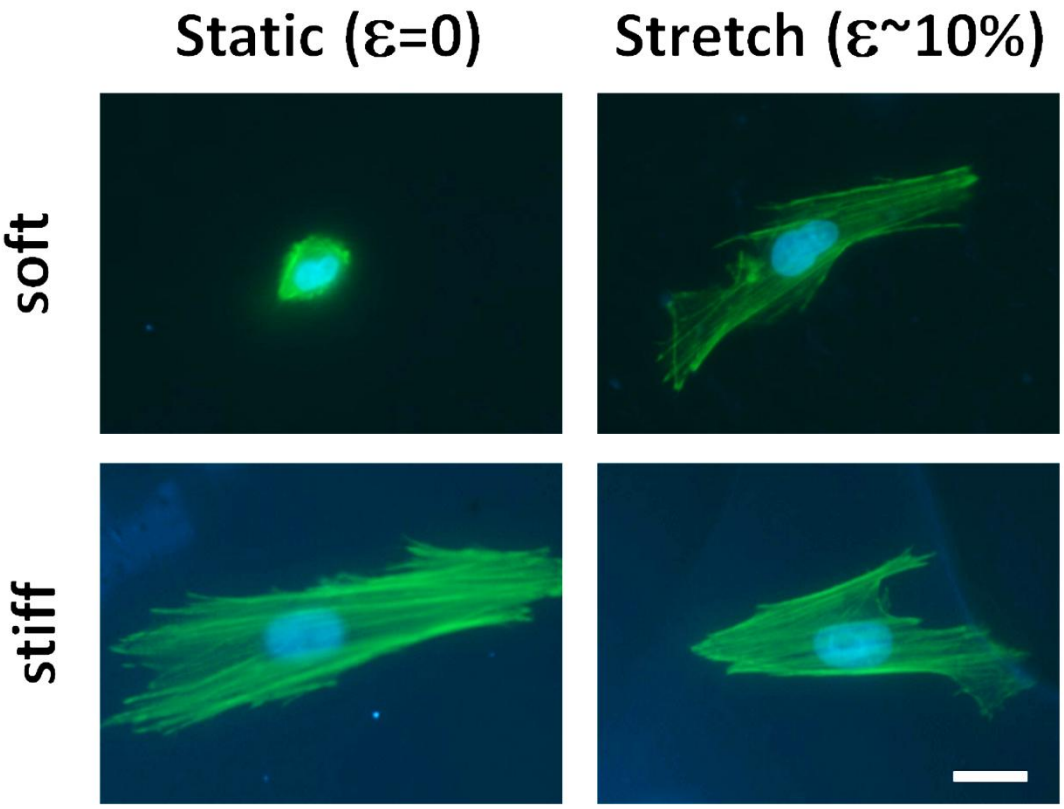

Figure 5.4. Cells cultured on soft substrate can sense and respond to stretch. Micrographs of VICs cultured statically (left column) and following ~10% cyclic equibiaxial strain (right column) for 6 hours on soft gels (0.3 kPa, top row) and stiff gels (50 kPa, bottom row). Staining for f-actin (green) and nuclei (blue) shows that stretch increases the spread area of the cells. Scale bar = 20 μm.[132]

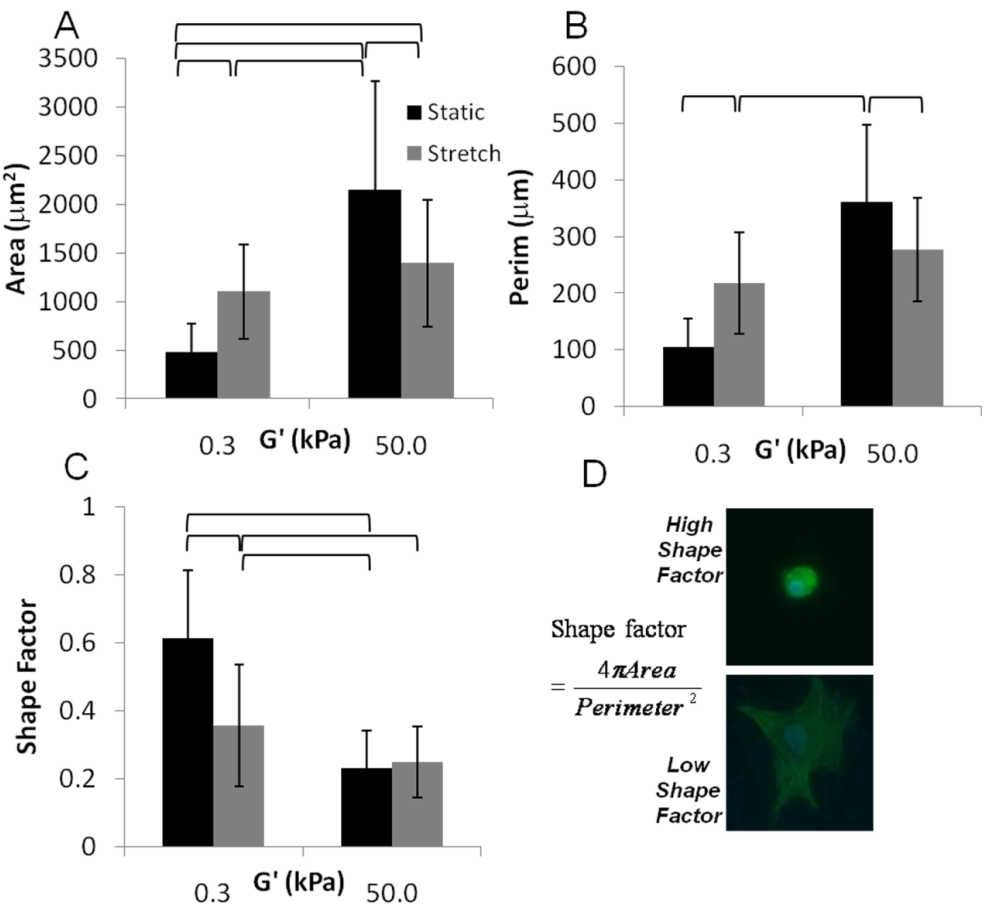

Figure 5.5. When cyclically stretched, cells on stiff substrates reduce spread area whereas cells on soft substrates increase spread area: Area (A) and perimeter (B) of VICs cultured on low (0.3 kPa) and high (50 kPa) stiffness gels subjected to 10% cyclic stretch at 1 Hz for 6 hours (grey bars) or static (black bars) culture. Shape factor (C) quantifies how rounded a cell is (a shape factor of 1 is perfectly circular, whereas a shape factor of 0 is extremely spread with many extensions). Cells of low and high shape factor are shown in D. Brackets above bars show significance between individual groups (two-way ANOVA, $p<0.05$).[132]

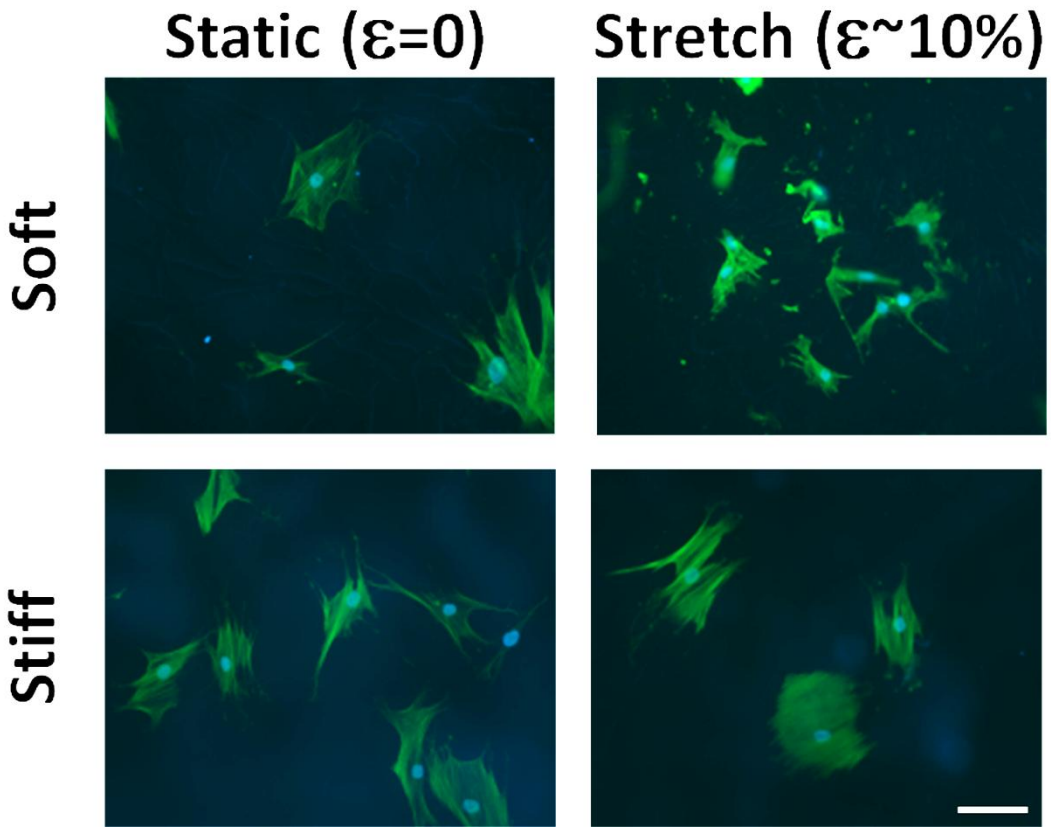

Figure 5.6. hMSC response to stretch is unclear due to spreading on static soft gels. Micrographs of hMSCs cultured statically (left column) and following ~10% cyclic equibiaxial strain (right column) for 6 hours on soft gels (0.3 kPa, top row) and stiff gels (50 kPa, bottom row). Staining for f-actin (green) and nuclei (blue) shows that hMSCs on soft gels (static and stretched) have unorganized actin fibers whereas cells on stiff gels have more organized actin fibers. Unlike VICs, hMSCs spread well on soft gels and stretch appears to increase the spread area of the cells slightly on stiff gels. Scale bar = 100 μm.[132]

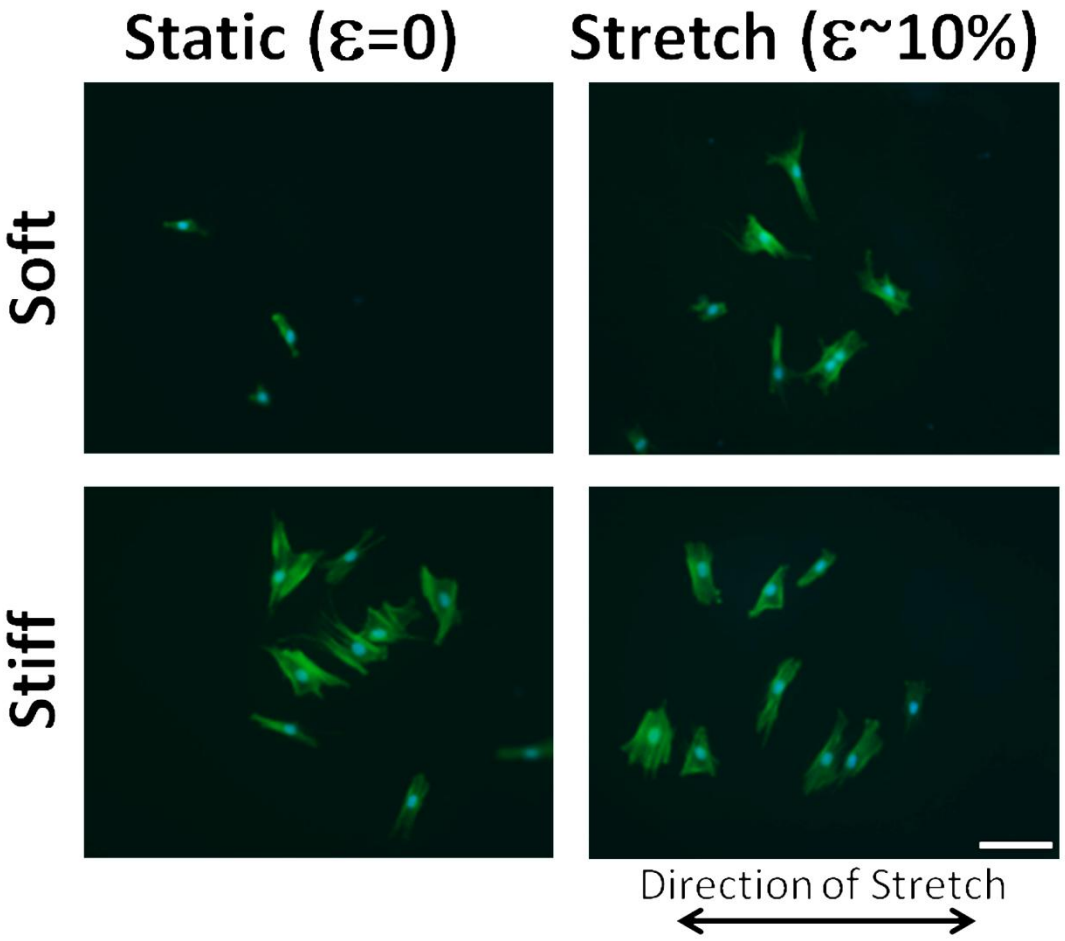

Figure 5.7. VICs on soft (0.3 kPa) and stiff (50 kPa) gels cultured under static and pure uniaxial stretch conditions (1 Hz, 10% stretch, 6 hrs). Cells cultured on soft substrates appear to have less realignment with stretch compared to the classic realignment perpendicular to the direction of stretch on the stiff substrates. Scale bar = 100 μm.[132]

5.5. Discussion

In this study, we developed a novel method for combining and independently controlling two important mechanical cues: the stiffness of the culture substrate and dynamic stretch. Our preliminary data confirm our hypothesis that the application of cyclic stretch to cells cultured on soft hydrogels induces responses indicative of culture on stiff substrates; most strikingly, VICs exhibited a rounded morphology on soft static substrates but spread to the same extent as those cultured on stiff substrates upon application of cyclic equibixial stretch. Previous studies have shown that cells remain mechanically sensitive when cultured on soft substrates,[76] yet it was unclear *a priori* if rounded cells on very soft substrates would retain mechanosensitivity or even be capable of remaining adhered to the substrates when subjected to large cyclic biaxial strains of extended duration. Our data indicate that cells on soft substrates remain well attached and have functional mechanical sensing mechanisms despite their rounded morphology and low basal tension level and that the application of stretch can override stiffness cues.

5.5.1. Cell Phenotypic Modulation and Differentiation

Our main purpose for developing the combined stretch and stiffness method was to facilitate the study of mechanical modulation of cell phenotype and differentiation in a more biofidelic mechanical environment. Cells within connective tissues reside in soft environments (relative to tissue culture plastic and silicone membranes) and are

dynamically stretched due to external loading of the tissues and traction forces from other cells. We are especially interested in the mechanical regulation of VIC phenotype due to the strong correlation of myofibroblasts and fibrotic pathology in areas of high stiffness and stretch in the valve. The valve leaflet environment is highly heterogeneous with very soft and stiff regions as well as extremely large dynamic strains. Our data indicate that VICs are highly sensitive to combinations of stretch and stiffness. Although determination of phenotypic shifts awaits analysis of functional outcomes such as gene/protein expression and traction force generation, these results may have implications for scaffold design. If a soft substrate is chosen to reduce cell tension and limit fibrotic behavior within a scaffold (to inhibit myofibroblast activation), the magnitude of stretch will be higher than in a stiff scaffold for a given loading, and the stretch stimulus may be sufficient to produce an equivalent (or potentially enhanced) fibrotic behavior as observed with a stiff scaffold.

The method developed herein is potentially applicable to the study of mechanoregulation of any adherent cell. Our experimentation with different cell types indicates that the threshold for responses to stiffness and stretch is likely different for each type of cell (compare Figure 5.4 and Figure 5.6). Mechanical regulation of stem cells is currently of great interest, and there is mounting evidence that stem cell lineage is directed, at least in part, by the local stiffness with osteogenic lineage favored on more rigid substrates, adipogenic or neuronal differentiation enhanced on soft substrates, and muscle markers expressed on intermediate stiffness substrates.[38,130] These findings have practical

implications for *in vitro* differentiation of stem cells for cell-based therapies in addition to the fate of the stem cells once implanted. For example, it has been suggested that the heightened stiffness of post-myocardial infarction scar tissue is not conducive to induction of stem cell differentiation to the proper (muscle) lineage.[134] It is conceivable that the cells may even be pushed towards an osteogenic lineage in a stiff scar. Similarly, cyclic stretch has been shown to induce differentiation of bone marrow stem cells into different cell lineages including ligament cells,[135] chondrocytes, osteogenic cells,[136] myocardial cells, and vascular cells[137,138] in a stretch anisotropy (uniaxial vs. equibiaxial)[139] and strain magnitude-dependent manner.[140,141] Although the effect of stretch on spreading of hMSCs (Figure 5.6) on soft substrates was inconclusive in this study since they did not demonstrate a rounded morphology on the low level stiffness gel, lower stiffness gels could be utilized in the present system (we have attached gels down to 50 Pa). Controlling combined levels of stretch and stiffness simultaneously holds the promise of providing more flexibility in the induction of specific stem cell lineage than stiffness or stretch alone.

5.5.2. Cell Contractility and Prestress

The ability of the cell to generate tension through its actin cytoskeleton is integral to the mechanoregulation of cell behavior. For example, stiffness-directed stem cell lineage specification is blocked by inhibiting nonmuscle myosin II,[38] and endothelial cell

reorientation with cyclic uniaxial stretch is blocked by abolishing stress fibers.[142] Cell traction force is, in turn, strongly modulated by the substrate stiffness.[63,143] Thus, tunable stiffness substrates offer a powerful alternative to chemical agents for the study of how cell prestress levels alter the transduction of dynamic stretch. More recently, dynamic substrates that utilize UV light to decrease stiffness were developed to evaluate the cellular effects of changes in stiffness in a single substrate during culture.[12,114] While these dynamic systems allow the study of the transition between multiple levels of stiffness, they do not address the differences in cell signaling between stiffness and stretch. Similar to previous chemical blocking experiments, stress fibers are absent on soft substrates; however, our data clearly demonstrate the ability of the cells to form stress fibers and remodel their cytoskeletons in response to cyclic stretch in the absence of high cell prestress (Figure 5.4). Not only are the potential side effects of chemical blocking agents removed by using PA gels, the prestress in the cell can be tuned to various levels by selecting the stiffness of the gel, and the traction force before, during, and after stretch can be assessed by utilizing traction force microscopy, a technique widely utilized with standard PA gels.[76,97,144] The incorporation of fluorescent microbeads in PA gels cast in between glass plates is relatively straight forward; however, care must be taken when selecting the type of beads as to not affect the polymerization or attachment to the silicone. We have found that beads with surface modifications such as carboxylate groups interfere with the gel polymerization and attachment. Our preferred method for incorporating beads into PA gels cast onto silicone

is to first cast a gel (as described above) and once polymerized, apply a thin layer of gel/(unmodified) bead solution on top. Only recently has cell traction forces in response to stretch been evaluated, and it was found that forces initially decreased and then slowly recovered after a single on-off stretch cycle.[76]

5.5.3. Cytoskeletal Changes (Cell Area and Stress Fibers)

Quantification of cell traction force is also critical for studying the mechanisms by which the cytoskeleton is remodeled in response to both stiffness and stretch. VICs cultured on high stiffness substrates, presumably at a high level of prestress based on their large spread area, actually reduced their spread area when stretched (Figure 5.4). This behavior has been observed previously with 1 Hz equibiaxial stretch of endothelial cells (but not 0.01 Hz stretch)[47] and is consistent with the stress fiber disassembly and reassembly to remain at a tension set-point. Interestingly, cell retraction was observed without an increase in the rate of disassembly and reassembly of stress fibers in the aforementioned study. Others have observed stress fiber shortening after only one cycle of quasistatic stretch of NIH 3T3 cells[145] and rapid fluidization of the cytoskeleton in human airway smooth muscle cells.[76] Although spreading due to cyclic stretch of cells on a soft substrate has not previously been shown, this behavior (Figure 5.4) is also consistent with the fibers remodeling and lengthening to reestablish a mean level of fiber tension when extended cyclically. Kaunas and colleagues[47] have developed a model incorporating

viscoelastic stress fibers which predicts high tension in the fibers at high strain rates, but a negligible perturbation in fiber tension at the low strain rate consistent with the observed data. Although this and other models have been successful in predicting the dynamics of cell reorientation with uniaxial stretch, cell spreading and retraction are not explicitly predicted by any model to the best of our knowledge. We presented preliminary data on cell re-alignment away from the direction of stretch. This has been described as cells "shielding" themselves from external forces caused by strain.[146] Cells and subsequently the stress fibers within the cells exposed to uniaxial strain will reorient themselves in-line with the lowest magnitude of strain.[147] Disruption of the stress fibers after application of strain demonstrated that stress fiber alignment, cellular retraction and MAPK activations occur in response to changes in stress fiber strain.[47] When cells are stretched at low frequencies, they are able to quickly relax to maintain fiber tension; however, at high frequencies, cells are unable to relax stress fibers fast enough to maintain homeostatic tension and an increase in stress fiber turn-over occurs.[47] Stress fiber turn-over decreases as the number of stress fibers oriented in the direction of the lowest strain increases.[47]

From a feedback-control system point of view, it is still controversial whether the cell has an extension (strain) set-point or a tension (stress) set-point;[148] or possibly it is a hybrid system controlling both the stress and strain state in the cell to control a basal energy level.[149] The feedback loop likely contains chemical diffusion and/or bond formation/dissociation and thus is sensitive not only to differences from the set-point

(proportional control) but also the rate of change of the signal (derivative control)[150] and the summation of signals over time (integral control). Further, the control is most likely nonlinear since the cells can actively adapt to the stimuli. Quantification of cell traction forces, dynamically varying the stiffness of the gel, applying additional non-equibiaxial, non-homogeneous strain patterns, and changing the rate of strain both for loading and unloading will provide new data for validation of computational models and will shed light upon the mechanical control system of the cell.

5.5.4. Mechanotransduction

The similarity of spread morphology of VICs with application of stretch on soft substrates to those cultured statically on higher stiffness substrates leads us to speculate that the mechanisms of "outside-in" sensing (of stretch) are similar to those for "inside-out" sensing (of stiffness). However, identification of the mechanosensors which transduce substrate stiffness and/or stretch is not trivial since they may be located anywhere along the mechanical pathway from outside the cell, to the interface between the cell and ECM, to deep within the cell. It is likely that there are multiple types of mechanosensors including mechanically actuated protein unfolding,[151] stretch-sensitive ion channels,[152] and changes in protein kinetics with loading such as actin stabilization.[47] Further, it is difficult to distinguish between inactivation of a mechanical or chemical pathway from inactivation of a mechanosensor itself since the physical linkages

necessary for relaying the mechanical signal to the sensor may be disrupted by experimental treatments. For example, blocking integrin expression may disrupt mechanotransduction due to the mechanosensitivity of the integrins themselves, or due to lack of sufficient attachment to the substrate as integrins are the critical for anchorage to the ECM. Independent stretch and stiffness control offers the possibility of separating the effects of outside-in vs. inside-out signaling.

5.5.5. Other Stiffness-Stretch Methods

Other materials and methods could be used to obtain combined levels of stiffness and stretch. For example, PEG, PDMS, or other soft polymers have been utilized for the study of stiffness-dependent biology and could be integrated into a similar stretch device.[153] Further, beds of microneedles of various dimensions have also been extensively used as tunable stiffness culture substrates[30,130] and could be stretched, although it is unclear if cells would attach to adjacent posts and spread once adhered to a given set of posts. The thickness of a thin (1-10 μm) collagen gel[26] or PA gel[154] layer attached to a silicone membrane could also be altered to modulate the effective stiffness sensed by the cells if the thickness could be controlled and the gel affixed tightly. For the development of our method, we chose to use a relatively thick layer (70 μm) of the most common tunable-stiffness substrate, PA, due to the known conjugation chemistries for various ECM coating proteins and the extensive traction force microscopy methods developed for PA

gels. We chose to affix PA onto the most common commercial stretching device (Flexcell®), although we have also affixed PA to other commercial cell stretching devices (e.g., STREX, B-Bridge) and custom devices utilizing silicone sheeting (e.g., Specialty Manufacturing). Alternatively, the previously mentioned elegant indenter-based device for stretching individual cells on PA[76] could be scaled up to stretch larger numbers of cells simultaneously.

5.5.6. Limitations/Future

As we have shown in this study, the ability to independently control the stiffness and stretch of a 2D culture substrate represents a substantial advance for studies of mechanobiology; however, cells have repeatedly been shown to behave differently in 2D culture than in 3D systems.[101] The cell shape, motility, proliferation, and protein biosynthesis are often very different in cells cultured on 2D substrates compared to those cultured within 3D synthetic and biopolymer gels. Further, cells cultured within soft biopolymer gels orient towards the direction of stretch[155] whereas the opposite response is found for cells cultured on 2D stiff substrates.[156] This response could be attributed to contact guidance, but could also be a result of the compliance of the gel. Despite these differences, 2D systems remain important for the study of mechanobiology due to the wealth of powerful techniques available to interrogate the cells in 2D and the ability to control other important factors which may affect cell responses including nanotopography and ligand density offered to the cell.

Here we focused on studying relatively large cell populations in parallel for statistical changes and to allow for future gene/protein quantification. Clearly there is a need to integrate the PA layer onto flex units on a microscope stage to track single cell behavior over time (e.g., using the STREX system). Further, dynamic changes in substrate stiffness should be investigated to study their interaction with changes in stretch.[12,114] Finally, chemical signals are integrated with mechanical signals within the cell, thus combinations of growth factors and mechanical stimuli should be examined in concert in future studies.

In summary, we report on a novel method for the study of mechanobiology which enables independent control of stretch and stiffness of the culture substrate. To facilitate adoption by other research groups, the method combines the most highly utilized tunable-stiffness substrate with the most common stretching apparatus available. Preliminary results demonstrate, for the first time, spreading of rounded cells on soft substrates in response to cyclic equibiaxial stretch. Studies using this method may increase our understanding of mechanical regulation of cell differentiation and phenotype, validate computational models of dynamic cell remodeling in response to stretch, and help elucidate molecular mechanisms involved in mechanotransduction of both outside-in and inside-out signaling.

5.6. Acknowledgements

We would like to thank our undergraduate researchers Cathryn Bedard and Mike Drnek

for testing countless gel formulation and covalent bonding techniques, Bhavika Shah and Heather Cirka for rheological testing, and Mehmet Kural for MATLAB expertise. We thank John McDonald, Peter Driscoll, Eftim Milkani for advising on the covalent bonding techniques. We would also like to thank Glenn Gaudette and Jeremy Skorinko for assistance with HDM, and Marsha Rolle and Tracy Gwyther for guidance on the culture of hMSCs.

Chapter 6 - Conclusions and Future Work

The work presented herein describes three distinct model systems for controlled modulation of the mechanical environment of cells cultured *in vitro*. We probed different aspects of VIC mechanobiology with each system and found VICs to be highly sensitive to both static and dynamic mechanical stimuli.

Data presented here and elsewhere[12,43] indicate that the level of stiffness required to maintain the quiescent VIC phoneotype is potentially too low for a material to both act as matrix to support cell growth in the non-activated state and also to withstand the mechanical loading that occurs during the cardiac cycle. If a very soft material is required to support the growth of an optimal VIC phenotype, a culture system prepared from a laminate material or a "supported" soft material could be beneficial. Alternatively, other cell types could be used.

In both the studies using 2D PA gels and 3D VIC populated gels, we observed an increase in activation (determined by aSMA expression, remodeling, contractile force, etc.) with TGF-β1 supplementation but only at the higher levels of stiffness tested. These results were in agreement with studies performed using lung fibroblasts[40] and give us some insight into the interactions between mechanical tension (stiffness) and TGF-β1.

The value in a high-throughput 2D PA gel system is to quickly and easily evaluate cells' response to a large range of stiffness levels which would be beneficial when selecting material properties for a tissue engineered product. Alternatively, numerous cell types or

media additives (drug candidates) can be screened.[40] Fluorescent microbeads could be incorporated into the gels in order to perform traction force microscopy[41] measurements of the force exerted on the gel by the cells in response to the stiffness of the gel or an externally applied chemical or biochemical stimuli. The semi-high-throughput method for evaluating the response of cells to a wide range of stiffness levels presented here has potential to be used in numerous other studies of both VICs and other adherent cells types. Understanding the response of cells to stiffness cues is important for basic mechanobiology research, designing materials and culture systems for tissue engineered products as well as developing other therapies, such as surgical intervention which could alter the mechanical environment and thus the stiffness of the cellular environment.[157]

An obvious follow-up to the study of the effects of 2D stiffness and of TGF-β1 on VICs is to broaden the range of TGF-β1 concentrations. Additionally, protein levels of αSMA expressed in response to stiffness and cytokine cues could be measured using semi-quantitative methods such as Western Blotting or ELISA. However, given the experimental format, the cells would require culturing at high densities and cell lysates from multiple wells would need to be pooled to obtain adequate quantities of protein for Western Blotting. Also of interest, is the expression levels of other biomarkers in myofibroblasts such as cofilin, in which cellular expression coincides with αSMA expression and is required for cell contraction.[11] In future studies, additional markers need be evaluated including those indicative of valve calcification. Wang et al. showed reversal of activated VIC phenotype using a gel system that softens when exposed to

light.[43] A high-throughput gel system capable of softening would be of interested for future studies in order to further evaluate the threshold stiffness levels for activation and subsequently reversal of the myofibroblast phenotype.

In native valves, cell density of adult valves is 10% of the fetal valve density.[158] Cells start in close contact and as the valve matures, the distance between the cells increases. These studies primarily used VICs seeded at a low or medium density in order to study the effects of substrate stiffness without the confounding effects of cell-cell interactions. *In vivo* however, cell-cell interactions are vital for cell function. These cell-cell interactions could take the form of secretion of soluble factors into the media or forces transferred through the surrounding ECM and/or adjacent cells. We show in Figure 3.1 how the cell morphology changes with increased cell density. The relationship between cell density and stiffness is further confounded in a 3D culture system where cells can interact on all sides. The overall cell density is higher but cells are not necessarily touching, validating our 2D model of low cell density. Future studies should be designed to evaluate the role of cell density in cellular response to substrate stiffness in order to optimize VIC density for TEHVs.

The 3D controlled boundary stiffness model is a powerful method for measuring the contractile forces the cell exerts on its surroundings in response to physical or chemical cues. This system could be used for a number of additional evaluations of stiffness levels, of other cell types, or of alternative gel materials such as synthetic or biopolymer systems. The addition of actuators to the controlled boundary stiffness device would

allow for the concomitant evaluation of tension (stiffness) and stretch similar to the 2D study presented in Chapter 5.

A number of additional studies could be performed using the modified Flexcell® system. Of particular interest are the mechanisms involved in the cells; "sensing" of stiffness and stretch. While there have been numerous studies with the aim of elucidating the sensing pathways, it remains unknown whether the same or independent pathways are involved in the sensing of stiffness and stretch. Many of these studies blocked specific receptors or pathways and evaluated the cellular response. Using the culture system described in Chapter 5, a well understood pathway, such as one involved in stiffness sensing, could be blocked and the responses to stretch alone could be evaluated. Could stretch function in place of stiffness to create a "stiff" environment? Further, could the cessation of stretch of a soft substrate cause a myofibroblast phenotype to revert back to the quiescent fibroblast phenotype? These are important questions that have relevance to both preparation of tissue engineered valves as well as to fundamental research on the onset and progression of valvular and other fibrotic diseases. A large scale culture system with defined stiffness and stretch levels could be used to condition cells prior to implantation in a tissue-engineered construct. Finally, the modified Flexcell® system could be used to evaluate other disease models such as idiopathic lung fibrosis or for the direction of stem cells down a specific lineage using both stiffness and stretch cues. Mesenchymal stem cells cultured in osteogenic media and cyclically stretched had decreased proliferation and increased mineralization compared to static controls[136]; a similar study using VICs

could provide insight on the role of stretch in valve calcification.These findings have numerous implications for understanding and treating heart valve disease and for heart valve tissue engineering. Understanding the role of mechanical stimulation of heart valves could lead to surgical intervention such as mechanical modifications of the valve geometry that reduce stresses across the valve tissue.[157] The same findings can be applied to the development of tissue engineered heart valves. While high levels of VIC activation are considered detrimental and characteristic of diseased valves, it is possible that during the development of TEHVs, activated VICs could be beneficial in their ability to produce collagen. Given the growing knowledge base around VIC activation, it may be possible to use activated VICs during valve development and then induce VICs return to the "quiescent" state prior to implantation through chemical or mechanical means. Like the native valve, an ideal TEHV would have predominantly quiescent VICs that are capable of activation to myofibroblasts for valve maintenance and repair. Towards this, several groups have developed gels capable of softening upon exposure to light.[114,159] Utilizing this system with VICs, demonstrated that softening the culture substrate from 32 kPa (similar stiffness to pre-calcified disease tissue) to 7 kPa (similar stiffness to healthy cardiac valve fibrosa) caused myofibroblasts to de-activate to quiescent fibroblasts.[159] The de-differentiation of VICs was reversible indicating that VICs could be activated during valve development and return to the quiescent state prior to implantation. These studies add to the general state of the field mechanobiology as a whole and are positioned to help elucidate the relationship between mechanical deformation and the biological

response of VICs.[160]

In summary, these studies provide information that is critical for understanding how VICs respond to mechanical stimuli, data that are important for the development of tissue engineered heart valves and contribute to the understanding of the role of mechanical cues on valve pathology and disease onset and progression. While this work is focused on VICs, the culture conditions and methods for applying mechanical stimulation could be applied to numerous other adherent cell types providing information on the response to mechanical stimuli relevant for optimizing cell culture, tissue engineering or fundamental research of disease states.

References

1. Barnett SD, Ad N. Surgery for aortic and mitral valve disease in the United States: a trend of change in surgical practice between 1998 and 2005. J Thorac Cardiovasc Surg. 2009;137(6):1422-9.
2. Deck JD, Thubrikar MJ, Schneider PJ, Nolan SP. Structure, stress, and tissue repair in aortic valve leaflets. Cardiovasc Res 1988;22(1):7-16.
3. Levitt LC, Thubrikar MJ, Nolan SP. Patterns and pathogenesis of calcification in pathologic human aortic valves. Curr Surg. 1984;41(1):17-9.
4. Thubrikar MJ, Aouad J, Nolan SP. Patterns of calcific deposits in operatively excised stenotic or purely regurgitant aortic valves and their relation to mechanical stress. Am J Cardiol. 1986;58(3):304-8.
5. Merryman WD, Youn I, Lukoff HD, Krueger PM, Guilak F, Hopkins RA, Sacks MS. Correlation between heart valve interstitial cell stiffness and transvalvular pressure: implications for collagen biosynthesis. Am J Physiol Heart Circ Physiol 2006;290(1):H224-31.
6. Mulholland DL, Gotlieb AI. Cell biology of valvular interstitial cells. Can J Cardiol 1996;12(3):231-6.
7. Olsson M, Rosenqvist M, Nilsson J. Expression of HLA-DR antigen and smooth muscle cell differentiation markers by valvular fibroblasts in degenerative aortic stenosis. J Am Coll Cardiol 1994;24(7):1664-71.
8. Rabkin-Aikawa E, Farber M, Aikawa M, Schoen FJ. Dynamic and reversible changes of interstitial cell phenotype during remodeling of cardiac valves. J Heart Valve Dis 2004;13(5):841-7.
9. Darby I, Skalli O, Gabbiani G. Alpha-smooth muscle actin is transiently expressed by myofibroblasts during experimental wound healing. Lab Invest. 1990;63(1):21-9.
10. Walker GA, Masters KS, Shah DN, Anseth KS, Leinwand LA. Valvular Myofibroblast Activation by Transforming Growth Factor-{beta}. Implications for Pathological Extracellular Matrix Remodeling in Heart Valve Disease. Circ Res 2004;24:24.
11. Pho M, Lee W, Watt DR, Laschinger C, Simmons CA, McCulloch CA. Cofilin is a marker of myofibroblast differentiation in cells from porcine aortic cardiac valves. Am J Physiol Heart Circ Physiol 2008;294(4):H1767-78.
12. Kloxin AM, Benton JA, Anseth KS. In situ elasticity modulation with dynamic substrates to direct cell phenotype. 2009.
13. Balachandran K, Konduri S, Sucosky P, Jo H, Yoganathan AP. An ex vivo study of the biological properties of porcine aortic valves in response to circumferential cyclic stretch. Ann Biomed Eng. 2006;34(11):1655-65.
14. Ku CH, Johnson PH, Batten P, Sarathchandra P, Chambers RC, Taylor PM, Yacoub MH, Chester AH. Collagen synthesis by mesenchymal stem cells and

aortic valve interstitial cells in response to mechanical stretch. Cardiovasc Res. 2006;71(3):548-56.
15. Engelmayr GC, Jr., Rabkin E, Sutherland FW, Schoen FJ, Mayer JE, Jr., Sacks MM. The independent role of cyclic flexure in the early in vitro development of an engineered heart valve tissue. Biomaterials 2005;26(2):175-87.
16. Balachandran K, Sucosky P, Jo H, Yoganathan AP. Elevated cyclic stretch induces aortic valve calcification in a bone morphogenic protein-dependent manner. Am J. Pathol. 2010;177(1):49-57.
17. Yetkin E, Waltenberger J. Molecular and cellular mechanisms of aortic stenosis. Int J Cardiol. 2009;135(1):4-13.
18. Otto CM, Kuusisto J, Reichenbach DD, Gown AM, O'Brien KD. Characterization of the early lesion of 'degenerative' valvular aortic stenosis. Histological and immunohistochemical studies. Circulation. 1994;90(2):844-53.
19. Chen JH, Simmons CA. Cell-matrix interactions in the pathobiology of calcific aortic valve disease: critical roles for matricellular, matricrine, and matrix mechanics cues. Circ Res 2011;108(12):1510-24.
20. Balachandran K, Sucosky P, Yoganathan AP. Hemodynamics and mechanobiology of aortic valve inflammation and calcification. Int J. Inflam 2011.
21. Merryman WD, Huang HY, Schoen FJ, Sacks MS. The effects of cellular contraction on aortic valve leaflet flexural stiffness. J Biomech 2006;39(1):88-96.
22. Filip DA, Radu A, Simionescu M. Interstitial cells of the heart valves possess characteristics similar to smooth muscle cells. Circ Res 1986;59(3):310-20.
23. Messier RH, Jr., Bass BL, Aly HM, Jones JL, Domkowski PW, Wallace RB, Hopkins RA. Dual structural and functional phenotypes of the porcine aortic valve interstitial population: characteristics of the leaflet myofibroblast. J Surg Res 1994;57(1):1-21.
24. Taylor PM, Batten P, Brand NJ, Thomas PS, Yacoub MH. The cardiac valve interstitial cell. Int J Biochem Cell Biol 2003;35(2):113-8.
25. Cushing MC, Liao JT, Anseth KS. Activation of valvular interstitial cells is mediated by transforming growth factor-beta1 interactions with matrix molecules. Matrix Biol. 2005;24(6):428-37.
26. Yip CY, Chen JH, Zhao R, Simmons CA. Calcification by valve interstitial cells is regulated by the stiffness of the extracellular matrix. Arterioscler Thromb Vasc Biol 2009;29(6):936-42.
27. Monzack EL, Masters KS. Can valvular interstitial cells become true osteoblasts? A side-by-side comparison. J Valve Dis. 2011;20(4):449-63.
28. Schenke-Layland K, Riemann I, Opitz F, Konig K, Halbhuber KJ, Stock UA. Comparative study of cellular and extracellular matrix composition of native and tissue engineered heart valves. Matrix Biol 2004;23(2):113-25.
29. Xing Y, He Z, Warnock JN, Hilbert SL, Yoganathan AP. Effects of constant static pressure on the biological properties of porcine aortic valve leaflets. Ann Biomed

Eng 2004;32(4):555-62.
30. Gabbiani G. The myofibroblast in wound healing and fibrocontractive diseases. J Pathol 2003;200(4):500-3.
31. Discher DE, Janmey P, Wang YL. Tissue cells feel and respond to the stiffness of their substrate. Science 2005;310(5751):1139-43.
32. Tomasek JJ, Gabbiani G, Hinz B, Chaponnier C, Brown RA. Myofibroblasts and mechano-regulation of connective tissue remodelling. Nat Rev Mol Cell Biol 2002;3(5):349-63.
33. Hinz B, Mastrangelo D, Iselin CE, Chaponnier C, Gabbiani G. Mechanical tension controls granulation tissue contractile activity and myofibroblast differentiation. Am J Pathol 2001;159(3):1009-20.
34. Eastwood M, Mudera VC, McGrouther DA, Brown RA. Effect of precise mechanical loading on fibroblast populated collagen lattices: morphological changes. Cell Motil Cytoskeleton 1998;40(1):13-21.
35. Grouf JL, Throm AM, Balestrini JL, Bush KA, Billiar KL. Differential effects of EGF and TGF-beta1 on fibroblast activity in fibrin-based tissue equivalents. Tissue Eng. 2007;13(4):799-807.
36. Grinnell F. Fibroblast biology in three-dimensional collagen matrices. Trends Cell Biol. 2003;13(5):264-9.
37. Tibbitt MW, Anseth KS. Hydrogels as extracellular matrix mimics for 3D cell culture. Biotechnol Bioeng. 2009;103(4):655-63.
38. Engler AJ, Sen S, Sweeney HL, Discher DE. Matrix elasticity directs stem cell lineage specification. Cell 2006;126(4):677-89.
39. Zemel A, Rehfeldt F, Brown AE, Discher DE, Safran SA. Optimal matrix rigidity for stress fiber polarization in stem cells. Nat Phys 2010;6(6):468-473.
40. Mih JD, Sharif AS, Liu F, Marinkovic A, Symer MM, Tschumperlin DJ. A multiwell platform for studying stiffness-dependent cell biology. PLoS 2011;6(5):e19929.
41. Marinkovic A, Mih JD, Park JA, Liu F, Tschumperlin DJ. Improved throughput traction microscopy reveals pivotal role for matrix stiffness in fibroblast contractility and TGF-beta responsiveness. Am J Physiol Lung Cell Mol Physiol 2012;2012:1.
42. Benton JA, Kern HB, Anseth KS. Substrate properties influence calcification in valvular interstitial cell culture. J Heart Valve Dis. 2008;17(6):689-99.
43. Wang H, Haeger S, Kloxin A, Leinwand L, Anseth K. Redirecting Valvular Myofibroblasts into Dormant Fibroblasts through Light-mediated Reduction in Substrate Modulus. PLoS 2012;7(7):e39969.
44. Leung DY, Glagov S, Mathews MB. Cyclic stretching stimulates synthesis of matrix components by arterial smooth muscle cells in vitro. Science 1976;191(4226):475-7.
45. Banes A, Tsuzaki M, Yamamoto J, Fischer T, Brigman B, Brown T, Miller L. Mechanoreception at the cellular level: the detection, interpretation, and diversity

of responses to mechanical signals. Biochem Cell Biol. 1995;73(7-8):349-65.
46. Shirinsky V, Antonov A, Birukov K, Sobolevsky A, Romanov Y, Kabaeva N, Antonova G, Smirnov V. Mechano-chemical control of human endothelium orientation and size. J Cell Biol. 1989;109(1):331-9.
47. Hsu HJ, Lee CF, Locke A, Vanderzyl SQ, Kaunas R. Stretch-induced stress fiber remodeling and the activations of JNK and ERK depend on mechanical strain rate, but not FAK. PLoS 2010;5(8):e12470.
48. Dartsch P, Betz E. Response of cultured endothelial cells to mechanical stimulation. Basic Res Cardiol. 1989;84(3):268-81.
49. Michalopoulos E, Knight RL, Korossis S, Kearney JN, Fisher J, Ingham E. Development of methods for studying the differentiation of human mesenchymal stem cells under cyclic compressive strain. Tissue Eng Part C Methods. 2011;18(4):252-62.
50. Park JS, Chu JS, Cheng C, Chen F, Chen D, Li S. Differential effects of equiaxial and uniaxial strain on mesenchymal stem cells. Biotechnol Bioeng. 2004;88(3):359-68.
51. Cassino TR, Drowley L, Okada M, Beckman SA, Keller B, Tobita K, Leduc PR, Huard J. Mechanical loading of stem cells for improvement of transplantation outcome in a model of acute myocardial infarction: the role of loading history. Tissue Eng Part A 2012;18(11-12):1101-8.
52. Yap CH, Kim HS, Balachandran K, Weiler M, Haj-Ali R, Yoganathan AP. Dynamic deformation characteristics of porcine aortic valve leaflet under normal and hypertensive conditions. Am J Physiol Heart Circ Physiol 2009;298(2):H395-405.
53. Thubrikar MJ, Nolan SP, Aouad J, Deck JD. Stress sharing between the sinus and leaflets of canine aortic valve. Ann Thorac Surg. 1986;42(4):434-40.
54. Liu AC, Gotlieb AI. Transforming growth factor-beta regulates in vitro heart valve repair by activated valve interstitial cells. Am J Pathol. 2008;173(5):1275-85.
55. Villar AV, Cobo M, Llano M, Montalvo C, Gonzalez-Vilchez F, Martin-Duran R, Hurle MA, Nistal JF. Plasma levels of transforming growth factor-beta1 reflect left ventricular remodeling in aortic stenosis. PLoS One. 2009;4(12):e8476.
56. Anscher MS, Peters WP, Reisenbichler H, Petros WP, Jirtle RL. Transforming growth factor beta as a predictor of liver and lung fibrosis after autologous bone marrow transplantation for advanced breast cancer. N Engl J Med. 1993;328(22):1592-8.
57. Jian B, Narula N, Li QY, Mohler ER, 3rd, Levy RJ. Progression of aortic valve stenosis: TGF-beta1 is present in calcified aortic valve cusps and promotes aortic valve interstitial cell calcification via apoptosis. Ann Thorac Surg 2003;75(2):457-65; discussion 465-6.
58. DeForest CA, Anseth KS. Advances in bioactive hydrogels to probe and direct cell fate. Annu Chem Biomol Eng. 2012;3:421-44.

59. Harris AK, Wild P, Stopak D. Silicone rubber substrata: a new wrinkle in the study of cell locomotion. Science 1980;208(4440):177-9.
60. Brown XQ, Ookawa K, Wong JY. Evaluation of polydimethylsiloxane scaffolds with physiologically-relevant elastic moduli: interplay of substrate mechanics and surface chemistry effects on vascular smooth muscle cell response. Biomaterials 2005;26(16):3123-9.
61. Pelham RJ, Jr., Wang Y. Cell locomotion and focal adhesions are regulated by substrate flexibility. Proc Natl Acad Sci U S A 1997;94(25):13661-5.
62. Engler A, Bacakova L, Newman C, Hategan A, Griffin M, Discher D. Substrate compliance versus ligand density in cell on gel responses. Biophys J 2004;86(1 Pt 1):617-28.
63. Lo CM, Wang HB, Dembo M, Wang YL. Cell movement is guided by the rigidity of the substrate. Biophys J 2000;79(1):144-52.
64. Wang YL, Pelham RJ, Jr. Preparation of a flexible, porous polyacrylamide substrate for mechanical studies of cultured cells. Methods Enzymol 1998;298:489-96.
65. Benigo KA, Lo CM, Wang YL. Flexible polyacrylamide substrata for the analysis of mechanical interactions at cell-substratum adhesions. Methods in Cell Biology: Elsevier Science; 2002. p 325-339.
66. Marganski WA, Dembo M, Wang YL. Measurements of cell-generated deformations on flexible substrata using correlation-based optical flow. Methods Enzymol 2003;361:197-211.
67. Tan JL, Tien J, Pirone DM, Gray DS, Bhadriraju K, Chen CS. Cells lying on a bed of microneedles: an approach to isolate mechanical force. Proc Natl Acad Sci U S A 2003;100(4):1484-9.
68. Cukierman E, Pankov R, Yamada KM. Cell interactions with three-dimensional matrices. Curr Opin Cell Biol. 2002;14(5):633-9.
69. Pedersen JA, Swartz MA. Mechanobiology in the third dimension. Ann Biomed Eng 2005;33(11):1469-90.
70. Elsdale T, Bard J. Collagen substrata for studies on cell behavior. J Cell Biol 1972;54(3):626-37.
71. Arora PD, Narani N, McCulloch CA. The compliance of collagen gels regulates transforming growth factor-beta induction of alpha-smooth muscle actin in fibroblasts. Am J Pathol 1999;154(3):871-82.
72. Knezevic V, Sim AJ, Borg TK, Holmes JW. Isotonic biaxial loading of fibroblast-populated collagen gels: a versatile, low-cost system for the study of mechanobiology. Biomech Model Mechanobiol. 2002;1(1):59-67.
73. Brown TD. Techniques for mechanical stimulation of cells in vitro: a review. J Biomech. 2000;33(1):3-14.
74. Tschumperlin DJ, Margulies SS. Equibiaxial deformation-induced injury of alveolar epithelial cells in vitro. Am J Physiol. 1998;275(6 Pt 1):L1173-83.
75. Deng L, Fairbank NJ, Cole DJ, Fredberg JJ, Maksym GN. Airway smooth muscle

tone modulates mechanically induced cytoskeletal stiffening and remodeling. J Appl Physiol. 2005;99(2):634-41.
76. Krishnan R, Park C, Lin Y, Mead J, Jaspers R, Trepat X, Lenormand G, Tambe D, Smolensky A, Knoll A and others. Reinforcement versus fluidization in cytoskeletal mechanoresponsiveness. PLoS One 2009;4(5):e5486.
77. Nagayama K, Adachi A, Matsumoto T. Heterogeneous response of traction force at focal adhesions of vascular smooth muscle cells subjected to macroscopic stretch on a micropillar substrate. J 2011;44(15):2699-705.
78. Mann JM, Lam RH, Weng S, Sun Y, Fu J. A silicone-based stretchable micropost array membrane for monitoring live-cell subcellular cytoskeletal response. Lab 2011;12(4):731-40.
79. Ingber DE. Tensegrity II. How structural networks influence cellular information processing networks. J Cell Sci. 2003;116(Pt 8):1397-408.
80. Rabkin E, Aikawa M, Stone JR, Fukumoto Y, Libby P, Schoen FJ. Activated interstitial myofibroblasts express catabolic enzymes and mediate matrix remodeling in myxomatous heart valves. Circulation 2001;104(21):2525-32.
81. Hinz B. The myofibroblast: paradigm for a mechanically active cell. J Biomech 2010;43(1):146-55.
82. Della Rocca F, Sartore S, Guidolin D, Bertiplaglia B, Gerosa G, Casarotto D, Pauletto P. Cell composition of the human pulmonary valve: a comparative study with the aortic valve--the VESALIO Project. Vitalitate Exornatum Succedaneum Aorticum labore Ingegnoso Obtinebitur. Ann Thorac Surg 2000;70(5):1594-600.
83. Liao J, Joyce EM, Sacks MS. Effects of decellularization on the mechanical and structural properties of the porcine aortic valve leaflet. Biomaterials 2008;29(8):1065-74.
84. Wang HB, Dembo M, Wang YL. Substrate flexibility regulates growth and apoptosis of normal but not transformed cells. Am J Physiol Cell Physiol 2000;279(5):C1345-50.
85. Yperman J, De Visscher G, Holvoet P, Flameng W. Molecular and functional characterization of ovine cardiac valve-derived interstitial cells in primary isolates and cultures. Tissue Eng 2004;10(9-10):1368-75.
86. Taylor PM, Allen SP, Yacoub MH. Phenotypic and functional characterization of interstitial cells from human heart valves, pericardium and skin. J Heart Valve Dis 2000;9(1):150-8.
87. Guo WH, Frey MT, Burnham NA, Wang YL. Substrate rigidity regulates the formation and maintenance of tissues. Biophys J 2006;90(6):2213-20.
88. Reinhart-King CA, Dembo M, Hammer DA. Cell-cell mechanical communication through compliant substrates. Biophys J 2008;95(12):6044-51.
89. Billiar KL, Sacks MS. Biaxial mechanical properties of the natural and glutaraldehyde treated aortic valve cusp: Part I - Experimental results. Journal of Biomechanical Engineering 2000;122(1):23-30.
90. Liu F, Mih JD, Shea BS, Kho AT, Sharif AS, Tager AM, Tschumperlin DJ.

Feedback amplification of fibrosis through matrix stiffening and COX-2 suppression. J Cell Biol 2010;190(4):693-706.
91. Wang M, Hill RJ. Electric-field-induced displacement of charged spherical colloids in compressible hydrogels. Soft Matter 2008;4(5):1048-1058.
92. Bryant S, Anseth, KS. Photopolymerization of hydrogel scaffold. In: Ma P, Elisseeff, J, editor. Scaffolding in tissue engineering. Boca Raton, FL: Taylor and Francis Group; 2005. p 71-90.
93. Young R, Lovell, PA. Introduction to Polymers. London, UK: Chapman & Hall; 1991.
94. Hoerstrup SP, Kadner A, Melnitchouk S, Trojan A, Eid K, Tracy J, Sodian R, Visjager JF, Kolb SA, Grunenfelder J and others. Tissue engineering of functional trileaflet heart valves from human marrow stromal cells. Circulation 2002;106(12 Suppl 1):I143-50.
95. Munevar S, Wang Y, Dembo M. Traction force microscopy of migrating normal and H-ras transformed 3T3 fibroblasts. Biophys J 2001;80(4):1744-57.
96. Dembo M, Oliver T, Ishihara A, Jacobson K. Imaging the traction stresses exerted by locomoting cells with the elastic substratum method. Biophys J 1996;70(4):2008-22.
97. Dembo M, Wang YL. Stresses at the cell-to-substrate interface during locomotion of fibroblasts. Biophys J 1999;76(4):2307-16.
98. Quinlan AM, Billiar KL. Investigating the role of substrate stiffness in the persistence of valvular interstitial cell activation. J Biomed Mater Res A 2012;2012(12).
99. Goffin JM, Pittet P, Csucs G, Lussi JW, Meister JJ, Hinz B. Focal adhesion size controls tension-dependent recruitment of alpha-smooth muscle actin to stress fibers. J Cell Biol 2006;172(2):259-68.
100. Engler AJ, Carag-Krieger C, Johnson CP, Raab M, Tang HY, Speicher DW, Sanger JW, Sanger JM, Discher DE. Embryonic cardiomyocytes beat best on a matrix with heart-like elasticity: scar-like rigidity inhibits beating. J Cell Sci 2008;121(Pt 22):3794-802.
101. Pedersen J, Swartz M. Mechanobiology in the third dimension. Ann Biomed Eng. 2005;33(11):1469-90.
102. Robinson PS, Tranquillo RT. Planar biaxial behavior of fibrin-based tissue-engineered heart valve leaflets. Tissue Eng Part A. 2009;15(10):2763-72.
103. Jiao T, Clifton RJ, Converse GL, Hopkins RA. Measurements of the Effects of Decellularization on Viscoelastic Properties of Tissues in Ovine, Baboon, and Human Heart Valves. Tissue Eng Part A 2011:26.
104. Cushing MC, Liao JT, Jaeggli MP, Anseth KS. Material-based regulation of the myofibroblast phenotype. Biomaterials 2007;28(23):3378-87.
105. Masters KS, Darshita NS, Gennyne W, Leslie AL, Kristi SA. Designing scaffolds for valvular interstitial cells: Cell adhesion and function on naturally derived materials. Journal of Biomedical Materials Research Part A 2004;71A(1):172-

180.
106. Chen WL, Likhitpanichkul M, Ho A, Simmons CA. Integration of statistical modeling and high-content microscopy to systematically investigate cell-substrate interactions. Biomaterials 2010;31(9):2489-97.
107. Chen CS, Mrksich M, Huang S, Whitesides GM, Ingber DE. Geometric control of cell life and death. Science 1997;276(5317):1425-8.
108. Liu AC, Gotlieb AI. Characterization of cell motility in single heart valve interstitial cells in vitro. Histol Histopathol 2007;22(8):873-82.
109. Beningo KA, Dembo M, Kaverina I, Small JV, Wang YL. Nascent focal adhesions are responsible for the generation of strong propulsive forces in migrating fibroblasts. J Cell Biol 2001;153(4):881-8.
110. Li C, Gotlieb AI. Transforming growth factor-beta regulates the growth of valve interstitial cells in vitro. Am J Pathol 2011;179(4):1746-55.
111. Smith S, Taylor PM, Chester AH, Allen SP, Dreger SA, Eastwood M, Yacoub MH. Force generation of different human cardiac valve interstitial cells: relevance to individual valve function and tissue engineering. J Heart Valve Dis. 2007;16(4):440-6.
112. Martin P. Wound healing--aiming for perfect skin regeneration. Science 1997;276(5309):75-81.
113. Rowlands AS, George PA, Cooper-White JJ. Directing osteogenic and myogenic differentiation of MSCs: interplay of stiffness and adhesive ligand presentation. Am J Physiol Cell Physiol 2008;295(4):C1037-44.
114. Frey MT, Wang YL. A photo-modulatable material for probing cellular responses to substrate rigidity. Soft Matter 2009;5:1918-1924.
115. John J, Quinlan AT, Silvestri C, Billiar K. Boundary stiffness regulates fibroblast behavior in collagen gels. Ann Biomed Eng 2010;38(3):658-73.
116. Grinnell F, Petroll WM. Cell motility and mechanics in three-dimensional collagen matrices. Annu Cell Dev Biol. 2010;26:335-61.
117. Grinnell F. Fibroblasts, myofibroblasts, and wound contraction. J Cell Biol. 1994;124(4):401-4.
118. Bell E, Ivarsson B, Merrill C. Production of a tissue-like structure by contraction of collagen lattices by human fibroblasts of different proliferative potential in vitro. Proc Natl Acad Sci U S A. 1979;76(3):1274-8.
119. Thomopoulos S, Fomovsky GM, Holmes JW. The development of structural and mechanical anisotropy in fibroblast populated collagen gels. J Biomech Eng. 2005;127(5):742-50.
120. Kershaw JD, Misfeld M, Sievers HH, Yacoub MH, Chester AH. Specific regional and directional contractile responses of aortic cusp tissue. J Heart Valve Dis. 2004;13(5):798-803.
121. Ingber DE, Prusty D, Sun Z, Betensky H, Wang N. Cell shape, cytoskeletal mechanics, and cell cycle control in angiogenesis. J Biomech. 1995;28(12):1471-84.

122. Tamariz E, Grinnell F. Modulation of fibroblast morphology and adhesion during collagen matrix remodeling. Mol Biol Cell. 2002;13(11):3915-29.
123. Billiar KL, Throm AM, Frey MT. Biaxial failure properties of planar living tissue equivalents. J Biomed Mater Res A. 2005;73(2):182-91.
124. Legant WR, Pathak A, Yang MT, Deshpande VS, McMeeking RM, Chen CS. Microfabricated tissue gauges to measure and manipulate forces from 3D microtissues. Proc Natl Acad Sci U S A. 2009;106(25):10097-102.
125. Wang JH, Thampatty BP. An introductory review of cell mechanobiology. Biomech Model Mechanobiol 2006;5(1):1-16.
126. Kaunas R, Nguyen P, Usami S, Chien S. Cooperative effects of Rho and mechanical stretch on stress fiber organization. Proc Natl Acad Sci U S A 2005;102(44):15895-900.
127. Tschumperlin DJ, Margulies SS. Equibiaxial deformation-induced injury of alveolar epithelial cells in vitro. Am J Physiol 1998;275(6 Pt 1):L1173-83.
128. Solon J, Levental I, Sengupta K, Georges PC, Janmey PA. Fibroblast adaptation and stiffness matching to soft elastic substrates. Biophys J 2007;93(12):4453-61.
129. Jacot JG, McCulloch AD, Omens JH. Substrate stiffness affects the functional maturation of neonatal rat ventricular myocytes. Biophys J 2008;95(7):3479-87.
130. Fu J, Wang YK, Yang MT, Desai RA, Yu X, Liu Z, Chen CS. Mechanical regulation of cell function with geometrically modulated elastomeric substrates. Nat 2010;7(9):733-6.
131. Silver JH, Lin JC, Lim F, Tegoulia VA, Chaudhury MK, Cooper SL. Surface properties and hemocompatibility of alkyl-siloxane monolayers supported on silicone rubber: effect of alkyl chain length and ionic functionality. Biomaterials 1999;20(17):1533-43.
132. Throm QAM, Sierad LN, Capulli AK, Firstenberg LE, Billiar KL. Combining dynamic stretch and tunable stiffness to probe cell mechanobiology in vitro. PLoS 2011;6(8):e23272.
133. Kelly DJ, Azeloglu EU, Kochupura PV, Sharma GS, Gaudette GR. Accuracy and reproducibility of a subpixel extended phase correlation method to determine micron level displacements in the heart. Med Eng Phys 2007;29(1):154-62.
134. Berry MF, Engler AJ, Woo YJ, Pirolli TJ, Bish LT, Jayasankar V, Morine KJ, Gardner TJ, Discher DE, Sweeney HL. Mesenchymal stem cell injection after myocardial infarction improves myocardial compliance. Am J Physiol Heart Circ Physiol 2006;290(6):H2196-203.
135. Altman GH, Lu HH, Horan RL, Calabro T, Ryder D, Kaplan DL, Stark P, Martin I, Richmond JC, Vunjak-Novakovic G. Advanced bioreactor with controlled application of multi-dimensional strain for tissue engineering. J Biomech Eng 2002;124(6):742-9.
136. Simmons CA, Matlis S, Thornton AJ, Chen S, Wang CY, Mooney DJ. Cyclic strain enhances matrix mineralization by adult human mesenchymal stem cells via the extracellular signal-regulated kinase (ERK1/2) signaling pathway. J Biomech

2003;36(8):1087-96.
137. Huang H, Kamm RD, Lee RT. Cell mechanics and mechanotransduction: pathways, probes, and physiology. Am J Physiol Cell Physiol 2004;287(1):C1-11.
138. Park JS, Huang NF, Kurpinski KT, Patel S, Hsu S, Li S. Mechanobiology of mesenchymal stem cells and their use in cardiovascular repair. Front Biosci 2007;12:5098-116.
139. Kurpinski K, Chu J, Hashi C, Li S. Anisotropic mechanosensing by mesenchymal stem cells. Proc Natl Acad Sci U S A 2006;103(44):16095-100.
140. Zhang J, Wang JH. Mechanobiological response of tendon stem cells: implications of tendon homeostasis and pathogenesis of tendinopathy. J Orthop Res. 2010;28(5):639-43.
141. Chen YJ, Huang CH, Lee IC, Lee YT, Chen MH, Young TH. Effects of cyclic mechanical stretching on the mRNA expression of tendon/ligament-related and osteoblast-specific genes in human mesenchymal stem cells. Connect Tissue Res 2008;49(1):7-14.
142. Wang JH, Goldschmidt-Clermont P, Yin FC. Contractility affects stress fiber remodeling and reorientation of endothelial cells subjected to cyclic mechanical stretching. Ann Biomed Eng 2000;28(10):1165-71.
143. Califano JP, Reinhart-King CA. Substrate Stiffness and Cell Area Predict Cellular Traction Stresses in Single Cells and Cells in Contact. Cell 2010;3(1):68-75.
144. Chen J, Li H, SundarRaj N, Wang J. Alpha-smooth muscle actin expression enhances cell traction force. Cell Motil Cytoskeleton. 2007;64(4):248-57.
145. Wang D, Xie Y, Yuan B, Xu J, Gong P, Jiang X. A stretching device for imaging real-time molecular dynamics of live cells adhering to elastic membranes on inverted microscopes during the entire process of the stretch. Integr 2010;2(5-6):288-93.
146. Neidlinger-Wilke C, Grood ES, Wang JHC, Brand RA, Claes L. Cell alignment is induced by cyclic changes in cell length: studies of cells grown in cyclically stretched substrates. J Orthop Res. 2001;19(2):286-93.
147. Wang JH, Goldschmidt-Clermont P, Wille J, Yin FC. Specificity of endothelial cell reorientation in response to cyclic mechanical stretching. J Biomech. 2001;34(12):1563-72.
148. Hsu HJ, Lee CF, Kaunas R. A dynamic stochastic model of frequency-dependent stress fiber alignment induced by cyclic stretch. PLoS One 2009;4(3):e4853.
149. Wang JH. Substrate deformation determines actin cytoskeleton reorganization: A mathematical modeling and experimental study. J Theor Biol 2000;202(1):33-41.
150. Humphrey JD, Rajagopal KR. A constrained mixture model for arterial adaptations to a sustained step change in blood flow. Biomech Model Mechanobiol 2003;2(2):109-26.
151. Gao M, Craig D, Vogel V, Schulten K. Identifying unfolding intermediates of FN-III(10) by steered molecular dynamics. J Mol Biol. 2002;323(5):939-50.
152. Martinac B. Mechanosensitive ion channels: molecules of mechanotransduction. J

Cell Sci. 2004;117(Pt 12):2449-60.
153. Nemir S, West JL. Synthetic materials in the study of cell response to substrate rigidity. Ann Biomed Eng 2009;38(1):2-20.
154. Buxboim A, Rajagopal K, Brown A, Discher D. How deeply cells feel: methods for thin gels. J Condens Matter 2010;22(19).
155. Seliktar D, Black RA, Vito RP, Nerem RM. Dynamic mechanical conditioning of collagen-gel blood vessel constructs induces remodeling in vitro. Ann Biomed Eng 2000;28(4):351-62.
156. Balestrini JL, Billiar KL. Equibiaxial cyclic stretch stimulates fibroblasts to rapidly remodel fibrin. J Biomech 2005;28.
157. Salgo IS, Gorman JH, 3rd, Gorman RC, Jackson BM, Bowen FW, Plappert T, St JSMG, Edmunds LH, Jr. Effect of annular shape on leaflet curvature in reducing mitral leaflet stress. Circulation. 2002;106(6):711-7.
158. Aikawa E, Whittaker P, Farber M, Mendelson K, Padera RF, Aikawa M, Schoen FJ. Human semilunar cardiac valve remodeling by activated cells from fetus to adult: implications for postnatal adaptation, pathology, and tissue engineering. Circulation. 2006;113(10):1344-52.
159. Wang H, Haeger SM, Kloxin AM, Leinwand LA, Anseth KS. Redirecting Valvular Myofibroblasts into Dormant Fibroblasts through Light-mediated Reduction in Substrate Modulus. PLoS 2012;7(7):e39969.
160. David MW, Engler AJ. Innovations in cell mechanobiology. J Biomech 2009;43(1):1.

•

Appendices

Appendix A Aortic and Mitral VIC Isolation Protocol

Source: Messier 1994, Taylor 2002, Butcher 2004 – also modified from personal experiences

Materials:

- Collagenase (Worthington Collagenase, Type I (650 U/mL)
- Sterile PBS
- DMEM + Penicillin/Streptomycin (1 µg/mL)
- DMEM +10% FBS + Penicillin/Streptomycin (1 µg/mL)
- Cell scrapers
- Culture dishes
- Nylon mesh conical tube filters
- Sterile 15 mL conical tubes
- Sterile scissors

Collagenase Preparation:

- Determine the volume of collagenase solution required for digestion.
  - Aortic valves (for up to 6 cusps) – 3 mL for endothelium digestion and (for up to 3 cusps) 3 mL for cell removal.
  - Mitral valves (for up to 2 cups) – 3 mL for endothelium digestion and 3 mL for cell removal.
- Calculate the mass of collagenase needed to make a 600 U/mL solution. (the units/mg are batch specific and can be found on the collagenase bottle).

$$v_{solution} \times \frac{600 Units}{ml} \times \frac{mg_{collagenase}}{Units_{collagenase}}$$

- Weigh out the collagenase and add to the appropriate volume of DMEM with P/S (NO Serum!!!)

Valve Dissection:

- Remove mitral and/or aortic valves and place individual cusp types in beakers with 15 mL sterile PBS to rinse. Continue rinsing valves to remove blood.
- Remove the cusps and place each in a 15 mL conical tube with 3 mL collagenase (per 6 aortic cusps or 2 mitral cusps).
- Place on rocker tray for 30 minutes at 37°C.
- Rinse cusps in sterile PBS.
- Place cusp in culture dish and scrape both sides with cell scraper to remove endothelial cells.
- Rinse in sterile PBS.
- Place rinsed cusp in new culture dish and mince into pieces approximately 1-2 mm^2 with sterile scissors or scalpel blade.
- Place minced cusp in new 15 mL conical tube.
- Add 3 mL of collagenase solution.
- Place on rocker tray for ~2 hr at 37°C or until valves are digested. You will need to keep checking the tubes so they don't digest for too long.
- Filter solution through nylon mesh into new 15 mL conical tube.
- Centrifuge at $1.2X10^3$ rpm and resuspend in DMEM +10% FBS.
- Perform cell count and plate.

Appendix B Glass Activation Protocol

Source: (Modified from) Yu-li Wang Laboratory January 4, 2006

Materials:

- No. 1 Coverslip, 43x50 mm rectangle coverslip - GoldSeal, cat# 3329
- Cell scraper
- NaOH, 0.1 N, 100 mL
- 3-aminopropyltrimethoxy silane - Acros, cat # 31325100
- 1x PBS
- Glutaraldehyde, 0.5% (prepared) in PBS (stock glutaraldehyde, Electron Microscopy Sciences, 70% solution, EM grade cat# 16360)

Glass Activation:

Make sure you keep track of which side is being activated!!

- If the gels are to be used for AFM, do not attach the activated glass to a petri dish, it won't fit on the AFM stage
- If the gels are to be used for cell culture, cut a hole in a 60 mm diameter Petri dish using a drill press and hole bit. Use 45 mm round coverslips. Attach the activated coverslip with PDMS. Or use custom made holders – use 43x50 mm coverslips attach coverslip with vacuum grease

- Pass one side of a 43x50 mm rectangle coverslip over inner flame of ethanol burner, place flamed side up on benchtop.
- Once cool, transfer to a plastic test tube rack. (The NaOH will react with an Aluminum rack.)
- Using a plastic pipet in the chemical hood, add approximately 6-8 drops of 0.1 N NaOH to the flamed side of the coverslip. Using a cell scraper, smear the NaOH until

it covers the entire coverslip. Let dry. Dry is indicated by a white substance on the surface of the coverslip.

- Using a glass pipet in the chemical hood, add approximately 6-8 drops of 3-aminopropyltrimethoxy silane. Smear with cell scraper until it covers entire coverslip.
- Incubate for 5 minutes at room temperature
- Place coverslips in dish with ddH_2O. Shake for 20-60 minutes, changing the water 3x (minimum) at room temperature or until the coverslips are clear. There will be a clear thick substance on glass – this should be rinsed off completely before continuing!!! (It is important to rinse well at this step, otherwise the coverslips will have a reddish tint after application of gluteraldehyde).
- Place coverslips back on plastic test tube racks and cover with 0.5% gluteraldehyde. Incubate for 30 minutes at room temperature.
- Place coverslips in ddH_2O dish and shake for 20-60 minutes, changing the water 3x (minimum) at room temperature or until the coverslips are clear.
- Dry coverslips vertically on test tubes racks to prevent water marks.
- Store at room temperature.
- Mount coverslips onto custom chambers with vacuum grease.

Appendix C Polyacrylamide Substrate Preparation and Protein Conjugation Protocol I

Source: (Modified from) Yu-li Wang Laboratory

Materials:

- Activated coverslips (see glass activation protocol)
- 22 mm round coverslips
- 1x PBS
- HEPES 1 M, pH 8.5, 1 mL
- HEPES 50 mM, pH 8.5, 500 mL
- Acrylamide 40% - Biorad, cat# 161-0140
- Bis 2% - Biorad, cat# 161-0142
- Ammonium Persulfate; 10 mg in 100 µL ddH_2O. Biorad, cat# 161-0700 (make fresh for each day of gel preparation)
- TEMED - Biorad, cat# 161-0801
- (If using gels for traction force microscopy) 0.2 µm diameter fluoresbrite yellow/green microspheres (unconjugated) – Polysciences cat# 17151
- Sulfo-SANPAH; 400 µL/22 mm gel at 0.5 mg/mL. Add 4 µL DMSO per 1 mg of sulfo-SANPAH. Use HEPES 50 mM at room temperature to bring to final volume. Prepare immediately before use. Pierce, cat# 22589
- Collagen (PureCol) 100 µg/mL diluted in 1x PBS ~1 mL solution per 22 mm diameter gel, enough to cover gel

Acrylamide Preparation:

- Make acrylamide solution in a 25 mL glass beaker according to the chart at the end of protocol. (if microbeads are required, replace 50 µL of the water with 50 µL of beads-sonacate beads for 1-2 minutes prior to adding to the solution).
- Place beaker in vacuum jar and degas solution for ~5 minutes. NOTE: Depending on the strength of your vacuum, the solution may start to bubble over or freeze. If this happens, RELEASE THE VACUUM SLOWLY!
- Add 30 µL ammonium persulfate and 20 µL TEMED to the acrylamide solution; mix gently.

- Pipet 20 µL onto activated coverslip and quickly place a 22 mm circular coverslip over acrylamide drop.
- Leave remaining acrylamide in beaker. It should polymerize in 20-30 minutes.
- Once polymerized, flood each gel with ~1 mL of 50 mM HEPES to assist in the removal of the 20 mm coverslip.
- Remove 20 mm coverslip by popping it off with the tip of a scalpel blade. Substrates can now be stored in PBS for 2 weeks at 4°C.

Final Acryl/Bis	40%Acrylamide	2%Bis	1M HEPES	H_20+Beads	Young's Modulus
12/0.6%	1500	1500	50	1950	70 kPa
8/0.08	1000	200	50	3750	10
5/0.10	625	250	50	4075	5
5/0.025	625	63	50	4262	1.5

Acrylamide Activation:

- Prepare Sulfo-SANPAH solution immediately before use.
- Remove as much liquid as possible without drying out the substrate. Add 200 µL Sulfo-SANPAH to substrate.
- Place 6 inches below 365 nm UV box for 6 minutes. Solution will become reddish brown when activated.
- Remove Sulfo-SANPAH and rinse with 50 mM Hepes.
- Add 200 µL Sulfo-SANPAH.
- Place on UV box for 6 minutes.
- Remove Sulfo-SANPAH.
- Wash with 50 mM HEPES and then flick off excess liquid.
- Add 1 mL collagen solution to each substrate and put on orbital shaker (slow rpm) for several hours at room temperature or overnight at 4°C.
- Rinse and store in PBS at 4°C for up to one week.
- Before plating, UV sterilize substrates for 15 minutes. (can be done in culture hood).

Appendix D Evaluating FN Density on NHS PA Gels with Antibody Conjugated Microbeads

Source: Lo et al. Biophysical Journal, 79, 2000, 144-152

Materials:

- NHS-PA gels on glass coverslips
- Vacuum grease
- Culture chambers
- 50 mL 0.5% BSA in PBS (0.25 g BSA, 50 mL PBS)
- Anti-fibronectin
- Anti-IgG conjugated microbeads
- 1x PBS

Procedure:

- Using a Kimwipre, dry the surface of the coverslip around gel.
- Apply a small amount of vacuum grease to the culture chambers.
- Seal the culture chambers to coverslips.
- Calculate volume of primary antibody needed (Use 1:100 dilution):
  - (# samples x 50 µL/sample) / = total volume of antibody solution

*Add one to the sample number to allow for volume loss during pipetting

Total volume / 100 (dilution factor) = volume of primary antibody stock solution

Total volume – volume of antibody stock = volume of BSA/PBS solution

- In an appropriate size tube, first add calculated volume of BSA/PBS solution, then add antibody stock and mix well.
- Rinse PA substrates 1x with PBS
- Remove PBS and block with 0.5% BSA in PBS for 10 minutes
- Aspirate BSA solution, add 50 µL antibody solution to each gel, and incubate 1 hr on orbital shaker at room temperature.
- Aspirate antibody solution.
- Rinse 3x – minutes each with BSA/PBS solution.

- Calculate volume of secondary antibody (1:40 dilution):
- (# samples x 50 µL/sample) / = total volume of antibody

*Add one to the sample number to allow for volume loss during pipetting

solution (make sure you account for secondary only controls)

Total volume / 40 (dilution factor) = volume of secondary antibody stock solution

Total volume – volume of antibody stock = volume of BSA/PBS solution

- Remove BSA/PBS solution and add 50 µL secondary antibody solution.
- Incubate for 30 minutes on orbital shaker at room temperature.
- Aspirate antibody solution.
- Rinse 3x – minutes each with BSA/PBS solution.
- Cover with PBS and image.

Appendix E Preparation of 5x DMEM for Fabrication of Fibroblast Populated Collagen Gels

Materials:

- Powdered DMEM
- Sodium bicarbonate ($NaHCO_3$)
- ddH_2O
- 100 mL beaker
- 2 graduated cylinders

Procedure:

- Pour 50 mL ddH_2O into a graduated cylinder.
- Remove 25 mL and add to a 100 mL beaker.
- Weigh out 3.37 g of powdered DMEM and 0.925 g of $NaHCO_3$ add both powders to the 100 mL beaker.
- Rinse the weigh boats with approximately 10 mL of ddH_2O (from the first graduated cylinder) to ensure all of the powder is removed.
- Place the beaker on a stir plate with stir bar. Once all of the powder is dissolved, pour the solution into the second graduated cylinder and bring the volume to 50 mL.
- Pour solution back into the beaker and stir until well mixed.
- In the tissue culture hood, sterile filter solution using a 50 mL filter-top conical tube.
- Label and store solution in fridge.

Appendix F Preparation of 5 mg/mL Collagen Solution for Fibroblast Populated Collagen Gels

Materials:

- Dry rat tail tendon collagen
- 5 mM HCl
- 50 mL conical tube

Procedure:

- Freeze dried rat tail tendon type I collagen is in the fridge in a plastic ziplock bag.
- Weigh out 150 mg (weigh twice for accuracy) and place a 50 mL conical tube.
- Pour 30 mL of sterile 5mM HCl into the 50 mL conical tube.
- Wrap tube with paraffin and attach to rotator in fridge.
- Mix for 12 hours. If bubbles are in the solution, centrifuge for 10 minutes at 1000 rpm prior to use.
- Label and store in the fridge.
- To check the collagen concentration of the solution, use the Sircol assay.

Appendix G Protocol for Fabrication of Fibroblast Populated Collagen Gels

Materials:

- 5 mg/mL collagen solution
- 5x DMEM (Dulbuccos Modified Eagles Medium)
- 0.1 M NaOH
- ATCC fibroblasts (Passage 5-9)
- DMEM with 10% FBS
- Trypsin
- Culture plate (specific type depends on experiment)

Aliquot and label the proper amounts (see spreadsheet) of the following, place in ice:

To calculate the correct volumes of solution needed for one experiment, use the excel spreadsheet (Collagen gel calculation spreadsheet).

- Collagen at 5 mg/mL (see preparation of collagen solution protocol) measure the necessary volume using a syringe
- 5X DMEM (see preparation of 5x DMEM protocol)
- 0.1 M NaOH

To obtain fibroblasts cells from T-150 flasks:

- Remove T-150 plates from incubator, look at under microscope to ensure viability and 80-90% confluency, then perform the following in sterile hood.
  Note: if cells are over 90% confluent, they should not be used. Cells change morphology at this density, which will alter the behavior of the cells.

- Aspirate media.
- Add 8 mL Trypsin with EDTA.

- Place each plate in the incubator, let sit for 5-10 minutes until cells have become unattached (there should be a yellowish cloudy appearance to the solution).
- Add 8 mL of warm media (1X DMEM, 10% FBS with penicillin/streptomycin) to each plate to deactivate the trypsin.
- Remove the liquid from the flask with a pipette, place into a 50 mL conical tube and centrifuge the cell solution at 1200 rpm for 6 minutes.
- Aspirate supernatant from tubes being careful not to disturb the pellet of cells in bottom.
- Resuspend the cells in a small volume (1-2 mL) of DMEM with 10% FBS noting the volume of liquid in mL for cell count.
- Mix the solution well and remove 100 µL of the cell-media solution from the center of the conical tube (this ensures an appropriate representation of the cell solution), and place in a 1-2 mL microcentrifuge tube. Add 100 µL of Trypan blue dye to the microcentrifuge tube and mix well (do not vortex, this will kill the cells). Place ~10 µL of this solution into the hematocytometer and perform a cell count.
- Add media to the tube in order to bring the cell concentration (cells/mL) to that listed on the Collagen Gel Calculation Sheet.
- Place the cells on ice immediately, and aliquot proper amounts for gel fabrication (per calculation spreadsheet). Proceed to next header OR
- For continued cell culture:
  - Resuspend cells with 5 mL of DMEM with 10% FBS.
  - Place cells in a T-150 flask. For cell passage, each T-150 flask should have 25 mL of DMEM with 10% FBS, penicillin/streptomysin, and amphatericin B and $1x10^6$ cells.
  - Slide flask in a figure 8 motion.
  - Place in incubator.

To fabricate gels:

NOTE: If a large volume of collagen gel solution is required, it may be advantageous to make 2 batches of gels to prevent the solution from polymerizing before all of the gels are plated.

- First add 5X DMEM, 0.1 M NaOH, and FBS to an appropriate sized conical tube mix well and then add the appropriate cell volume last (refer to calculation spreadsheet). Note: Since the DMEM-NaOH solution is very basic, it is important that cells are added last to minimize the time in this solution.

- Using a syringe, add the collagen to the aliquot of cell-media-5X DMEM-NaOH mixture, mix well with pipette until color is homogonous throughout, taking care not to add air bubbles to the mixture.
- Quickly add the desired volume of the collagen-cell solution to each well. Aspirate any bubbles off the top and swirl gently to assure solution is level and covers entire plate.
- Place gels in 37° incubator for 1 hour.
- Add 2 mL of media to each well (for 6-well plate) and place in incubator.
- Replace media every other day.

Appendix H Triple Stain Protocol (Phalloidin, αSMA, Hoechst)

Source: Modified protocol from Katie Bush

Materials:

- Fixing Solution (use .5 mL per sample)
    - 12 mL of 1.33X PBS with 4 mL of 16% formaldehyde and 32 µL of 100X Triton
        - 1.33X PBS = 1.6 mL of 10X PBS + 10.4 mL of ddH_2O
        - 16% formaldehyde (Ted Pella, prod #18505)
        - 100X Triton (Calbiochem)
- 1X PBS
    - 20 mL of 10X PBS (VWR) + 180 mL of ddH_2O
- Heat Denatured PBS/BSA solution (make around 300mL) – already made, use 0.25-0.5 mL/sample
    - 1X PBS
    - 1% BSA = For every 100 mL of PBS add 1 g of BSA (CAT)
    - Bring to 80˚ C for 10 minutes then aliquot as necessary, store at -20˚ C.
    - Let cool before applying to samples
- Phallotoxin
    - Working solution
        - For each well to be evaluated, 5 µL stock + 200 µL 1X PBS (Protect from light)
        - Need 4 mL – Add 100 µL of phallotoxin stock solution to 4 mL 1X PBS
- Anti-αSMA Solution (1:500 dilution)
    - For each well to be evaluated, 200 µL antibody solution
    - Need 4 mL – Add 8 µL Anti-αSMA stock to 4 mL PBS/BSA
- Anti-Mouse IgG Alexafluor 584 Solution (1:500 dilution)
    - For each well to be evaluated, 200 µL antibody solution
    - Need 5.2 mL – Add 10.4 µL IgG Alexafluor 584 to 5.2 mL PBS/BSA

- Hoechst Staining Solution
    - For each well, 200 µL antibody
    - 18.3 µL Hoechst Stock Solution +5.5 mL ddH_2O

Procedure:

- Warm 1X PBS and Fixing Solutions. Bring PBS/BSA to room temperature.
- Drain media from culture dishes, rinse 2X with warm 1X PBS (~0.5 mL per sample)
- Add 0.5 mL Fixing Solution to each sample. Put on orbital shaker for 10 minutes.
- Prepare Anti-αSMA solution.
- Remove Fixing solution and put in Hazardous Waste.
- Rinse plates 2X with warm 1X PBS.
- Add PBS/BSA solution (0.25-0.5 mL per sample). Put on orbital shaker for 10 minutes.
- Remove liquid, and add 200 µL anti-αSMA to each sample (except secondary only samples)
- Seal and put on orbital shaker for 1 hr
- Prepare Working solution, anti-mouse IgG solution, and Hoechst Staining Solution. Put on ice and protect from light until solutions are required.
- Remove antibody solution and rinse 3x with BSA/PBS for 10 minutes each (on orbital shaker).
- Remove final wash of PBS/BSA solution and add 200 µL working solution to designated samples and 200 µL anti-mouse IgG solution to every sample. Seal and place on orbital shaker for 30 minutes.
- Remove solution and wash 2X with PBS/BSA.
- Remove solution and add 200 µL Hoechst staining solution to every sample. Seal and place in incubator for 5 minutes.
- Remove solution and wash the samples 2x with PBS/BSA.
- Keep hydrated! Store in PBS, wrap plates in parafilm and protect from light until samples are imaged.

Appendix I Preparing Flexcell Plates with PA Gels

Source: Leach, J. Neural Eng., vol 4, 26-34 (2007), Schnaar, Analy Biochem, vol 151, 268-281 (1985)

Materials:

- Untreated Flexcell plate
- Glass syringe with gradations (200 µL)
- Glass pipettes with gradations (5 and 10 mL)
- Manual pipettor
- Plasma Prep, plasma oxidizer (chemistry. department)
- 3-(Trichlorosilyl)propyl methacrylate (TPM, Sigma 64205, store in fridge under desiccate and N_2)
- Heptane
- Carbon tetrachloride
- Hexane
- Vacuum
- Vacuum desiccator
- 40% Acrylamide (Biorad) - refrigerator
- 2% Bis-acrylamide (Biorad) - refrigerator
- 1x PBS
- TEMED (Biorad) – Chemical shelf
- 1% aqueous solution of APS in ddH_2O (1g APS /100 mL ddH_2O – prepare fresh)
- ddH_2O
- 22 mm round coverslips
- Surfacil
- Methanol
- Kimwipes
- 60 mm Petri dishes or mounting chambers for glass coverslips
- Nitrogen tank

- Sterile PBS
- DMEM with 10% FBS

Procedure:

Before plasma cleaning, place the following in the chemical hood, the chemicals will need to be applied immediately after coating:

- Glass syringe (200 µL)
- 50 mL glass beaker(s)
- Glass pipettes (5 and 10 mL)
- Manual pipettor
- 3-(Trichlorosilyl)porpyl methacrylate (Sigma 64205, store in fridge under desiccate, keep in sealed jar until ready to use)
- Heptane
- Carbon tetrachloride
- Hexane
- Vacuum
- Vacuum desiccator (plastic only – do not use glass)
- Timer

- Do the following in the chemical hood:
- Treat 22 mm coverslips with surfacil as per protocol. Add a small volume (few mL) of Surfacil to a glass beaker and dip coverslips in Surfacil solution to coat. Rub dry with a Kimwipe. Rinse coverslips by washing in methanol. Let dry by standing coverslips on end to prevent spotting.

Begin to prepare PA – it is important to work very quickly after the silicone surface has been functionalized…have EVERYTHING ready to go.

See below for calculating necessary volumes.

For each 1 mL of prepolymer:

- Weigh out ~10 mg of APS.
  - Zero balance
  - Label a 1.5 mL eppendorf tube with APS
  - Weigh the tube and write the mass on the side
  - Add 1-2 mg APS to the tube
  - Write the final mass on the side
  - Add appropriate volume of ddH_2O for 1% solution
- Mix the following according to the chart below:
  - 40% acrylamide
  - 2% bis-acrylamide
  - PBS
  - TEMED

Leave PA samples on the bench while you plasma clean the Flexcell plate.

Return to the chemical hood and prepare the following solution:
- 8 mL heptane in the 50 mL glass beaker (use the glass pipette).
- Add 2 mL carbon tetrachloride.

(This solution will evaporate so it is important to work quickly after this step).

(using Plasma Prep II)
Created by: Lee Sierad v 1.0 4/26/2007

- Ensure that the "meter" switch is up and the other two switches are down.
- Turn on the Plasma Prep II (press the square red button on the front).
- Let the machine warm up for at least three minutes.

- Turn on the O_2. Make sure the main valve is completely open – also check side valve and flow rate (big knob on front of regulator). It is important to have oxygen flow!
- Turn on large vacuum pump.
- CAREFULLY remove sample container from device.
- Place sample inside of container.
- CAREFULLY replace sample container into device.
- Turn "vacuum" to on position (switch – up).
- Ensure a vacuum has been reached.

- Perform the next set of steps quickly so the sample is not under plasma oxidation for an extended period of time.

    - Turn power on (switch – up).
    - Turn level up so meter reads about 40.
    - Tune counterclockwise until area becomes magenta.
    - Turn level all the way up – about 100.
    - Tune clockwise slowly until area is at its greatest intensity of magenta.
    - Let sit for 2 minutes.
    - Turn level all the way down.
    - Turn power switch off.
    - Turn vacuum switch off.
    - Wait for vacuum to release.
    - Remove the sample.
    - Repeat steps 7 through 22 as needed for multiple samples.
    - Turn large vacuum off.
    - Turn O_2 off.
    - Turn Plasma Prep II off.

- It is important to chemically activate the plates immediately after plasma coating. (all chemicals are very toxic, wear gloves and always work in the hood).
- Using the glass syringe remove 20 µL TPM (puncture septum with needle, never open container to the air). Submerge the end of the needle in the heptane/carbon tetrachloride solution and expel the TPM. Swirl to mix.
- Apply ~2 mL of the activation solution to each Flexcell well and cover with lid.
- Set timer for 5 minutes.
- Note: solution will begin to evaporate, it will turn the lid white, and will cause the silicone to swell.
- After 5 minutes, dispose of in hazardous waste (chlorinated flammable) and apply ~2 mL hexane to each well to rinse. Dispose of hexane in same waste container. At this point the silicone is relatively fragile, do not puncture with the glass pipette.

- Place flexcell plate in vacuum desiccator and pull hard vacuum (not house vac) for 5 minutes. After 5 minutes the silicone should return to its normal geometry.
- Close valve to vacuum desiccator. Remove tube from desiccator (vent vac to atm) then quickly turn off vac. (keep desiccator sealed).
- Bring desiccator to bench top and connect to nitrogen source. Slowly release the vacuum while pumping nitrogen into the dessicator – it is EXTREMELY important to only use a plastic dessicator with a light lid. When the chamber has filled with nitrogen it will lift allowing for excess gas to escape.
- Add 100 µL of 1% aqueous solution of APS to first tube of PA and vortex.
- Open desiccator and apply 50 µL of PA solution to each well (while under the flow of Nitrogen)
- Using forceps, "rinse" each coverslip under nitrogen flow prior to placing on top of the PA droplet.
- Try to get it in the center when placing the coverslip – forceps sometimes help.
- DO NOT MOVE THE COVERSLIP ONCE IT IS DOWN. Sliding the CS around will cause the PA gel to stick to the CS upon removal.
- Put the lid back on the dessicator and continue flowing nitrogen over the gels for 15 minutes. (for softer gels increase time to 30 minutes)
- After 15 minutes, turn off the nitrogen tank but DO NOT OPEN THE DESICCATOR. Let sit for another 15 minutes undisturbed.
- After 15 minutes remove the flexcell plate from the desiccator and add PBS to each well.
- Let sit for 10 minutes.
- To remove the coverslips, gently press down (into the well) with forceps. You will see the coverslip lift off the gel.
- Remove the coverslip from the well with forceps being sure not to disturb the gel.
- Activate gels with sulfa-Sanpah (per manufacturer protocol) and apply collagen solution
- After incubation, cover gels with PBS and place under UV light for 10 minutes to sterilize
- Remove PBS and add 200 µL of media (note: only apply media to the PA, try to avoid getting media on glass surrounding PA gel) and incubate for 45 minutes at room temperature.
- Remove media and add cells (For most experiments, a concentration of 5000 cells in 200 µL media was used). Again, only put the cell solution on the PA gel.
- Allow 1 hr for cell attachment and fill well with media (~2 mL)

	1	**2**	**3**	**4**	**5**	**6**	**7**	**8**	**9**	**10**	**11**
Estimated G' (Pa)	**50**	**100**	**200**	**400**	**800**	**1600**	**3200**	**6400**	**12800**	**25600**	**51200**
% Acrylamide	3.0	3.0	3.0	3.0	7.5	7.5	7.5	7.5	12.0	12.0	12.0
% Bisacrylamide	0.040	0.048	0.058	0.107	0.034	0.053	0.117	0.236	0.118	0.242	0.585

POLYMERIZATION MIXTURE (µL) for 1 mL											
40% Acrylamide	75	75	75	75	188	188	188	188	300	300	300
2% Bisacrylamide	20.0	24.2	29.1	53.7	16.8	26.7	58.4	118.2	58.8	120.9	292.5
Water	804	799	794	770	694	684	653	593	540	478	306
TEMED	1.5	1.5	1.5	1.5	1.5	1.5	1.5	1.5	1.5	1.5	1.5
TOTAL	900	900	900	900	900	900	900	900	900	900	900
add 1% APS	100	100	100	100	100	100	100	100	100	100	100
Final volume = 1 mL											

Appendix J Cell Lysis Protocol for Western Blot

Materials:

- Sterile, protease free 1.5 mL eppendorf tubes
- Lab Marker
- Sterile 1x PBS (warmed)
- Tissue homogenizer
- Centrifuge
- Ice

Cell lysis buffer (volume depends on # and cell density of samples):

ALWAYS KEEP SOLUTION COLD!!!

- 500 µL NP-40 lysis buffer (aliquotted in tubes, 500 µL/tube) (Biosource: cat# FNN0021)
- 1.7 µL PMSF (Pierce: cat# 36978)
- 5 µL HALT protease inhibitor (Pierce: cat# 78410)

Procedure:

For tissue or biopolymer gels:

- *3 mL per gram of whole tissue or biopolymer gel*
- Pre-weigh 1.5 mL eppendorf tubes
- Rinse tissue in sterile 1X PBS and place in tube.
- Weigh tube+tissue and subtract tube mass to get mass of tissue
- Add appropriate volume of lysis buffer and homogenize until tissue is pulverized
- Incubate on ice for 30 minutes. (vortex every 10 minutes)
- Centrifuge tubes for 10 minutes at 10,000 rpm.

- Transfer lysate to new 1.5 mL tube.
- Store at -80˚ C.

For plated cells:

- *0.6 mL per 100 mm diameter petri dish with subconfluent monolayer*
- Remove media from culture dish
- For a 100 mm Petri dish, add 0.5 mL PBS and scrape cell layer off with cell scraper
- Transfer PBS/cell solution to 1.5 mL eppendorf tube.
- Repeat 2 times (transfering to same tube) for a total of 1.5 mL PBS
- Centrifuge at 1200 rpm for 6 minutes.
- Aspirate PBS – be careful not to disturb the pellet.
- At this point, cell pellet can be stored in the -80˚ C freezer until all samples are ready. (not recommended for long term storage, but should be fine for a few days).
- Add 0.6 mL lysis buffer and pipette up and down to break up pellet.
- Incubate on ice for 30 minutes. (vortex every 10 minutes)
- Centrifuge tubes for 10 minutes at 13,000 rpm.
- Transfer lysate to new 1.5 mL tube.
- Store at -80˚ C.

For cells in suspension:

- 1 mL per 2e7 cells in suspension.

Appendix K Western Blot Protocol

Materials:

- Pouring Gel
- Acrylamide
- Bis-acrylamide
- TEMED
- Ammonium persulfate

Running Gel

- Running Buffer
- 6X Loading Buffer
- 1X Loading Buffer
- Protein samples
- 500 µL tubes
- Some sort of lane maker (Previously have not had success with Magic Mark XP marker).

Protein Transfer

- Razor blade
- Methanol
- Transfer Buffer
- PVDF membrane
- 10 sheets Whatman paper
- Glass pipette

Blotting

- 5% milk in PBS-T
- Anti-αSMA
- Anti-tubulin
- Anti-IgG-AP

- PBS-T
- Lumi Phos WB (AP substrate)

Procedure:

Sample Preparation

- Quantify the amount of protein using a BSA assay. For dermal fibroblasts or VICs, 10 µg of protein per lane is enough to get a good signal.
- Use 1-500 µL tube for each lane. Poke a hole in each lid with a push pin. Add 10 µg protein to each tube.
- To calculate volume of 6x Loading Buffer, divide the volume of the most dilute protein by 5.
- Add this amount to each tube.
- Bring the volume of each tube to 20 µL by adding 1x Loading Buffer. (it is helpful to create an excel spread sheet for the calculations)
- Boil tubes for 5 minutes. Centrifuge for 1 minutes at 1000 RPM.

Loading the gel

- Pour (or purchase) 12% bis-acrylamide gel with 4% stacker.
- Load into BioRad electrophoresis system. Short piece of glass should face the inner chamber of the holder. If only running one gel, put a second glass sandwich on other side of gel holder.
- Fill bucket with 1X Running Buffer until it is to the top of the gel. Note: do not pour over the top of both pieces of glass, this will prevent the current from flowing through the gel.
- Remove the comb and rinse each lane with 200 µL Running Buffer.
- Load 20 µL samples per lane.
- Load 20 µL standard ladder
- Load 20 µL 1x Loading Buffer to unused lanes.
- Run ~2 hr at 30 mA

Transferring Protein

- Take apart gel, notch one corner.

- Cut off unused lanes and stacking gel with razor blade.
- Rinse gel in Transfer Buffer for 10 minutes.
- Cut PVDF membrane to size of gel and notch one corner.
- Soak in methanol for 45 seconds, then soak in transfer buffer until ready to use.
- Cut Whattman paper to size of gel, soak in Transfer Buffer.
- To prepare the stack, place 5 sheets of Whatman paper on transfer apparatus. Roll out air bubbles with glass pipette.
- Place gel on Whatman paper, roll.
- Place PVDF membrane on gel, line up notches, roll.
- Place 5 sheets of Whatman paper on PVDF membrane, roll.
- Dry off anode around stack with paper towel and cover the unused area with parafilm. This allows the current to only flow through the unblocked area (aka the stack).
- Run 90 minutes at 60 mA.

Blotting

- Take apart stack.
- Place membrane in 5% milk for several hours ~3 hours
- Dilute anti-αSMA at 1:5000 and anti-tubulin (1:500) in PBS-T. (5 mL for bag, 10 mL for pipette box).
- Rock overnight at 4˚C or at room temperature for 1 hr.
- Pour off antibody (can reuse ~3x).
- Do 3 quick rinses with PBS-T.
- Do 4-10 minutes rinses on rocker at room temperature.
- Dilute anti-IgG 1:10,000 in PBS-T (same volume as primary antibody).
- Rock at room temperature for 1 hr.
- Pour off antibody (Do not reuse this one).
- Do 3 quick rinses with PBS-T.
- Do 6-10 minutes rinses on rocker at room temperature.
- Apply 0.125 mL Lumi Phos WB substrate per cm^2 of PVDF membrane.
- Incubate 5 minutes in dark at room temperature.
- Expose.